공학석사 학위논문

Structural Tests of Precast Beams with Geopolymer Concrete

지오폴리머 콘크리트를 사용한 프리캐스트 보의 구조성능평가

February 2023

Graduate School of Engineering

Seoul National University

Architecture and Archtectural Engineering

Do Hun Kim

Structural Tests of Precast Beams with Geopolymer Concrete

지도 교수 박 홍 근

이 논문을 공학석사 학위논문으로 제출함

2023년 2월

서울대학교 대학원

건축학과

김 도 훈

김도훈의 공학석사 학위논문을 인준함

2023년 2월

위 원 장 ______________________ (인)

부위원장 ______________________ (인)

위 원 ______________________ (인)

Abstract

Structural Tests of Precast Beams with Geopolymer Concrete

Kim, Do Hun
Department of Architecture and Architectural Engineering
College of Engineering
Seoul National University

As climate change and global warming become the serious threats to the health of human being, international organizations and countries are making considerable efforts to reduce carbon emissions and revitalize clean energy. Various efforts are being made in the building construction industry to reduce operational carbon emissions during the building use phase, but more attention should be paid to embodied carbon emissions because carbon emissions are known to account for about 7% of global emissions per year.

Flexural, shear and lap splice tests of beams were performed to evaluate whether geopolymer concrete can be designed based on the current design codes. In the flexural tests, test variables were concrete types, flexural rebar ratio, cross-section depth of specimens, and compressive strength of concrete, etc. In the shear tests, test variables were concrete types, shear span ratio, spacing of stirrups, and compressive strength of concrete, etc. In the lap splice tests, test variables were concrete types, lap splice length, presence or absence of stirrups in the lap splice section, and compressive strength of concrete.

All flexural specimens showed high strength exceeding the nominal strength and showed typical flexural failure mode. All shear specimens also showed high strength exceeding the nominal strength. Most of shear specimens showed diagonal tension failure, but some specimens showed flexural failure mode because the shear strength exceeded the flexural strength. All lap splice specimens also showed high strength exceeding the nominal strength. In the case of lap splice tests, there were differences in accordance with the lap splice length. The specimens that satisfied required KDS lap splice length reached the yield strength and the longitudinal rebars yielded. However, the specimens, which was intentionally reduced length by 50%, were failed without reaching yield strength.

Based on the experimental results, it was found that the precast geopolymer concrete beam can be used for ordinary moment resisting frames according to the current design code, KDS.

Keywords: Carbon Reduced Concrete, Geopolymer Concrete, Compressive Strength, Flexural Strength, Shear Strength, Bond Strength, Lap Splice, Precast Beam

Student Number: 2021-28039

Contents

List of Tables

List of Figures

Chapter 1. Introduction

1.1 Background

Recently, policies have been implemented to set targets for reducing greenhouse gas emissions in countries around the world to cope with climate change caused by increased greenhouse gas emissions worldwide. The Kyoto Protocol (1997) and the Paris Agreement (2015) stipulate the country's obligation to reduce carbon emissions, and the government announced a roadmap for reducing greenhouse gas emissions in 2030. The trend of reducing national greenhouse gas in response to climate change is leading to the implementation of carbon taxes.

In the construction field, carbon-reducing concrete, which reduces embedded carbon, which is carbon generated in the process of production, transportation and construction, and disposal of building materials, is being studied. When producing 1 ton of cement, about 1 ton of carbon dioxide is emitted. And this amount accounts for about 7 percent of global carbon dioxide emissions.

The research on carbon-reduced concrete at domestic and foreign began in the 1960s, and has been activated since the 2000s as environmental issues have become a social issue. Although it has been studied steadily in countries such as the United States, Australia, Japan and Europe, most of them are brick-like non-structural materials, and the construction of the Global Change Institute at Queen's University in Australia in 2013 was the first case for architectural structure in the world. According to the national research in Korea, a total of 86 studies related to carbon-reduced concrete have been invested and a total research cost of 25.8 billion won has been invested since 2005. Most of them were studies performed at the material level, and the studies including even a little structural content are a total of 13 cases and a total research cost of 1.16 billion won, which is very insignificant, 15.1% for the number of cases and 4.5% for the research cost.

According to the current concrete structure design code, KDS 14 20 01, cement should be equal to or greater than that specified in the Korean Industrial Standards. ACI 318-19 also restricts cement with the table that meets the ACI code. However, KDS stipulates that this code may not be applied when designing by special researches, and that the design code considering material strength variability and structural resistance variability is presented when designing by performance tests.

1.2 Scope and Objectives

Most of the previous studies on carbon-reduced concrete have been conducted at the material level, and research and examples at the structural level are very insignificant. In addition, when cement not specified in the industrial standard is used in accordance with KDS 14 20 00, a research through performance tests is essential. In response, this study aims to prove through experimental studies whether the member for ordinary moment resisting frame made of geopolymer concrete using industrial by product without cement based on CSA composites can secure structural performance according to KDS 14 20 00. The design compressive strength of geopolymer concrete is 45 MPa, and subject to application is restricted to PC ordinary moment resisting frame members subjected to bending, shear and compression.

Material Test

<Basic Material Test for Material Mechanical Properties>

→ Test for compressive strength of concrete

→ Test for flexural strength of concrete

→ Test for tensile splitting strength of concrete

Structural Test

<Basic Member Test for Strength Design>

→ Flexural test

→ Shear test

→ Lap splice test (bond strength)

Figure 1-1 Performance test

This study was conducted on geopolymer concrete manufactured with a specific mixing standard. The study is largely divided into 2 parts. One is structural test at material level and the other one is structural test at member level. In the case of material tests, to investigate mechanical properties of geopolymer concrete, external institutes performed compressive strength, splitting tensile strength, and flexural strength (modulus of rupture) tests, which are basic material tests in accordance with KS standards. In order to evaluate the structural performance of members, beam flexural tests, beam shear tests, and beam lap splice tests were performed.

Since the geopolymer concrete used in these tests is used as a PC member, it is necessary to consider the manufacturing and shipping characteristics of the PC members. The PC member is manufactured in the factory and shipped after the design standard compressive strength is developed within 5 to 14 days. Therefore, when planning beam tests (flexural, shear, and lap splice), tests were planned and performed at the design standard compressive strength of 45 MPa, which is the strength at the time of shipment of PC members, and at 60 MPa which is the long-term strength.

Chapter 2. Literature Review

2.1 Code Review

2.1.1 Flexural design provided by KDS 14 20 20 :2022

According to the design code for flexural and compressive design of concrete structures, the flexural design is as follows

4.1.1 Design assumption (KDS)

(1) The strength design of the bending moment and the axial force member shall be in accordance with the assumptions prescribed in subparagraphs (2) through (7), and shall satisfy the force equilibrium conditions and strain conformity conditions.

(2) It can be assumed that the strain of rebar and concrete is proportional to the distance from the neutral axis. However, the deep beams specified in 4.2.4 shall consider the nonlinear strain distribution. Instead of considering nonlinear strain distributions in the design of deep beams, the strut-tie model can also be applied.

(3) The extreme strain of the concrete compressive edge of the member subjected to the bending moment or bending moment and axial force is assumed to be 0.0033 when the design standard compressive strength of the concrete is less than 40 MPa, and is reduced by 0.0001 for every 10 MPa increase in strength. If the design standard compressive strength of concrete exceeds 90 MPa, the extreme strain

of the concrete compressive edge shall be selected by study through performance experiments and the basis shall be specified.

(4) When the stress of rebars is less than the design standard yield strength f_y, the stress of rebars shall be the strain multiplied by B_s, and if the strain of rebars is greater than the strain corresponding to f_y, the stress of rebars shall be f_y regardless of the strain.

(5) The tensile strength of concrete can be ignored in the calculation of axial strength and flexural strength of the cross section of reinforced concrete members, except as specified in KDS 14 20 60 (4.2.1).

(6) The relationship between the distribution of concrete compressive stress and concrete strain can be assumed to be any shape that is substantially consistent with the results of a wide range of experiments in the prediction of rectangular, trapezoidal, parabolic, or strength.

(7) Thre provisions of 4.1.1(6) may be expressed as the stress-strain relationship of a parabolic-straight shape, as defined below.

① The rising curve from the origin to the maximum stress is calculated by Equation (2.1) and then by Equation (2.2) until the extreme strain ε_{cu}.

$$f_c = 0.85 f_{ck}\left[1-\left(1-\frac{\varepsilon_c}{\varepsilon_{co}}\right)^n\right] \qquad (2.1)$$

$$f_c = 0.85 f_{ck} \qquad (2.2)$$

where, n is an index representing the shape of the rising curve, ε_c is the compressive strain of concrete, and ε_{co} is the strain when the maximum stress is first reached.

② If the compressive strength of concrete is 40 MPa or less, n, ε_{co}, and ε_{cu} shall be 2.0, 0.002, and 0.0033, respectively. If the compressive strength of concrete exceeds 40 MPa, n is determined according to Equation (2.3), and for every increase in strength of 10 MPa, increase the value of ε_{co} by 0.0001 as shown in Equation (2.4) and decrease the value of ε_{cu} by 0.0001 as shown in Equation (2.5).

$$n = 1.2+1.5\left(\frac{100\text{-}f_{ck}}{60}\right)^4 \leq 2.0 \tag{2.3}$$

$$\varepsilon_{co} = 0.002+\left(\frac{f_{ck}\text{-}40}{100{,}000}\right) \geq 0.002 \tag{2.4}$$

$$\varepsilon_{cu} = 0.0033\text{-}\left(\frac{f_{ck}\text{-}40}{100{,}000}\right) \leq 0.0033 \tag{2.5}$$

However, if the compressive strength of concrete exceeds 90 MPa, these values shall be selected by study through performance experiments and the basis shall be specified.

③ The average value of the compressive strength acting on concrete by the parabolic-straight stress-strain relationship is α $(0.85f_{ck})$, and the working position of the force from the compressive edge is expressed as the product of the neutral axis depth c and β, and each variable and coefficient of the stress distribution is applied in Table

2-1.

Table 2-1 variable and coefficient of the stress distribution

f_{ck} (MPa)	≤40	50	60	70	80	90
n	2.0	1.92	1.50	1.29	1.22	1.20
ε_{co}	0.002	0.0021	0.0022	0.0023	0.0024	0.0025
ε_{cu}	0.0033	0.0032	0.0031	0.0030	0.0029	0.0028
α	0.80	0.78	0.72	0.67	0.63	0.59
β	0.40	0.40	0.38	0.37	0.36	0.35

(8) The provisions of paragraph (6) above may be represented by an equivalent rectangular compressive stress block defined below instead of the parabolic-straight stress-strain relationship defined in paragraph (7) above.

① It is assumed that the concrete stress of η ($0.85f_{ck}$) is equally distributed in the equivalent compression region formed by straight line parallel to the neutral axis at $\alpha = \beta_1 c$ distance from the edge of the crosssection and the platform where the maximum compressive strain occurs.

② The distance c from the compressive edge to the neutral axis where the maximum strain occurs is measured in the direction perpendicular to the neutral axis.

③ The coefficients η and β_1 apply the values in Table 2-2.

Table 2-2 variable and coefficient of the stress distribution

f_{ck} (MPa)	≤40	50	60	70	80	90
ε_{cu}	0.0033	0.0032	0.0031	0.0030	0.0029	0.0028
η	1.00	0.97	0.95	0.91	0.87	0.84
β_1	0.80	0.80	0.76	0.74	0.72	0.70

2.1.2 Shear design provided by KDS 14 20 22 :2022

According to the design code for shear and torsional design code on concrete structure, the shear design is as follows.

4.1 Shear design principles (KDS)

4.1.1 Design assumption

V_n is the nominal shear strength calculated by the following Equation (2-6).

$$V_n = V_c + V_s \tag{2-6}$$

where, V_c is the cross-sectional nominal shear strength of concrete calculated by the equation 4.2 or 4.11, and Vs is the cross-sectional nominal shear strength of rebars calculated by the equation 4.3 or 4.9.2(5) or 4.11.

4.2.1 Shear strength of reinforced concrete member by concrete

(1) ① In the case of members subjected to only shear forces and bending moments, it can be calculataed by Equation (2-7).

$$V_c = \frac{1}{6}\lambda\sqrt{f_{ck}}b_w d \tag{2-7}$$

where, b_w is width of members.

4.3.3 Least stirrup

$$A_{v,min} = 0.0625\sqrt{f_{ck}}\frac{b_w s}{f_{yt}} \tag{2-8}$$

where, s is spacing of stirrups. However, the minimum stirrups shall not be less than $0.35b_w s/f_{yt}$. Where, the unit of b_w and s is mm.

4.3.4 Design of stirrup

(2) If stirrup that perpendicular to the member axis is used, the shear strength V_s shall be calculated according to the following Equation (2-9).

$$V_s = \frac{A_v f_{yt} d}{s} \tag{2-9}$$

where, A_v is the entire cross-sectional area of the stirrups within the distance s, and f_{yt} is the design standard yield strength of the stirrups.

2.1.3 Development length of rebars (KDS 14 20 52 :2022)

According to the development and splice design code on concrete structure, the development length and splice length of rebar are as follows.

4.1.2 Development of tensile deformed rebar or steel wire

(1) The development length of tensile deformed rebar, l_d can be applied by selecting either the method of considering the correction factor for the basic development length ldb as shown in the following (2) or the method according to the following (3). However, the development length l_d calculated by this way, must always be 300 mm or more.

(2) The basic development length of the tensile deformed rebar, ldb shall be calculated by the following Equation (2-10). In addition, the correction factor according to whether the rebar sucface coating or plating, the location of the rebars, and the type of concrete shall be calculated by Table 2-3.

$$l_{db} = \frac{0.6 d_b f_y}{\lambda \sqrt{f_{ck}}} \qquad (2\text{-}10)$$

Table 2-3 Correction factor

	D19 or less rebar and steel wire	D22 or bigger rebar
If the spcaing of the anchoraged or spliced rebars is greater than d_b, the cover thickness is greater than d_b, and the stirrups or hoops with a minimum amount of rebars specified in this code are placed in the entire l_d section, or the spacing of anchoraged or spliced rebars is greater than $2d_b$ and cover thickness is greater than d_b.	$0.8\alpha\beta$	$\alpha\beta$
Et cetra	$1.2\alpha\beta$	$1.5\alpha\beta$

where, α, and β shown in Table 2-3 can be calculated as follows.

① α is location factor of rebar layout

i. Upper rebars (transverse rebars with non-hardended concrete exceeding 300 mm below development length or lap splice section) 1.3

ii. Et cetra 1.0

② β is paint skin factor

i. Epoxy coating or zinc-epoxy double coating rebar or steel wire with a cove thickness less than 3 db or a spacing less than 6 db 1.5

ii. Et cetra epoxy coating or zinc-epoxy double coating rebar or steel wire 1.2

iii. Zinc coating or non-coating rebar or steel wire 1.0

③ When the epoxy coating rebar is an upper rebar, $\alpha\beta$ which is the product of the upper rebar location factor α and the paint skin factor β does not need to be greater than 1.7.

④ λ follows KDS 14 20 10 (4.4).

(3) The development length of tensile deformed rebar, l_d can be calculated by the following Equation (2-11).

$$l_d = \frac{0.90 d_b f_y}{\lambda\sqrt{f_{ck}}} \frac{\alpha\beta\gamma}{\left(\frac{c+K_{tr}}{d_b}\right)} \geq 300 \text{ mm} \quad (2\text{-}11)$$

In equation (2-11), $(c+K_{tr})/d_b$ shall be less than 2.5. In addition, factor γ, c, and K_{tr} in the Equation (2-11) are as follows.

① γ is size factor of rebar or steel wire

i. D19 or less rebar and steel wire 0.8

ii. D22 or bigger rebar 1.0

② c is dimensions related to rebar spacing or cover thickness

The smallest of shortest distance from the center of the rebar or wire to the concrete surface or 1/2 of the distance between the centers of the rebar or wire being anchoraged is expressed in mm.

③ K_{tr} is dimensions of transverse rebar = $40A_{tr}/sn$

Even if transverse rebars are placed, they can be used as 0 to simplify the design.

(4) If the amount of rebars placed on the flexural member exceeds the required amount of rebars required by the analysis, the calculated development length can be multiplied by ((required A_s/placed A_s)) to reduce the development length l_d. However, at this time, the reduced development length l_d shall be 300 mm or more. In addition, this does not apply if anchorage is specifically required to exert f_y.

(5) For rebars with design basis yield strength greater than 550 MPa, the following shall be satisfied.

① If transverse rebars are not placed, c/db shall not be less than 2.5

② If transverse rebars are placed, Ktr/db≥0.25 and (c+Ktr)/db≥2.25 shall be satisfied.

4.5.2 Splice of tensile deformed rebar or steel wire

(1) The lap splice length of the deformed rebars and deformed steel wires subjected to tensile forsce shall be classified into Class A and Class B, and shall not be less than 300 mm.

① Class A splice: 1.0ld

② Class B splice: 1.3ld

Where, the development length of tensile deformed rebars is calculated in accordance with 4.1.2, at this time, the minimum value of 300 mm specified in 4.1.2(1) is not applied, and the correction factor of 4.1.2(4) is not applied, either.

(2) In lap splice, Class A and Class B splices are classified as follows.

① Class A splice: The amount of rebar placed is more than twice the required amount of rebar as a result of analysis in the entire section of the lap splice, and the amount of lap splice rebar within the required lap splice length is less than 1/2 of the total rebar amount

② Class B slplice: Not applicable to ①

Table 2-4 shows the development length of rebar specified in current design codes and methods.

Table 2-4 Development length of rebar according to design codes

Design Codes and Methods	Development Length (MPa and mm)	
KDS 14 20 52 [1)]	$l_d = \frac{0.90 d_b f_y}{\lambda\sqrt{f_{ck}}} \frac{\alpha\beta\gamma}{\left(\frac{c+K_{tr}}{d_b}\right)} \geq 300$ mm $c+K_{tr}/d_b \leq 2.5$ $c = \min(c_b, c_{so}, c_{si}) + 0.5d_b$ $K_{tr} = 40A_{tr}/sn$	(2-12)
KDS 14 20 52 (simplified eq.)	$l_d = \frac{0.6\alpha\beta d_b f_y}{\lambda\sqrt{f_{ck}}} \geq 300$ mm $\alpha\beta \leq 1.7$	(2-13)
ACI 318-19 [2)]	$l_d = \frac{f_y d_b}{1.1\lambda\sqrt{f_c'}} \frac{\psi_t\psi_e\psi_s\psi_g}{\left(c_f+K_{tr}\right)/d_b} \geq 300$ mm $(c_f+K_{tr})/d_b \leq 2.5$ $c_f = \min(c_b, c_{so}, c_{si}) + 0.5d_b$ $K_{tr} = 40A_{tr}/(s_t n_s)$	(2-14)

1) λ = lightweight concrete factor (0.75 ~ 1.0)
α = location factor of rebar layout (1.0 ~ 1.3)
β = paint skin factor (1.0 ~ 1.5)
γ = size factor of rebar or steel wire (0.8 ~ 1.0)
c = dimensions related to rebar spacing or cover thickness, the smallest of shortest distance from the center of the rebar or wire to the concrete surface or 1/2 of the distance between the centers of the rebar or wire being anchoraged is expressed in mm
K_{tr} = dimensions of transverse rebars = $40A_{tr}/sn$
A_{tr} = the total cross-sectional area of the transverse rebars within the spacing placed across the face that is likely to split along the anchorage rebars
s = maximum spacing between the centers of transverse rebars within the development length l_d section

n = number of rebars or steel wires that are anchoraged or spliced along a plane that is likely to split

2) λ = lightweight concrete factor (0.75 ~ 1.0)
ψ_t = location factor of rebar layout (1.0 ~ 1.3)
ψ_e = paint skin factor (1.0 ~ 1.5)
ψ_s = factor according to diameter of rebar (0.8 ~ 1.0)
ψ_g = factor according to yield strength of rebar (1.0 ~ 1.3)
c_b = bottom cover thickness
c_{so} = left anf right cover thickness
c_{si} = 1/2 of distance between centers of rebars
A_{tr} = the total cross-sectional area of the transverse rebars within the spacing placed across the face that is likely to split along the anchorage rebars
n_s = number of the transverse rebars within the spacing placed across the face that is likely to split along the anchorage rebars
s_t = spacing of transverse rebars

2.1.4 Flexural strength provided by ACI 318-19

According to ACI 318-19 [16], Maximum strain at the extreme concrete compression fiber shall be assumed equal to 0.003. Tensile strength of concrete shall be neglected in flexural and axial strength calculations. The relationship between concrete compressive stress and strain shall be represented by a rectangular, trapezoidal, parabolic, or other shape that results in prediction of strength in substantial agreement with results of comprehensive tests. The equivalent rectangular concrete stress distribution (stress block) in accordance with Equation (2-15).

Concrete stress of $0.85f_c'$ shall be assumed uniformly distributed over an equivalent compression zone bounded by edges of the cross section and a line parallel to the neutral axis located a distance a from the fiber of maximum compressive strain, as calculated by:

$$a = \beta_1 c \tag{2-15}$$

Distance from the fiber of maximum compressive strain to the neutral axis, c, shall be measured perpendicular to the neutral axis. Values of β_1 shall be in accordance with Table 2-5.

Table 2-5 Values of β_1 for equivalent rectangular concrete stess distribution (ACI)

f_c', MPa	β_1	
$17 \leq f_c' \leq 28$	0.85	(a)
$28 < f_c' < 55$	$0.85-0.05(f_c'-28)/7$	(b)
$f_c' \geq 55$	0.65	(c)

2.1.5 Shear strength provided by ACI 318-19

ACI 318-19 [16] addresses the shear strength of reinforced concrete beams. Shear strength is composed of concrete part and shear reinforcement part.

$$V_n = V_c + V_s \text{ (ACI 318-19)} \tag{2-16}$$

For non-prestressed members, V_c shall be calculated in accordance with Table 2-6.

Table 2-6 V_c for nonprestressed members (ACI)

Criteria	V_c		
$A_v \geq A_{v.min}$	Either of:	$\left[0.17\lambda\sqrt{f'_c}+\frac{N_u}{6A_g}\right]b_w d$	(a)
		$\left[0.66\lambda(\rho_w)^{1/3}\sqrt{f'_c}+\frac{N_u}{6A_g}\right]b_w d$	(b)
$A_v < A_{v.min}$	$\left[0.66\lambda_s\lambda(\rho_w)^{1/3}\sqrt{f'_c}+\frac{N_u}{6A_g}\right]b_w d$		(c)

For presstreseed members, V_c shall be calculated in accordance with Table 2-7, but need not be less than $0.17\lambda\sqrt{f'_c}b_w d$.

Table 2-7 Approximate method for calculating V_c (ACI)

V_c		
Least of (a), (b), and (c)	$(0.05\lambda\sqrt{f'_c}+4.8\frac{V_u d_p}{M_u})b_w d$	(a)
	$(0.05\lambda\sqrt{f'_c}+4.8)b_w d$	(b)
	$0.42\lambda\sqrt{f'_c}b_w d$	(c)

V_s for shear reinforcement shall be calculated by:

$$Vs=\frac{A_v f_{yt} d}{s}\ \text{(ACI 318-19)} \tag{2-17}$$

where, s is the spiral pitch or the longitudinal spacing of the shear reinforcement, and A_v shall be the effective area of all bar legs or wires within spacing s.

V_s for inclined shear reinforcement shall be calculated by:

where α is the angle between the inclined stirrups and the longitudinal axis of the member, s it measured parallel to the longitudinal reinforcement.

$$Vs=\frac{A_v f_{yt}(\sin\alpha+\cos\alpha)d}{s}\ \text{(ACI 318-19)} \tag{2-18}$$

2.1.6 Eurocode 2

Eurocode 2 [21] addresses the rectangular stress distribution. A rectangular stress distribution (see Figure 2-1) may be assumed. The factor λ, defining the effective height of the compression zone and the factor η, defining the effective strength, follow from

$\lambda = 0.8$	for $f_{ck} \leq 50$ MPa	(EC2) (2-19)
$\lambda = 0.8-(f_{ck}-50)/400$	for $50 \leq f_{ck} \leq 90$ MPa	(EC2) (2-20)
$\eta = 1.0$	for $f_{ck} \leq 50$ MPa	(EC2) (2-21)
$\eta = 1.0-(f_{ck}-50)/200$	for $50 \leq f_{ck} \leq 90$ MPa	(EC2) (2-22)

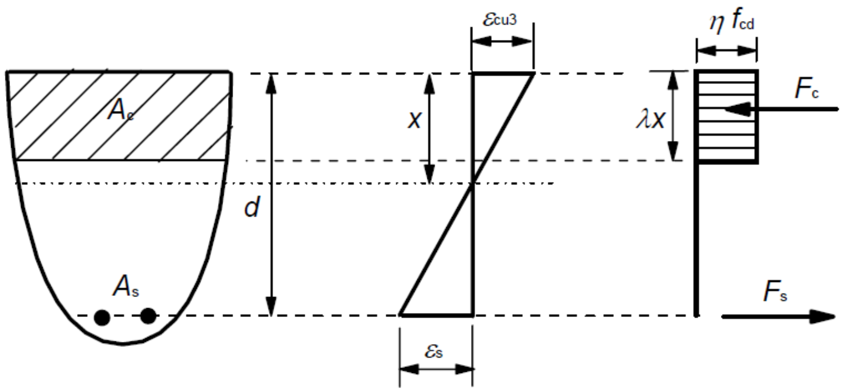

Figure 2-1 Rectangular stress distribution (EC2)

The design bond stress is limited to a value depending on the surface characteristics of the reinforcement, the tensile strength of the concrete and confinement of surrounding concrete. This depends on cover, transverse reinforcement and transverse pressure. The length necessary for developing the required tensile force in an anchorage or lap is calculated on the basis of a constant bond stress.

The arrangement of lapped bars should comply with Figure 2-2 (EC2).

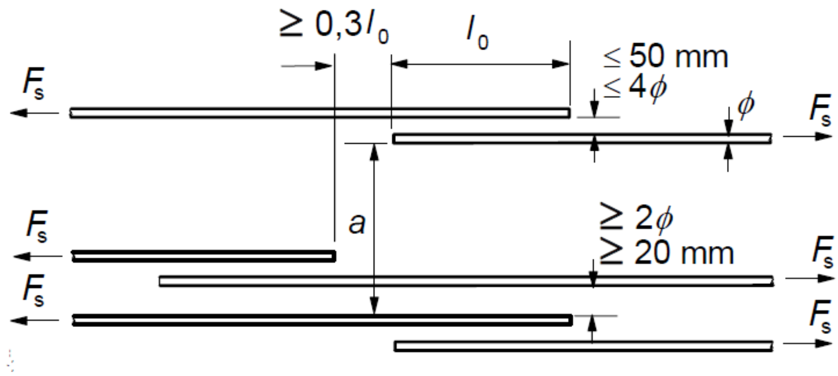

Figure 2-2 Adjacent laps (EC2)

The design lap length is

$$l_0 = \alpha_1\alpha_2\alpha_3\alpha_5\alpha_6 l_{b,\,rqd} \geq l_{0,\,min} \text{ (EC2)} \qquad (2\text{-}23)$$

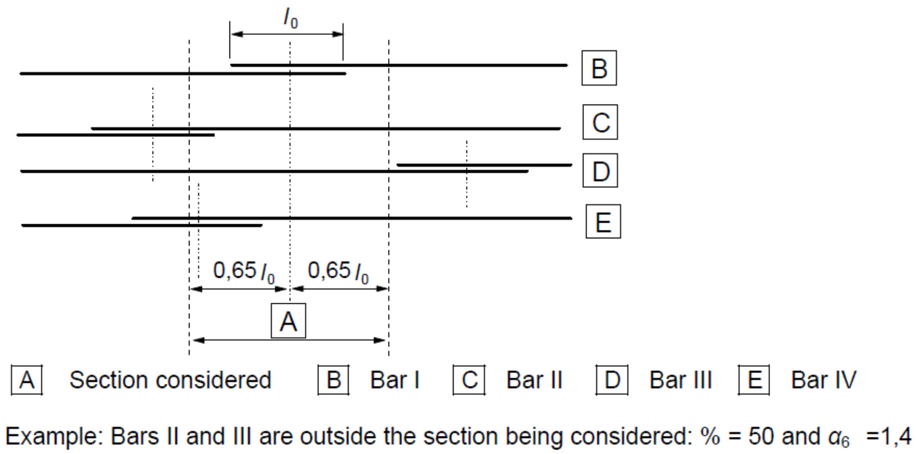

Figure 2-3 Percentage of lapped bars in one lapped section (EC2)

2.2 Literature Review

2.2.1 Flexural Test for Low Calcium Fly Ash Concrete Beam (GPC)

Alex et al. [22] studied flexural behavior of low calcium fly ash concrete beam. The cross section of sepcimens used in this study was 125×250×3200 mm. Three beams were used as fly ash concrete and three beams were used as control cement concrete. The grade of concrete was M20, and compressive strength was 20 MPa. In the test, four-point force test was conducted and LVDT's were placed at the mid-span below the specimens.

a

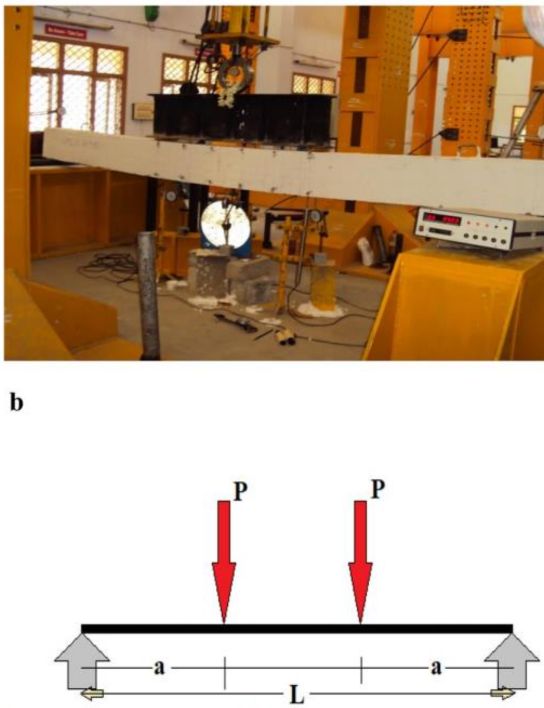

Fig. 4 a Beam testing set up. b Loading arrangement.

Figure 2-4 Test setup

The crack and failure patterns of specimens are very similar. GPC beams showed a 16.66 kN average first crack load, and CB (control concrete beam) showed a 13.66 kN. The load-deflection curves of specimens are shown in Figure 2-5. The theoretical value is calculated by Equation 2-24.

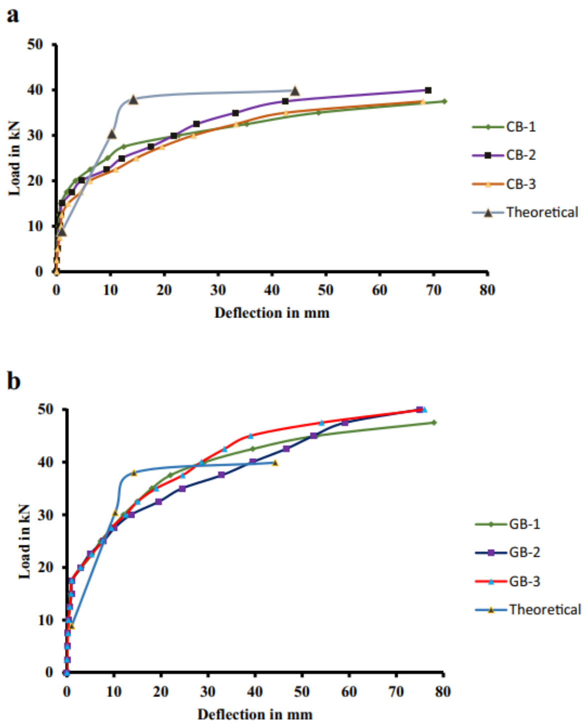

Fig. 6 **a** Mid span deflection of CB. **b** Mid span deflection of GPC.

Figure 2-5 Mid span deflection

$$\delta_{max} = \frac{Pa}{24EI}(3l^2\text{-}4a^2) \tag{2-24}$$

where, P = load (kN), a = distance from point (mm), l = effective length of beam (mm), E = young's moudulus (N/mm^2), and I = moment of inertia (mm^4).

GPC showed better performance in the load carrying and deflection compared to control concrete in the service stage and yield stage. Also, the average spacing of cracks in GPC is more when compared to control concrete. Therefore, the application of low calcium fly ash concrete was suggested effectively.

2.2.2 Shear Test for Fly Ash-Based Geopolymer Concrete Beams

Chang et al. [23] studied shear behaviour of reinforced low calcium fly ash-based geopolymer concrete beams. A total of nine beams were cast and their size was each with a rectangular cross section of 200 mm × 300 mm and length of 2000 mm. The beams were divided into three series in accordance with the longitudinal rebars ratio (each two of N24 mm, N28 mm, and N32 mm bars) (see Figure 2-2). All longitudinal rebars were designed to provide minimum yield strength of 500 MPa. The variables of the specimens were the stirrup spacing which was 125 mm, 100 mm, and 75 mm. Figure 2-6 shows the setup for loading.

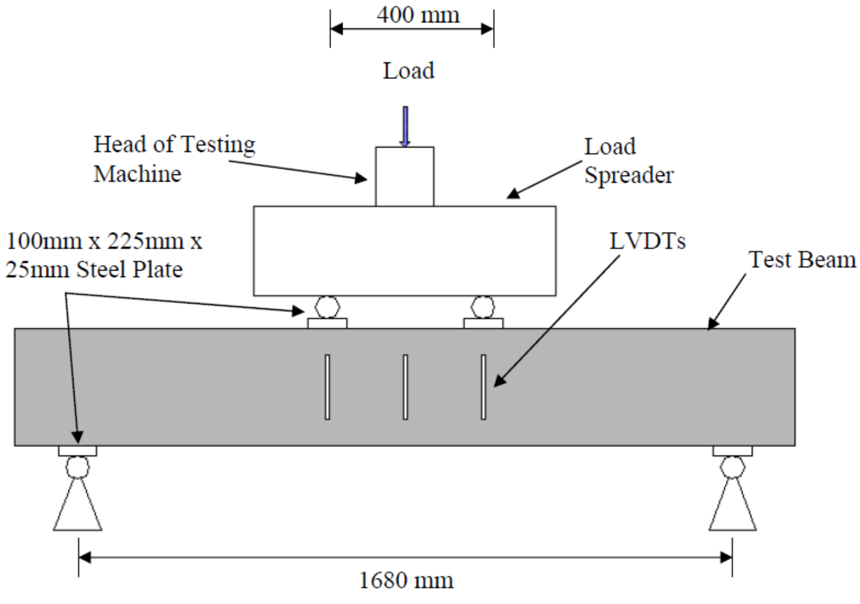

Figure 3.15: Loading Arrangement for Beam Tests

Figure 2-6 Test setup

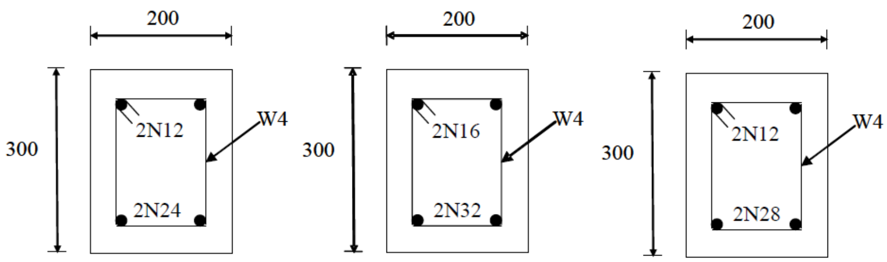

Figure 2-7 Specimen detail

There were two types of failure mode which were the diagonal tension failure and shear compression failure.

In the case of the diagonal tension failure, flexural cracks first occurred in the center of the beam, and gradually spread towards the supports at early load stages. The diagonal cracks widened into a principal crack and extensively developed toward the loading point. At last, the failure occurred after longitudinal splitting near the load point.

In the case of shear compression failure, flexural cracks first occurred in the center of the beam, and gradually spread towards the supports (see Figure 2-8). The flexural-shear cracks propagated towards the compression zone. At last, the failure occurred by the crushing of concrete in the compression zone.

The failures of the diagonal tension failure beams were sudden, with a sharp drop-off after peak load. The failures of the shear compression failure beams were less sudden and exhibited post-peak ductility.

Figure 2-8 Failure mode of specimen (S1-2)

Table 2-8 Comparison between geopolymer and Portland cement (shear)

Models	Geopolymer Concrte Beams		Portland Cement Concrete Beams	
	Test/Predicted Ratio	COV (%)	Test/Predicted Ratio	COV (%)
Von Ramin (2004)	1.42	13.4	1.14	15.0
Kong and Rangan (1998)	1.64	12.7	1.23	32.8
Vecchio (2000)	1.08	8.3	1.00	20.3

According to Chang et al. [22], Table 2-8 shows the comparison between geopolymer and Portland cement using Vecchio (2000), Kong and Rangan (1998), and Von Ramin (2004). The comparison of the results between Portland cement concrete and low calcium geopolymer concrete shows that it is applicable for predicting the shear strength of low calcium geopolymer concrete beams.

2.2.3 Bond Test for Fly Ash-Based Geopolymer Concrete Beams

Chang et al. [23] studied bond behaviour of reinforced low calcium fly ash-based geopolymer concrete beams. A total of twelve lap spliced beams with a cross section of 200 mm x 300 mm and length of 2500 mm were cast. The size of beam was selected to suit the capacity of testing machine. The beams were divided into two series in accordance with the longitudinar rebar size (16 mm, 20mm, and 24 mm diameter) and splice lengths (300 mm, 450 mm, and 720 mm). No stirrup was provided in the lap splice section. The nominal compressive strengths of concrete were 30 to 35 MPa for normal strength geopolymer and 50 to 55 MPa for high strength geopolymer.

In the case of failure modes and crack pattenrs on the side and bottom of all beam specimens were similar regardless of the variables. The crack patterns at the lap splice section were similar for all beams regardless of the compressive strength of concrete.

Table 2-9 Comparison between geopolymer and Portland cement (bond)

Models	Geopolymer Concrte Beams		Portland Cement Concrete Beams	
	Test/Predicted Ratio	COV (%)	Test/Predicted Ratio	COV (%)
Orangun (1977)	1.42	13.4	1.14	15.0
Zuo and Darwin (2000)	1.64	12.7	1.23	32.8
ACI 408R-03 (2003)	1.08	8.3	1.00	20.3
Esfahani and Rangan (1998)	1.28	10.16	0.94	20.21

According to Chang et al. [22], Table 2-9 shows the comparison between geopolymer and Portland cement using Orangun (1977), Zuo and Darwin (2000), ACI 408R-03 (2003), and Esfahani and Rangan (1998). The comparison of the results between Portland cement concrete and low calcium geopolymer concrete shows that the bond strength of geopolymer concrete is about 20% more than of Portland cement concrete using the same prediction.

2.2.4 Bond Test for Spliced GFRP Reinforcement Bars in Alkali Activated Cement Concrete

Tekle et al. [24] studied bond of spliced glass fibre reinforced polymer (GFRP) bars in alkali activated cement (AAC) concrete. A total of seven beams were manufacture with the variables such as splice length, type of concrete, and diameter of spliced bars. The splice lengths were 400 mm and 600 mm. The types of concrete were AAC and OPC (Portland cement). The diameters of spliced bars were 12.7 mm and 15.9 mm. Figure 2-9 shows the cross-section and detail of tested beam.

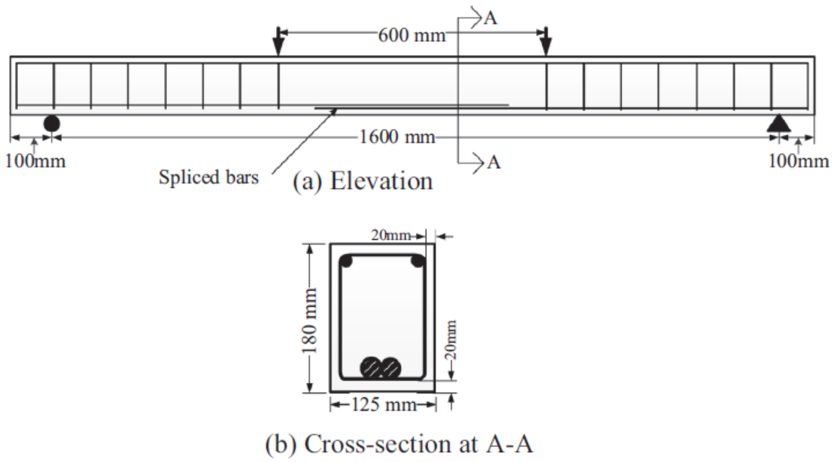

Fig. 2. Cross-section and detail of tested beam.

Figure 2-9 Cross-section and detail of tested beam.

In the case of cracking, flexural cracks were first initiated at both ends of the splice section. As the load increased, new flexural cracks occurred in the middle of the splice section. Finally, cracks forming in the shear span section. As the load further increased, the flexural cracks in the shear span section transformed to diagonal shear cracks.

All the beams failed by splitting of the concrete cover at the bottom part of the specimens. The splitting cracks ran from the bar surface to the concrete surface. After the cracking of the cover occurred, the covered concrete could not provide an increased splitting resistance, and thus load suddenly dropped.

Chapter 3. Material Test for Geopolymer Concrete

3.1 Properties

Carbon-reduced concrete used in this study was geopolymer concrete which was Portland cement-free concrete using CA composites and GGBS. The design compressive strength is 45 MPa. Table 3-1 shows the mix proportion of geopolymer concrete.

Table 3-1 Mix proportion of geopolymer concrete and normal concrete

<table>
<tr><th colspan="2">Material</th><th>Geopolymer concrete</th><th>Normal concrete</th></tr>
<tr><td rowspan="2">Powder</td><td>Cement</td><td>0%</td><td>70% (305)</td></tr>
<tr><td>GGBS</td><td>83%</td><td>30% (130)</td></tr>
<tr><td>Activator</td><td>Ca type composites</td><td>17%</td><td>0%</td></tr>
<tr><td rowspan="4"></td><td>Water</td><td>155</td><td>165</td></tr>
<tr><td>Sand</td><td>759</td><td>805</td></tr>
<tr><td>Coarse aggregate</td><td>862</td><td>978</td></tr>
<tr><td>Admixture</td><td>11</td><td>4</td></tr>
</table>

Unit: kg/m3
GGBS: ground granulated blast-furnance slag
Ca composites: calcium type material-based activator

The geopolymer concrete forms a cured product by reacting water and activator (Ca composites) directly with GGBS. However, GGBS does not react directly with water. The B/P production procedure can be produced in the same way as the normal concrete. The admixture (GGBS) and activator (Ca comprosites) are stored and used in silos, and the chemical agents are automatically metered.

The production procedure of geopolymer concrete is same as the normal concrete. Activators and industrial by-products (GGBS) are added to fine aggregates and coarse aggregates, and then, water and chemical agents are added to produce. The geopolymer concrete is produced for precast members and steam curing is carried out. After curing at the level of 20°C for 2 to 3 hours, the temperature is increased from 20°C to 35°C for 2 hours and maintained at 35°C for 8 hours. After that, curing ends by lowering 35°C to 20°C for 2 hours.

3.2 Test Results for Compressive Strength of Concrete

The compressive strength specimens were manufactured in a size of (Ø100×200 mm and Ø150×300 mm), and tests were performed on the 7^{th}, 14^{th}, and 28^{th} of the age [13]. Table 3-2 and Figure 3-1 show the test results. The strength was 21.6 MPa based on the 1^{st} day of age, which allows PC members to be deformed, and the strength on the 6^{th} of age was 45 MPa or more, which is the design standard compressive strength. The strength on the 28^{th} of age was 64.2 MPa.

Table 3-2 Compressive strength of concrete for each aging time (Ø100)

No.	Age						
	1^{st} day	3^{rd} day	5^{th} day	6^{th} day	7^{th} day	14^{th} day	28^{th} day
1^{st}	20.1	36.0	44.1	48.1	49.9	57.8	64.1
2^{nd}	23.6	36.4	44.2	48.6	51.0	57.7	62.6
3^{rd}	20.6	35.8	43.9	49.1	50.0	58.2	63.8
4^{th}	19.8	36.3	44.0	46.9	51.0	58.1	64.2
5^{th}	24.0	36.0	44.8	48.1	50.5	58.1	66.1
Avg.	21.6	36.1	44.2	48.2	50.5	58.0	64.2

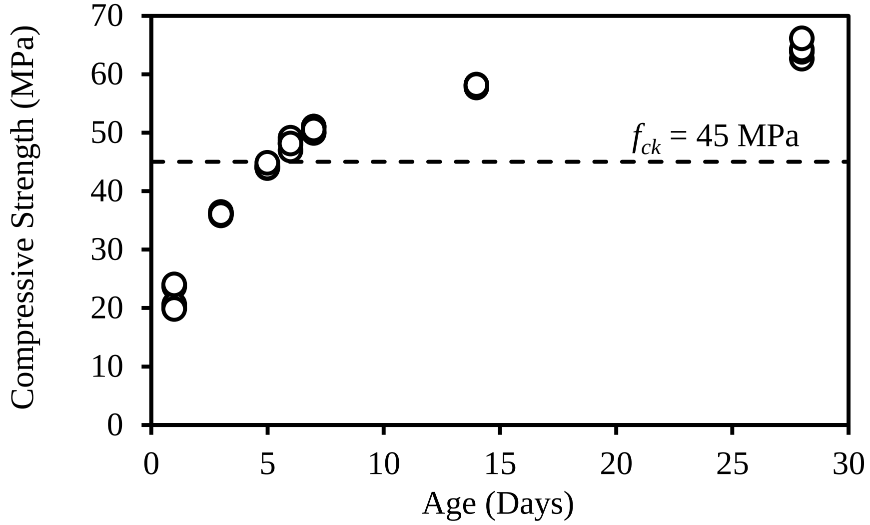

Figure 3-1 Compressive strength of concrete for each aging time (Ø100)

When performing compressive strength tests on the 7th, 14th, and 28th, the tests were conducted by attaching concrete strain gauges to both sides of the specimen, and the stress-strain relationship of the Ø150×300 mm is shown in Figure 3-2. The solid black line is the elastic modulus value calculated by the current KDS ($E_{c,\,KDS} = 8500\sqrt[3]{f_c'}$), and the black dotted line is $E_{c,\,test}$, which is the defined as the secant stiffness at 40% of the maximum strength.

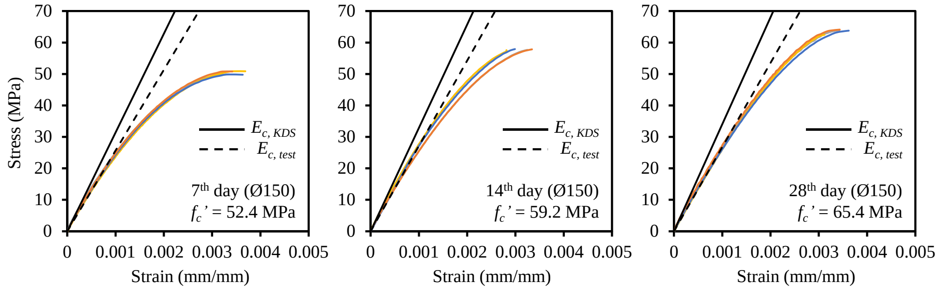

Figure 3-2 Stress-strain relationship of concrete (7, 14, 28 days) (Ø150)

The compressive strength and modulus of elasticity of the specimen (Ø150×300 mm) tested on the 7th, 14th, and 28th of the age are summarized in Table 3-3. The disconnection stiffness at 40% of the maximum strength calculated according to ASTM C469 was 0.86 to 0.90 times the current KDS elastic modulus, which tended to be similar to the current standard. The results of this test were conducted with a limited number of tests, making it difficult to judge as a general tendency.

Table 3-3 Compressive strength and elastic modulus of the specimen (Ø150)

Age	7th day	14th day	28th day
f_c' (MPa)	52.4	59.2	65.4
$E_{c,\,test}$ (MPa)	27430	29608	30717
$E_{c,\,KDS}$ (MPa)	31794	33126	34246
$E_{c,\,test}$ / $E_{c,\,KDS}$	0.86	0.89	0.90

3.3 Test Results for Flexural Strength of Concrete

The flexural strength specimens were manufactured in a size of (100×100×400) mm, and tests were performed on the 7th, 14th, and 28th of the age [14]. Table 3-4 and Figure 3-3 show the test results.

Table 3-4 Flexural strength of concrete (7, 14, 28 days) (MPa)

No.	Age		
	7th day (f_c' = 50.5 MPa)	14th day (f_c' = 58.0 MPa)	28th day (f_c' = 64.2 MPa)
1st	5.90	6.40	6.00
2nd	6.00	5.60	5.60
3rd	5.10	6.00	6.30
4th	5.80	6.20	6.00
5th	6.30	5.60	6.40
Avg.	5.82	5.96	6.06
StDev.	0.44	0.36	0.31

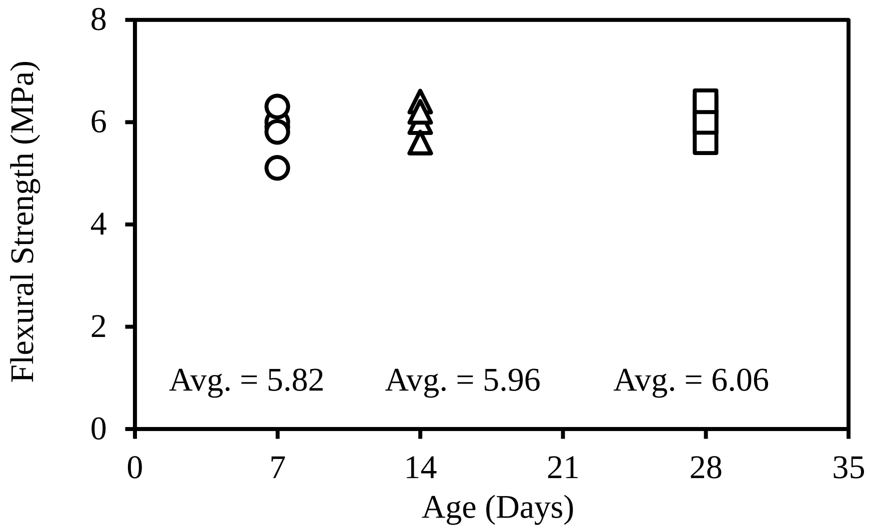

Figure 3-3 Flexural strength of concrete (7, 14, 28 days)

Table 3-5 and Figure 3-4 show the result of evaluating the experimental results of the flexural strength of concrete by the current KDS equation. The ratio of test results and current KDS equation was a range of 1.11 ~ 1.41, average was 1.25 and COV was 0.09. As a result, regardless of the aging date, the current KDS equation is evaluated to show the tendency of the flexural strength of geopolymer concrete. Therefore, it seems that there will be no difficulty in applying the current KDS equation.

Table 3-5 Comparison between flexural strength and current KDS

Age	Avg. f_c' (MPa)	$f_{r,\,KDS}$ (MPa)	$f_{r,\,test}$ (MPa)	$f_{r,\,test}$ / $f_{r,\,KDS}$
7	50.5	4.48	5.90	1.32
		4.48	6.00	1.34
		4.48	5.10	1.14
		4.48	5.80	1.29
		4.48	6.30	1.41
14	58.0	4.80	6.40	1.33
		4.80	5.60	1.17
		4.80	6.00	1.25
		4.80	6.20	1.29
		4.80	5.60	1.17
28	64.2	5.05	6.00	1.19
		5.05	5.60	1.11
		5.05	6.30	1.25
		5.05	6.00	1.19
		5.05	6.40	1.27

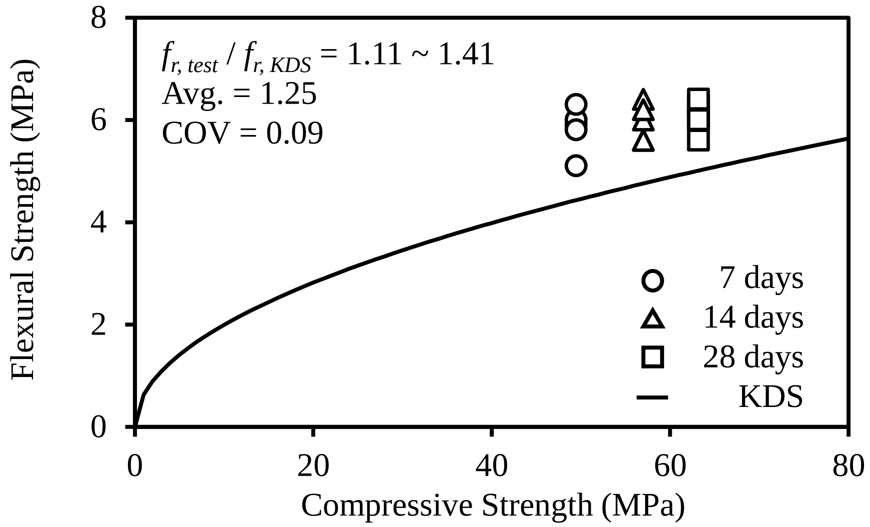

Figure 3-4 Comparison between flexural strength and current KDS

3.4 Test Results for Tensile Splitting Strength of Concrete

The tensile splitting strength specimens were manufactured in a size of Ø100×200 mm and Ø150×200 mm, and tests were performed on the 7th, 14th, and 28th of the age [15]. Table 3-6 and Figure 3-5 show the test results.

Table 3-6 Tensile splitting strength of concrete (7, 14, 28 days) (MPa)

No.	Age					
	7th day (f_c' = 50.5 MPa)		14th day (f_c' = 58.0 MPa)		28th day (f_c' = 64.2 MPa)	
	Ø100	Ø150	Ø100	Ø150	Ø100	Ø150
1st	4.8	4.0	5.3	5.0	5.6	5.6
2nd	4.5	4.8	5.4	5.1	5.6	5.4
3rd	4.9	4.7	5.5	4.8	4.9	6.1
4th	4.9	4.9	5.5	5.1	5.4	5.9
5th	5.3	4.9	5.3	5.5	5.7	4.5
Avg.	4.88	4.66	5.40	5.10	5.44	5.50
StDev.	0.29	0.38	0.10	0.25	0.32	0.62

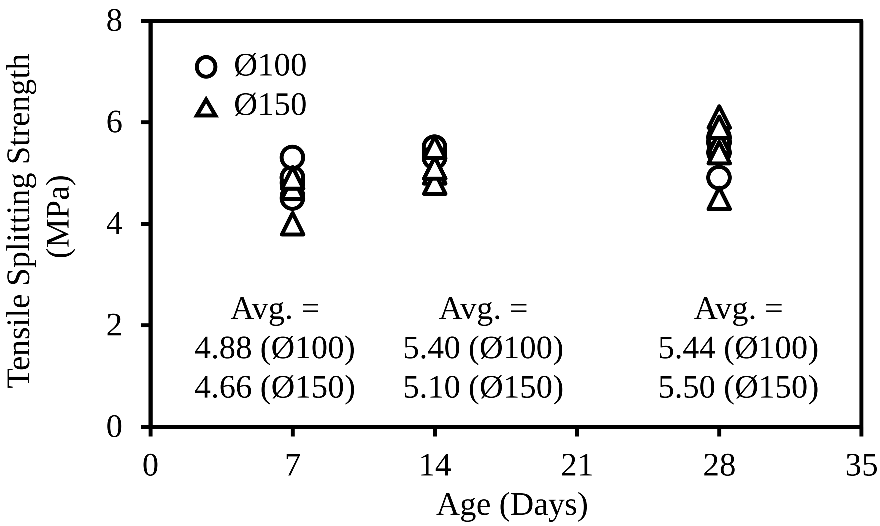

Figure 3-5 Tensile splitting strength of concrete (7, 14, 28 days)

There was no tensile splitting strength equation in KDS, so results were evaluated by foreign design code.

$$f_{tsp} = 0.59\sqrt{f_c'} \text{ (ACI 363R-92)} \quad (3\text{-}1)$$

$$f_{tsp} = 0.56\sqrt{f_c'} \text{ (ACI 318R-99)} \quad (3\text{-}2)$$

$$f_{tsp} = 0.3 f_c'^{\frac{2}{3}} \text{ (CEB-fib)} \quad (3\text{-}3)$$

where, f_{tsp} is tensile splitting strength.

Figure 3-6 show the comparison between tesile splitting strength and ACI equation. As a result, regardless of the aging date, the ACI equation is evaluated to show the tendency of the tensile splitting strength of geopolymer concrete.

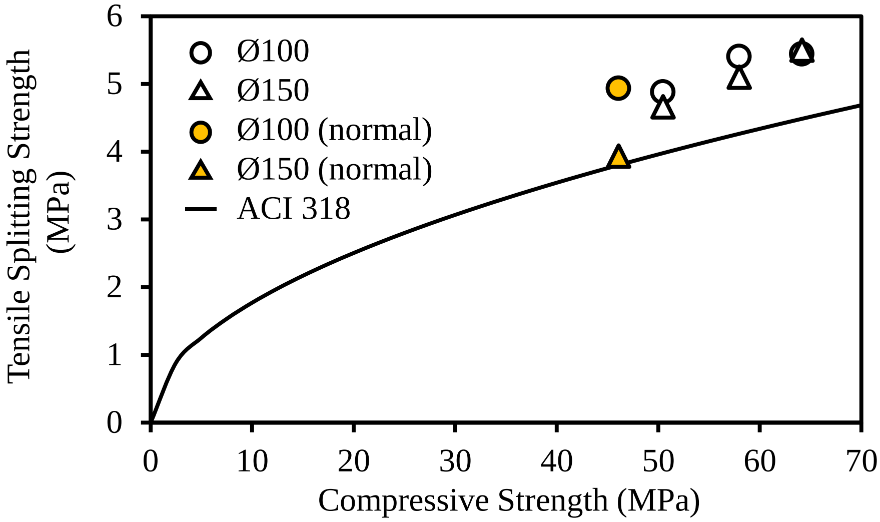

Figure 3-6 Comparison between tensile splitting strength and ACI

3.5 Discussion

In material test, the specimens were manufactured in accordance with KS F 2403 [12], and the compressive strength, flexural strength and tensile splitting strength were tested [13], [14], [15].

(1) In the test for compressive strength of concrete, a total of 70 specimens (55 of Ø100×200 mm and 15 of Ø150×300 mm) were performed for each aging date. As a result of the tests, the compressive strength was 21.6 MPa based on the 1st day of age, which allows PC members to be deformed, and the compressive strength on the 28th of age was 45 MPa or more, which is the design standard compressive strength.

(2) In the test for flexural strength of concrete, a total of 15 specimens (15 of (100×100×400) mm) were performed for each aging date. As a result of the tests, the flexural strength showed 1.11 to 1.41 times the current KDS 14 20 30: 2021 until the 28th of age. Therefore, the flexural strength of geopolymer concrete could be conservatively evaluated by the current KDS equation.

(3) In the test for tensile splitting strength of concrete, a total of 30 specimens (15 of Ø100×200 mm and 15 of Ø150×200 mm) were performed for each aging date. The tests were conducted by comparing the current specimen diameter Ø150 and the existing specimen diameter Ø100 [12]. Regardless of the size of the specimen, the tensile splitting strength of geopolymer concrete

could be conservatively evaluated by foreign design standard equation [17], [18], [20] on the 28^{th} of age.

In other words, the material test results of non-reduced concrete are considered to follow the equation of the design code.

Chapter 4. Flexural Test for Geopolymer Concrete Beams

4.1 Scope and Objectives

This test was planned to evaluate whether the flexural performance calcaulated by KDS 14 20 20: 2022 is satisfied for flexural failure, which is one of the main failure modes of the structure. In the flexural mode specimens, SD600 rebars were used for longitudinal reinforcement. Various reinforcement ratios from the minimum to maximum values were considered for test parameter. All specimens were designed to induce flexural yielding before shear failure.

4.2 Variables and Specimen Details

In the flexural tests, test variables are concrete types (normal concrete, geopolymer concrete), flexural rebar ratio (minimum, intermediate, maximum), cross-section, compressive strength of concrete and Table 4-1 shows test parameters. In specimen name, ‘F’ means flexural test specimen, ‘G’ and ‘N’ denote geopolymer concrete and normal concrete, respectively. F-N1 is a control specimen using normal concrete. F-G1, F-G2 and F-G3 are specimens with a flexural rebar ratio of 0.25% (minimum rebar ratio), 2.05% (maximum rebar ratio), and 0.98% (intermediate rebar ratio), respectively. In specimens F-G4 and F-G5, the beam height increased to h=700 mm. In specimen F-G6, higher strength of concrete, 60 MPa was considered due to longer concrete curing, 28 days. F-N1 and F-G3 are specimens with the same rebar ratio and details, and only different types of concrete. F-G6 is same with F-G3 with concrete type and rebar details. The concrete compressive strength of F-G6 is 60 MPa, which is considered in the actual site because it exceeds the design compressive strength of 45 MPa for 5 to 14 days when the PC members are shipped when aged on the 28th as described in the research plan.

Table 4-1 Variables of beam flexural tests

<table>
<tr><th>Variables</th><th>Speci mens</th><th>Length L (mm)</th><th>Shear span a (mm)</th><th>Height h (mm)</th><th>f_c'* (MPa)</th><th>Longit udinal bars</th><th>Rebar ratio (%)</th></tr>
<tr><td>Control Specimen (normal concrete)</td><td>F-N1</td><td rowspan="4">4000</td><td rowspan="4">1600</td><td rowspan="4">500</td><td rowspan="6">45</td><td>3-D25</td><td>0.98</td></tr>
<tr><td>Minimum rebar ratio</td><td>F-G1</td><td>2-D16</td><td>0.25</td></tr>
<tr><td>Maximum rebar ratio</td><td>F-G2</td><td>4-D32</td><td>2.05</td></tr>
<tr><td>Intermediate rebar ratio</td><td>F-G3</td><td>3-D25</td><td>0.98</td></tr>
<tr><td rowspan="2">Cross-section, Max. rebar ratio</td><td>F-G4</td><td rowspan="2">4800</td><td rowspan="2">2000</td><td rowspan="2">700</td><td>3-D32</td><td>1.06</td></tr>
<tr><td>F-G5</td><td>5-D32</td><td>1.76</td></tr>
<tr><td>Strength of concrete</td><td>F-G6</td><td>4000</td><td>1600</td><td>500</td><td>60</td><td>3-D25</td><td>0.98</td></tr>
</table>

*f_c'= 45 MPa (design compressive strength of geopolymer concrete, 5~14 days)
f_c'= 60 MPa (design compressive strength of geopolymer concrete, 28 days, strength difference according to age of same concrete)

Figure 4-1 shows the detail of beam flexural specimens. The rebar ratio and beam height are determined for the main variables to check flexural behavior of geopolymer concrete. The dimensions of F-N1, F-G1 ~ F-G3, F-G6 is 350 mm wide, 500 mm deep and the total length of sepcimens are 4,600 mm. F-G4 and F-G5 are specimens which increased depth, with a width of 350 mm, a depth of 700 mm, and a total length of 5,400 mm.

The minimum rebar ratio specimen F-G1 used 2-D16 (SD600) and intermediate rebar ratio specimen F-N1, F-G3, F-G6 used 3-D25 (SD600) for longitudinal bars. The maximum rebar ratio specimen F-G2 used 4-D32 (SD600). F-G4 and F-G5 used 3-D32, 5-D32 (SD600) for bottom longitudinal bars. For the shear reinforcement, D13 bars were used for transverse rebar at a spacing of 100-200 mm, and the V_n/V_m (nominal shear strength/shear force due to the beam flexural strength) was designed to be greater than 1. Table 4-2 shows design results of specimens.

To prevent local damage to the loading point and the reaction point during the test, transverse reinforcement was placed at spacings of 50 mm at the loding and reaction point.

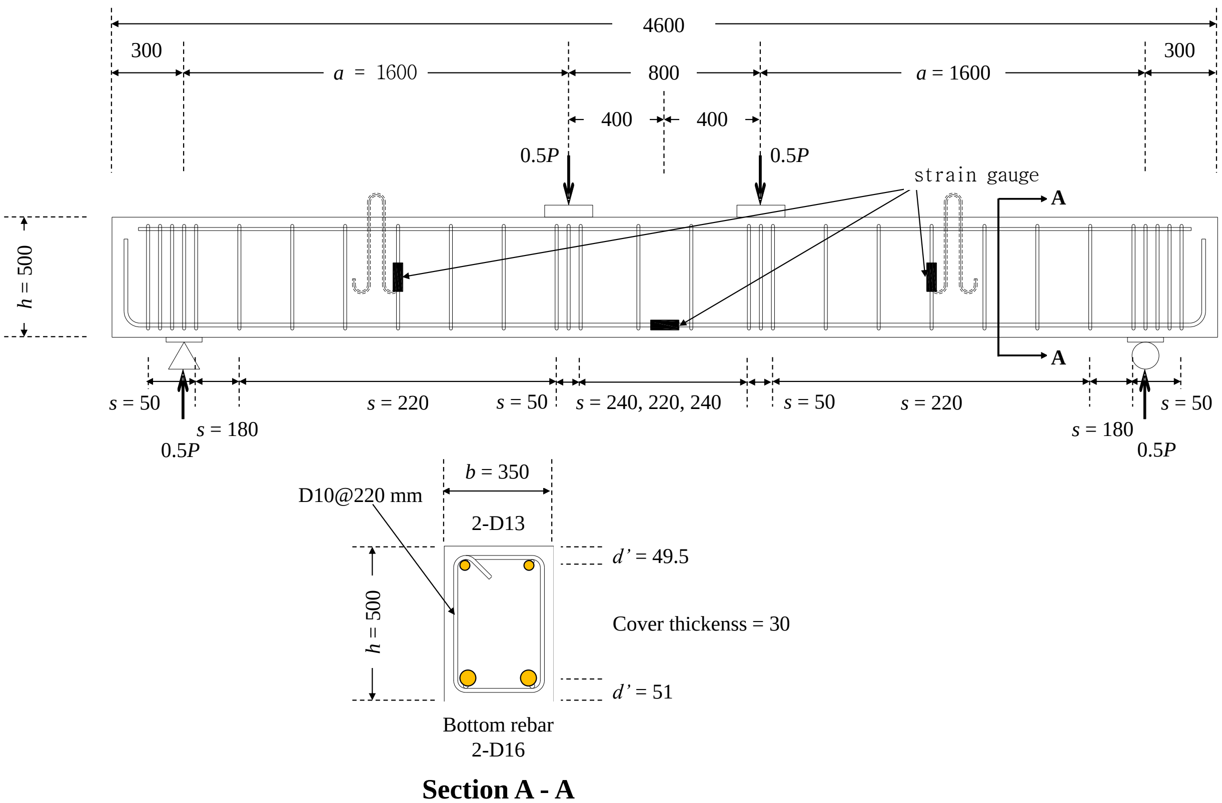

Figure 4-1 Flexural specimen detail (F-G1) (unit: mm)

Table 4-2 Design results of beam flexural tests

Specimens	Longitudinal bars	Rebar ratio (%)	a/d	Transverse bars	Spacing s (mm)	V_m (kN)	V_n (kN)	V_n/V_m
F-N1	3-D25	0.98%	3.60	SD500 D13	150	231.4	549.3	2.35
F-G1	2-D16	0.25%	3.56		220	65.8	434.2	6.63
F-G2	4-D32	2.05%	3.63		100	444.8	731.2	1.67
F-G3	3-D25	0.98%	3.60		150	233.2	549.3	2.35
F-G4	3-D32	1.06%	3.12		150	420.3	792.2	1.90
F-G5	5-D32	1.76%	3.12		100	662.5	1062.8	1.62
F-G6	3-D25	0.98%	3.60		150	236.3	576.2	2.41

V_m = Shear force due to the beam flexural strength(M_n)
V_n = Nominal shear strength

To measure the strain of rebar during the tests, 3 to 5 gauges were attached for each specimen. A total of three were attached by attaching one to the center of the bottom longitudinal bars, one to the transverse bar located in the center of the left and right shear span, respectively. F-G2 and F-G5 were measured with a total of 4 and 5 gauges by attaching 2 and 3 to the bottom longitudinal bars, respectively.

4.3 Test Setup

Figure 4-2 shows the setup for loading. 1500 kN actuator was used for the 4 points loading. During the test, the strain of the bottom rebars, load and displacement were measured in real time using a data logger. Loading was applied at a speed of 1 to 2 mm/min, and increased to speed of 4 to 8 mm/min after yielding of longitudinal bars.

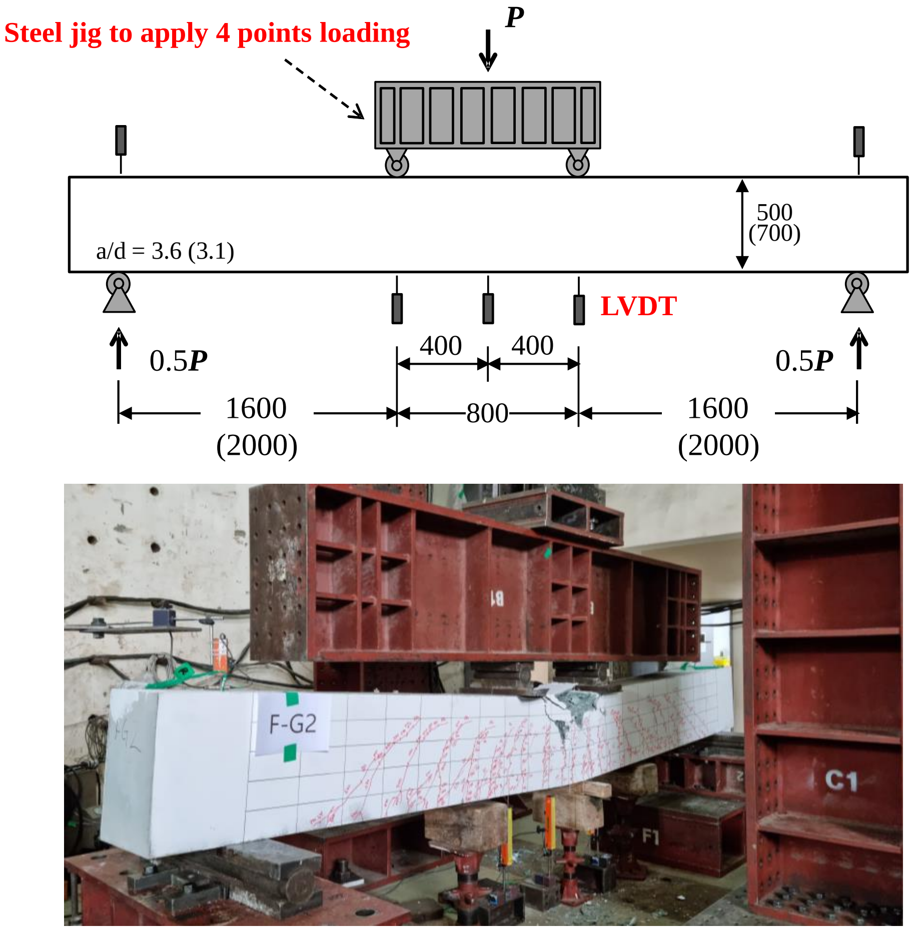

Figure 4-2 Beam flexural test setup (unit: mm)

4.4 Material Tests

The concrete of beam specimens was poured in each group for 9 days. When pouring concrete specimens, 15 for compressive strength tests (Ø100×200 mm), 6 for flexural strength tests (100×100×400 mm), and a total of 12 for tensile splitting strength tests (Ø100×200 mm, Ø150×200 mm, 6 each) were manufactured according to KS F 2403. Compressive strength specimens were manufactured in all groups, flexural strength specimens were manufactured only in the flexural test group, and tensile splitting strength specimens were manufactured in the shear and lap splice test groups. Table 4-3 shows the composition of specimens by beam group and the number of specimens manufactured by each group.

Table 4-3 Composition of specimens by beam group

Group	Beam specimens	Specimens (ea)		
		Compressive	Flexural	Tensile splitting
Group 1	F-G1, F-G2, F-G3, F-G4, F-G5	15	6	0
Group 2	S-G1, S-G2, S-G3, S-G4	15	0	12
Group 3	S-G9, S-G10, S-G11, S-G12	15	0	12
Group 4	L-G3, L-G4, L-G6, L-G7, L-G8, L-G9	15	0	12
Group 5	L-G1, L-G2, L-G5, L-G10	15	0	12
Group 6 (normal)	F-N1, S-N1, L-N1, L-N2	15	6	12
Group 7 (28 days)	S-G5, S-G6, S-G7, S-G8	15	0	12
Group 8 (28 days)	L-G11, L-G12, F-G6	15	6	12
Total	34 beams	120	18	84

On the day of beam tests, the compressive, flexural and tensile splitting strength tests were performed for each group in accordance with KS F 2405, KS F 2408, and KS F 2423, respectively, and the results of each group are shown as Table 4-4 ~ 4-6. The tests for compressive strength of concrete were performed as shown in Figure 4-3. The tests were performed at a speed of 0.4 MPa/s by applying load control according to KS F 2405, and the strain was measured by attaching concrete gauges to the left and right sides of the specimens.

(a) Before test

(b) After test

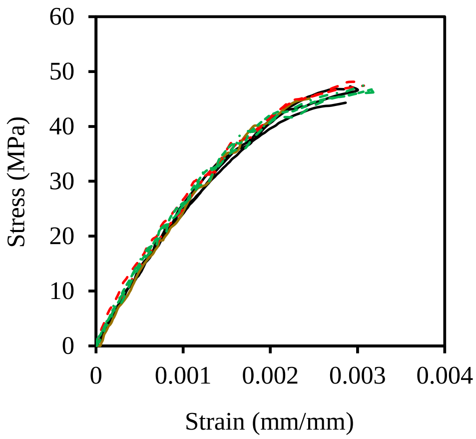

(c) Test result (s-s curve)

Figure 4-3 Test for compressive strength of concrete specimens

Table 4-4 Results of concrete compressive strength test by beam group

Group	∅100×200mm specimen				avg. f_c'
	1st	2nd	3rd	4th	
Group 1	51.1	48.5	50.4	50.3	50.1
Group 2	47.4	45.4	48.1	-	47.0
Group 3	42.9	43.4	41.4	43.3	42.7
Group 4	42.8	43.2	44.0	43.9	43.5
Group 5	46.4	47.9	46.8	-	47.0
Group 6 (normal)	44.3	47.3	46.8	-	46.1
Group 7 (28 days)	60.4	59.2	58.1	63.2	60.2
Group 8 (28 days)	61.6	63.6	57.8	60.1	60.8

Table 4-5 Results of concrete flexural strength test by beam group

Group	f_c'	100×100×400 mm specimen			avg. f_r
		1st	2nd	3rd	
Group 1	50.1	6.43	7.76	6.95	7.05
Group 6 (normal)	46.1	5.22	5.08	6.62	5.64
Group 8 (28 days)	60.8	7.47	8.44	7.69	7.87

Table 4-6 Results of concrete tensile splitting strength test by beam group

Group	f_c'	∅100×200mm specimen					∅150×200mm specimen				
		1st	2nd	3rd	4th	avg. f_{tsp}	1st	2nd	3rd	4th	avg. f_{tsp}
Group 2	47.0	5.01	4.46	4.81	-	4.76	4.40	3.85	3.53	-	3.93
Group 3	42.7	4.71	5.37	4.91	-	5.00	3.94	4.30	4.01	-	4.08
Group 4	43.5	4.78	4.69	4.90	-	4.79	3.94	3.99	3.97	-	3.97
Group 5	47.0	5.48	5.39	5.03	-	5.30	4.42	4.43	4.91	-	4.58
Group 6 (normal)	46.1	4.72	4.82	5.26	-	4.93	3.81	3.76	4.23	-	3.93
Group 7 (28 days)	60.2	6.46	5.21	5.24	5.89	5.70	4.86	5.01	5.37	5.31	5.14
Group 8 (28 days)	60.8	6.45	6.49	5.55	6.22	6.18	5.03	5.23	5.12	5.22	5.15

The stirrups used in the flexural beam tests were D13 rebars and longitudinal rebars were D16, D25, and D32 rebars, and 4 steel specimens of 600 mm length (700 mm for D32 rebars) were manufactured for each diameter. The steel tensile tests were performed in accordance with KS B 0802 as shown in Figure 4-4. The tests were performed at a speed of 2 ~ 4 mm/s by applying displacement control, and the strain was measured by attaching a rebar gauge to the center of the specimens. SD500 steel was used for D13 rebars and SD600 steel was used for D16, D25, and D32 rebars. The results of the steel tensile test are shown in Table 4-7 and Figure 4-5.

(a) Before test (b) Tensile failure (c) After test

Figure 4-4 Steel tensile test

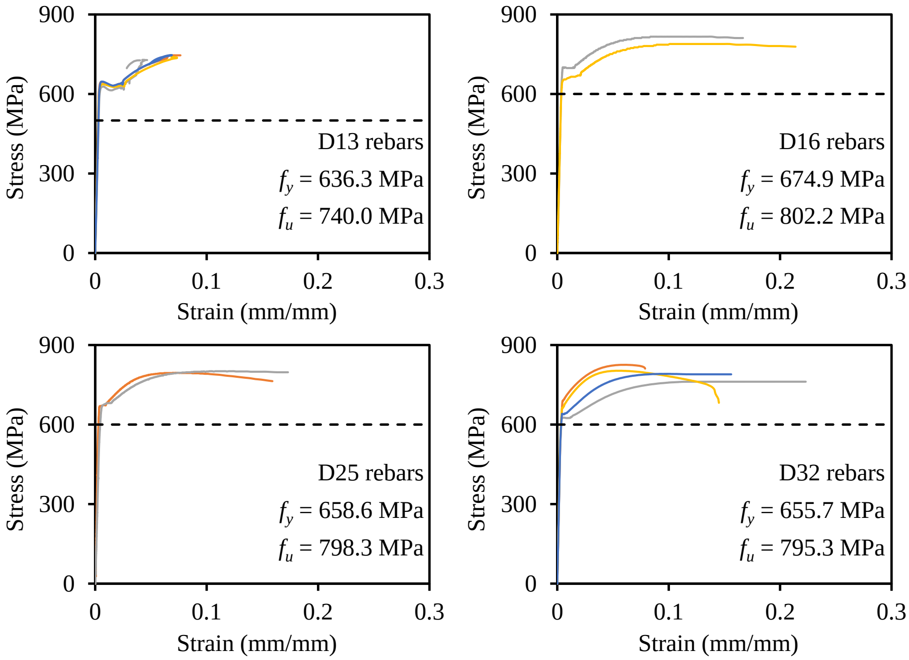

* Dotted line : Nominal yield strength

Figure 4-5 Results of the steel tensile test (flexural test)

Table 4-7 Results of the steel tensile test (flexural test)

Diameter	Yield strength, f_y (MPa)	Tensile strength, f_u (MPa)
D13	636.3	740.0
D16	674.9	802.2
D25	658.6	798.3
D32	655.7	795.3

4.5 Test Results

A total of 7 flexural tests were performed. The compressive strength of concrete specimens was 50.1 MPa and 46.1 MPa, respectively, and the tests were performed at the design strength of 45 MPa.

Figure 4-6 shows moment-deflection relationships of flexural test specimens. A horizontal dotted line represents nominal strength which was calculated using equivalent stress block method specified in current design code KDS. A triangular mark represents rebar yielding point and a circular mark represents peak bending moment.

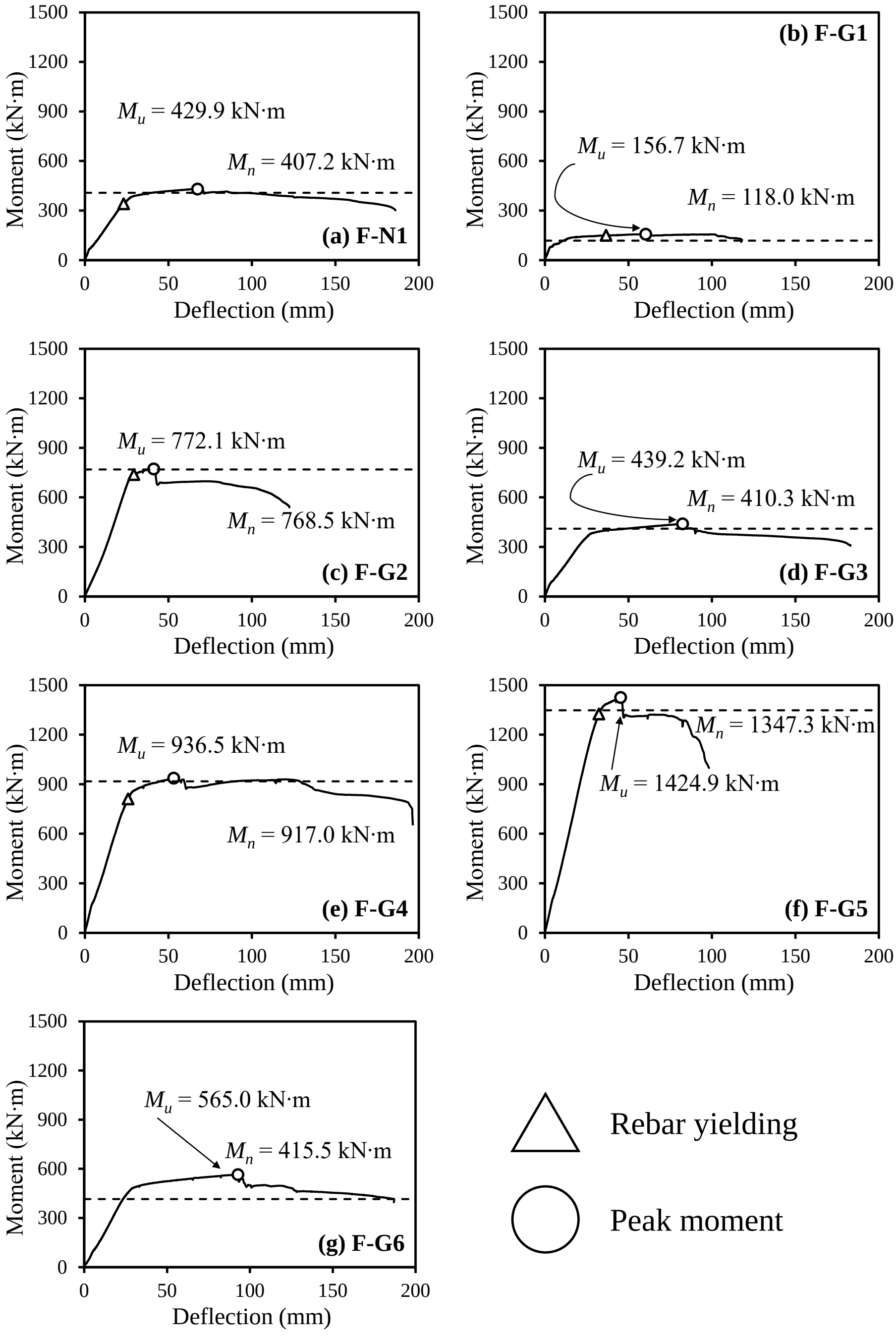

Figure 4-6 Moment-deflection relationships of specimens

The peak moment of F-N1 is 429.9 kN·m (Figure 4-6 (a)). F-N1 is a control specimen using normal concrete. A nominal strength which was calculated using equivalent stress block method specified in current design code KDS is 407.2 kN·m. The current design code safely predicted the test results, peak moment/nominal moment is 1.06.

$$a = \frac{A_s f_y}{0.85\eta f_c' b} = \frac{1520.1\times658.6}{0.85\times0.984\times45.25\times350} = 75.6\text{mm} \tag{4-1}$$

$$M_n = A_s f_y\left(d-\frac{a}{2}\right) = 1520.1\times658.6\left(444.5-\frac{75.6}{2}\right) = 407.2\text{kN·m} \tag{4-2}$$

where η is coefficient of equivalent stress block (=1.0 for 40MPa, 0.95 for 60MPa); a is depth of equivalent stress block; A_s is cross-section area of the rebar; f_y is yield strength of rebar; f_c' is compressive strength of concrete; b is beam width and d is effective depth.

The peak moment of F-G1 is 156.7 kN·m (Figure 4-6 (b)). F-G1 is a minimum rebar ratio specimen using geopolymer concrete. A nominal strength which was calculated using equivalent stress block method specified in current design code KDS is 118.0 kN·m. The current design code safely predicted the test results, peak moment/nominal moment is 1.33.

$$a = \frac{A_s f_y}{0.85\eta f_c' b} = \frac{397.1\times675.5}{0.85\times0.97\times50.1\times350} = 18.6\text{mm} \tag{4-3}$$

$$M_n = A_s f_y \left(d - \frac{a}{2}\right) = 397.1 \times 675.5 \left(449 - \frac{18.6}{2}\right) = 118.0\text{kN}\cdot\text{m} \tag{4-4}$$

The peak moment of F-G2 is 772.1 kN·m (Figure 4-6 (c)). F-G2 is a maximum rebar ratio specimen using geopolymer concrete. A nominal strength which was calculated using equivalent stress block method specified in current design code KDS is 768.5 kN·m. The current design code safely predicted the test results, peak moment/nominal moment is 1.00.

$$a = \frac{A_s f_y}{0.85 \eta f_c' b} = \frac{3176.9 \times 655.7}{0.85 \times 0.97 \times 50.1 \times 350} = 144.1\text{mm} \tag{4-5}$$

$$M_n = A_s f_y \left(d - \frac{a}{2}\right) = 3176.9 \times 655.7 \left(441 - \frac{144.1}{2}\right) = 768.5\text{kN}\cdot\text{m} \tag{4-6}$$

The peak moment of F-G3 is 439.2 kN·m (Figure 4-6 (d)). F-G3 is a intermediate rebar ratio specimen using geopolymer concrete. A nominal strength which was calculated using equivalent stress block method specified in current design code KDS is 410.3 kN·m. The current design code safely predicted the test results, peak moment/nominal moment is 1.07.

$$a = \frac{A_s f_y}{0.85 \eta f_c' b} = \frac{1520.1 \times 658.6}{0.85 \times 0.97 \times 50.1 \times 350} = 69.3\text{mm} \tag{4-7}$$

$$M_n = A_s f_y \left(d - \frac{a}{2}\right) = 1520.1 \times 658.6 \left(444.5 - \frac{69.3}{2}\right) = 410.3\text{kN}\cdot\text{m} \tag{4-8}$$

The peak moment of F-G4 is 936.5 kN·m (Figure 4-6 (e)). F-G4 is a intermediate rebar ratio specimen using geopolymer concrete and the beam height increased to h = 700 mm. A nominal strength which was calculated using equivalent stress block method specified in current design code KDS is 917.0 kN·m. The current design code safely predicted the test results, peak moment/nominal moment is 1.02.

$$a = \frac{A_s f_y}{0.85\eta f_c{}'b} = \frac{2382.7\times655.7}{0.85\times0.97\times50.1\times350} = 108.1\text{mm} \tag{4-9}$$

$$M_n = A_s f_y\left(d-\frac{a}{2}\right) = 2382.7\times655.7\left(641-\frac{108.1}{2}\right) = 917.0\text{kN·m} \tag{4-10}$$

The peak moment of F-G5 is 1424.9 kN·m (Figure 4-6 (f)). F-G5 is a maximum rebar ratio specimen using geopolymer concrete and the beam height increased to h = 700 mm. A nominal strength which was calculated using equivalent stress block method specified in current design code KDS is 1347.3 kN·m. The current design code safely predicted the test results, peak moment/nominal moment is 1.06.

$$a = \frac{A_s f_y}{0.85\eta f_c{}'b} = \frac{3971.1\times655.7}{0.85\times0.97\times50.1\times350} = 180.1\text{mm} \tag{4-11}$$

$$M_n = A_s f_y\left(d-\frac{a}{2}\right) = 3971.1\times655.7\left(607.5-\frac{180.1}{2}\right) = 1347.3\text{kN·m} \tag{4-12}$$

The peak moment of F-G6 is 560.9 kN·m (Figure 4-6 (g)). F-G6 is a specimen that was poured on the same day as F-G3 and tested after aging on the 28 days. Rebar detail is same with F-N1 and F-G3. A nominal strength which was calculated using equivalent stress block method specified in current design code KDS is 415.5 kN·m. The current design code safely predicted the test results, peak moment/nominal moment is 1.36.

$$a = \frac{A_s f_y}{0.85 \eta f_c' b} = \frac{1520.1 \times 658.6}{0.85 \times 0.95 \times 60.1 \times 350} = 59.0\text{mm} \tag{4-13}$$

$$M_n = A_s f_y \left(d - \frac{a}{2}\right) = 1520.1 \times 658.6 \left(444.5 - \frac{59.0}{2}\right) = 415.5\text{kN·m} \tag{4-14}$$

In all tests, the peak strength was greater than the nominal strength calculated by the equivalent stress block method specified in current design code KDS. Especially, when comparing F-N1 (normal concrete), F-G3 (geopolymer concrete), and F-G6 (geopolymer concrete, 28 days aging) which have the same details, the test results of normal and geopolymer concrete showed the same results in terms of strength and ductility.

Figure 4-7 compares the measured peak strength and nominal strength of all specimens. y=x graph is baseline and the result above the baseline indicates the measured peak strength is greater than nominal strength. All specimens are located above the baseline. The current design code safely predicted the test results, showing the average value of M_u/M_n = 1.13 and COV. = 0.13.

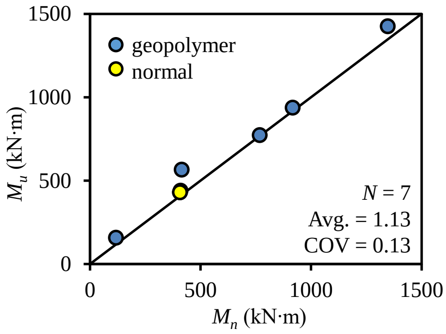

(a) KDS

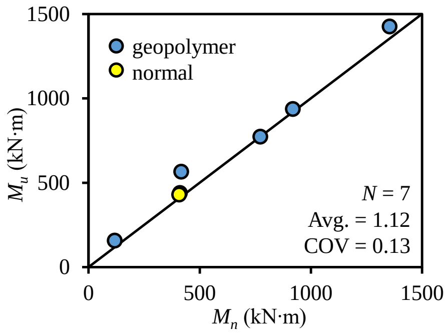

(b) ACI

Figure 4-7 Comparison between the peak and nominal moment (Flexural)

Table 4-8 summarizes the flexural test results for all specimens. In all specimens, M_u/M_n values are 1.00 to 1.36 and it means that they can be safely designed based on current design code KDS for all specimens. Also, there was no big difference compared to normal concrete specimens. In other words, the flexural rebar ratio (minimum, intermediate, maximum) and beam height (h = 500, 700 mm), which are the design variables considered in these tests, can be safely designed with the current strength equation in all specimens.

Table 4-8 Summary of flexural test results

Specimens	f_c' (MPa)	Flexural rebar ratio	h (mm)	M_u(kN-m)	M_n(kN-m)	M_u/M_n	Failure mode
F-N1	46.1	0.98%	500	429.9	407.2	1.05	Flexural
F-G1	50.1	0.25%	500	156.7	118.0	1.33	Flexural
F-G2	50.1	2.05%	500	772.1	768.5	1.00	Flexural
F-G3	50.1	0.98%	500	439.2	410.3	1.07	Flexural
F-G4	50.1	1.06%	700	936.5	917.0	1.02	Flexural
F-G5	50.1	1.76%	700	1424.9	1347.3	1.06	Flexural
F-G6	60.8	0.98%	500	565.0	415.5	1.36	Flexural

where f_c' is compressive strength of concrete specimens
h is beam height
M_n = nominal bending moment calculating equivalent stress block method (no reduction coefficient)
M_u is peak moment

4.6 Failure Mode

Figure 4-8 to Figure 4-14 show the failure mods of flexural test speicmens. All seven specimens failed due to concrete crushing and rebar yielding, showing typical flexural failure mode. Before rebar yielding, flexural cracks and diagonal tension cracks occurred at the bottom of the beam. After rebar yielding, flexural cracks increased and as the load increased, the upper concrete crushing within the load point, indicating the maximum load. The loading capacity gradually decreased as the depth of concrete crushing increased, and the test was end at 70% of the peak strength.

The test of F-N1 specimen ended by simultaneous fracture of 3 bottom longitudinal rebars at the 70% of the peak load as the concrete crushing became worse after the peak load, and Figure 4-8 shows the specimen after the cutting of the upper longitudinal rebars. The intermediate rebar ratio specimen, F-G3 (Figure 4-11) also ended by bottom rebar fracture. In other words, there was no difference between normal and geopolymer concrete and all flexural specimens showed typical flexural failure mode.

(a) Left shear span

(b) Right shear span

(c) Left shear span cross-section

(d) Right shear span cross-section

(e) Failure – Bottom longitudinal rebar fracture

Figure 4-8 Failure mode of F-N1


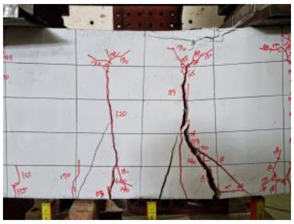


(a) Left shear span (b) Uniform *M* section (c) Right shear span

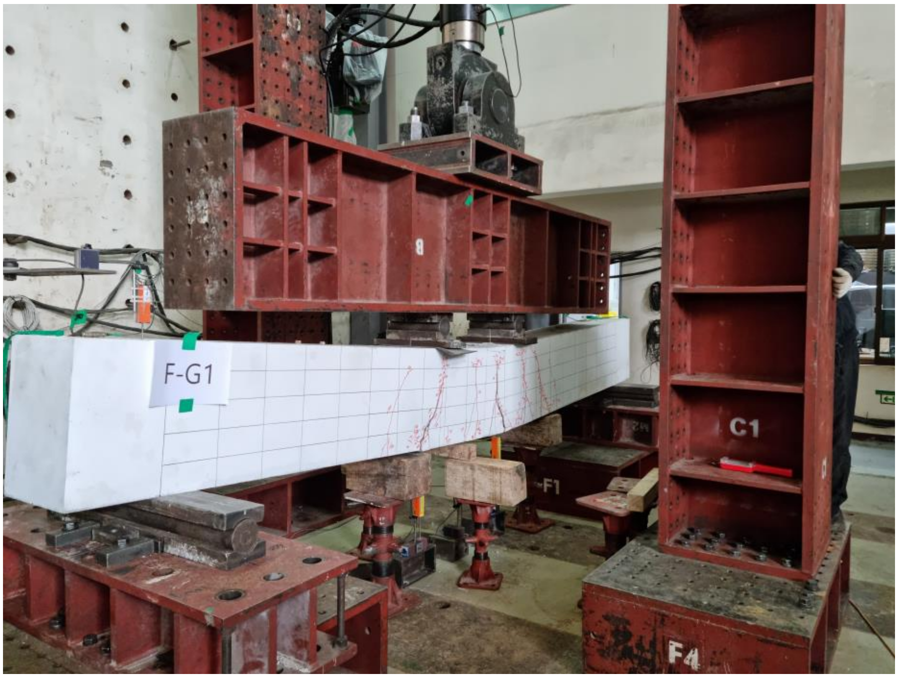

(d) Failure – Concrete collapse at right load point

Figure 4-9 Failure mode of F-G1

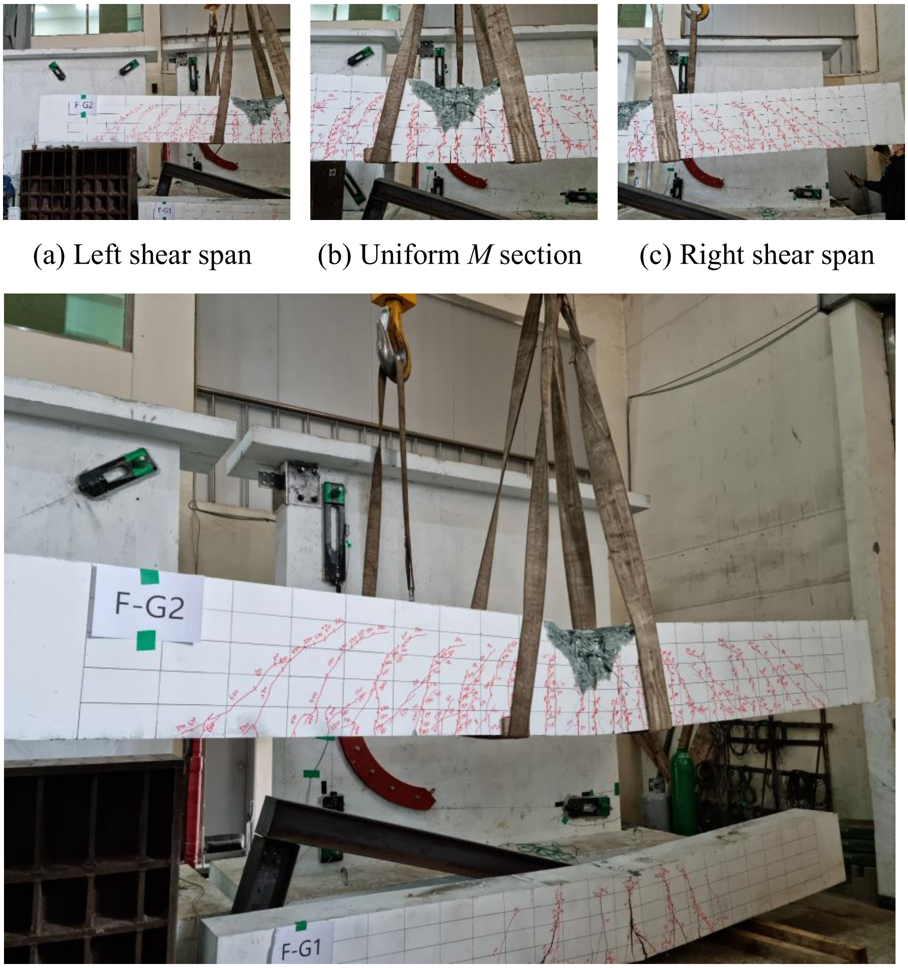

(a) Left shear span (b) Uniform *M* section (c) Right shear span

(d) Failure – Concrete collapse at right load point

Figure 4-10 Failure mode of F-G2

(a) Left shear span (b) Uniform *M* section (c) Right shear span

Failure – Concrete collapse at left load point

Figure 4-11 Failure mode of F-G3

(a) Left shear span

(b) Uniform M section

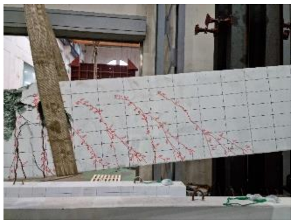

(c) Right shear span

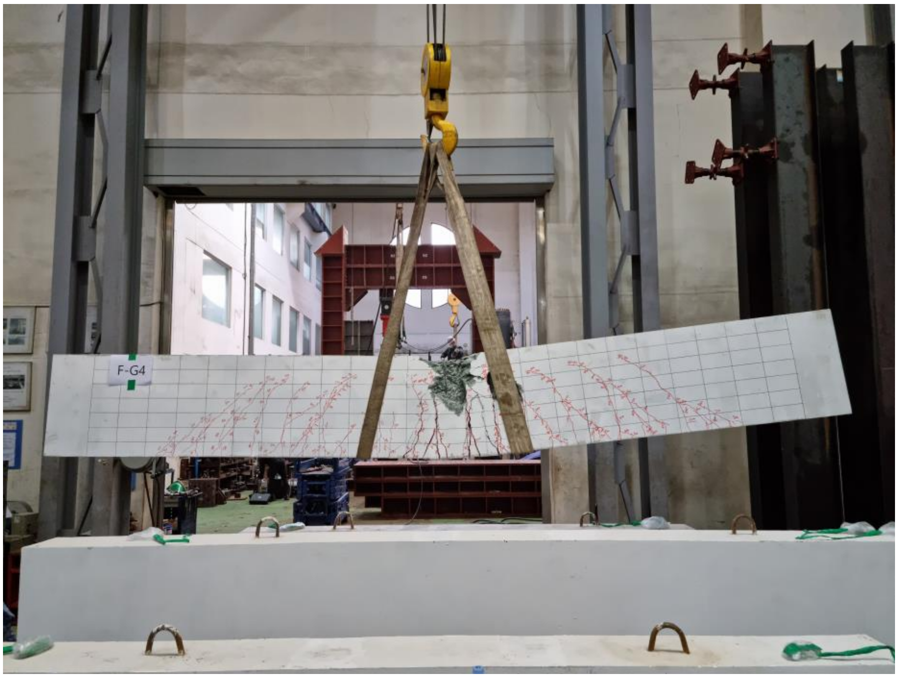

(d) Failure – Concrete collapse at right load point

Figure 4-12 Failure mode of F-G4

(a) Left shear span (b) Uniform M section (c) Right shear span

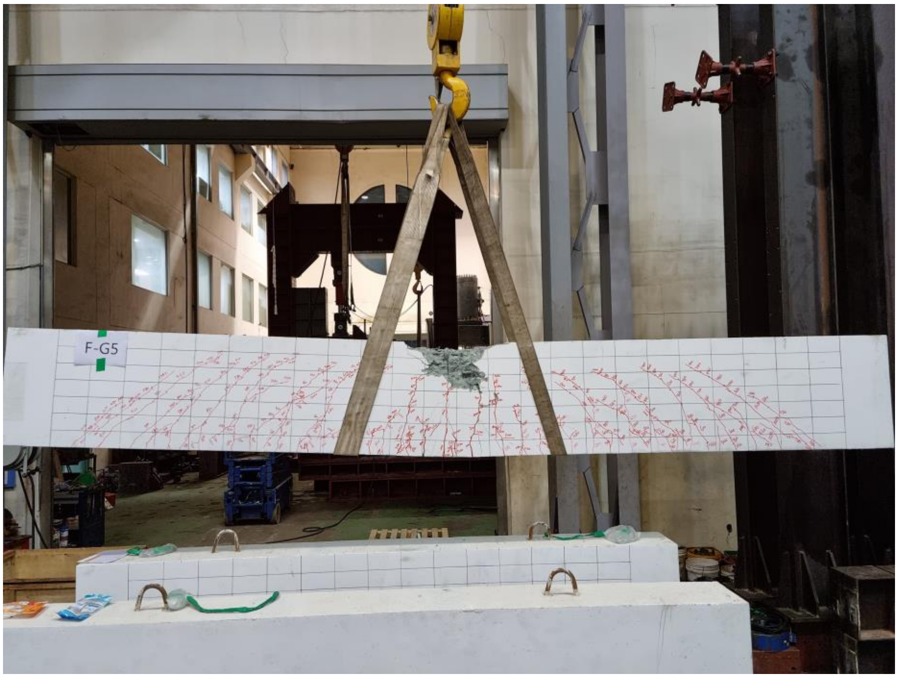

(d) Failure – Concrete collapse at right load point

Figure 4-13 Failure mode of F-G5

(a) Left shear span

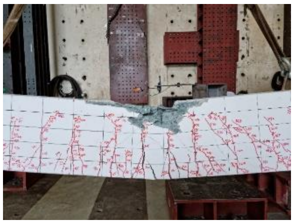

(b) Uniform M section

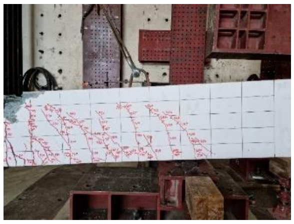

(c) Right shear span

(d) Failure – Concrete collapse at right load point

Figure 4-14 Failure mode of F-G6

Table 4-9 Approximate numbers and spacing of cracks (unit: ea, mm)

Specimens	Cracks	Left shear span	Mid span	Right shear span
F-N1	numbers	10	9 (collapse)	12
	spacing (avg.)	127.2	50	107.6
F-G1	numbers	4	9	5
	spacing (avg.)	120	80	100
F-G2	numbers	14	7	13
	spacing (avg.)	93.3	100	100
F-G3	numbers	13	13	11
	spacing (avg.)	85.7	57.1	116.6
F-G4	numbers	13	10	14
	spacing (avg.)	114.2	72.7	106.6
F-G5	numbers	17	10	16
	spacing (avg.)	111.1	72.7	117.6
F-G6	numbers	10	12	9
	spacing (avg.)	140	66.67	120

4.7 Strain of Longitudinal Bars

Figure 4-15 shows the longitudinal rebar strain for the mid span deflection. Specimen F-G3 and F-G6 could not be measured due to damage to the attached rebar gauge during manufacture. In all other specimens, the longitudinal rebar yielded near the peak strength.

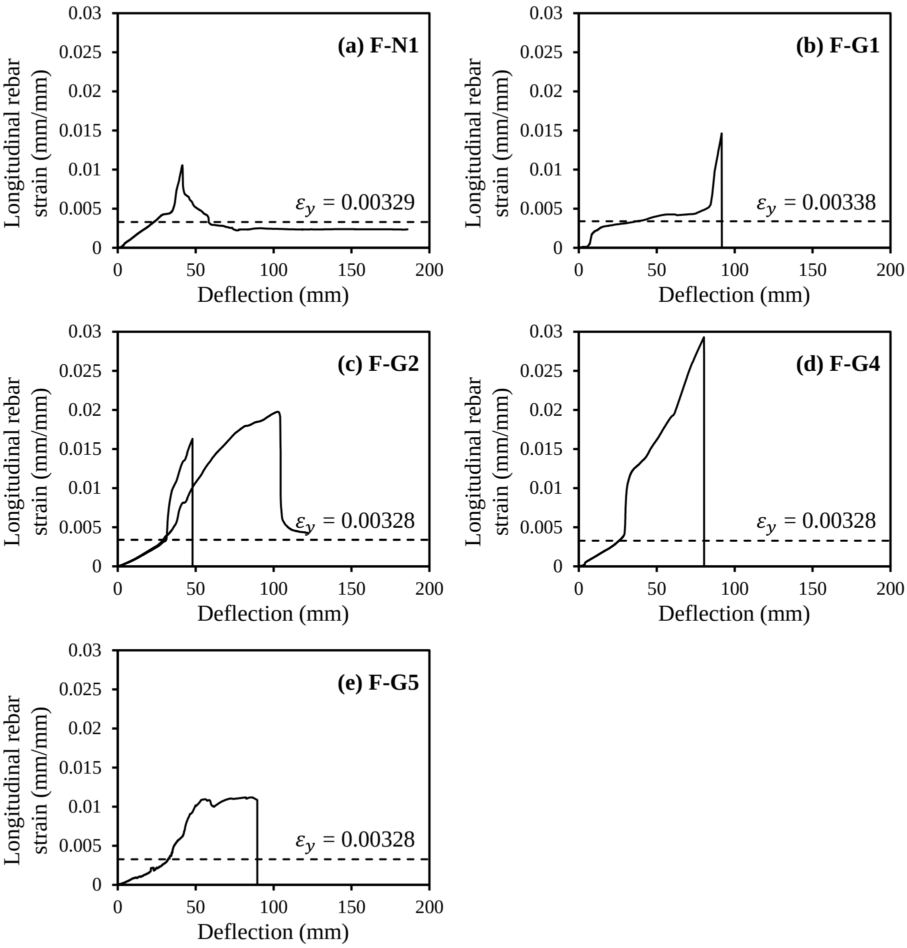

Figure 4-15 Longitudinal rebar strain

4.8 Discussion

In the flexural test, a four-point loading test was performed with a total of 7 members as variables such as rebar ratio (minimum, intermediate, maximum), depth of cross-section of the specimens (h = 500 mm, 700 mm), and compressive strength of concrete (45 MPa, 60 MPa). The longitudinal bar of the specimens was SD600 rebars, and the results showed greater than flexural strength calculated by KDS 14 20 20: 2022 at the design strength level of 45 MPa and the long-term strength of 60 MPa for the range from minimum rebar ratio (0.25%) to the maximum rebar ratio (2.0%). The ratio of the nominal strength to the experimental strength was 1.00 to 1.36, with an average of 1.13 and the coefficient of variation of 0.13, which can be reasonably predicted. All the flexural specimens showed typical flexural failure mode.

When comparing F-N1, a normal concrete specimen which is a control specimen, with F-G3, a specimen with the same cross-section and different materials, the ratio between the experimental strength and the nominal strength is very similar to 1.05 and 1.07. In the case of the failure modes of the two specimens, they were also equally failed by the fraction of the lower longitunidal rebars. The average spacing of cracks at the bottom of the mid-span of the two specimens was similar to 50 to 57.1 mm, and the maximum length of cracks was also similar to about 400 mm.

The Du et al. models are very similar to the models of this study. The settings and the compositions of experimental parameters are the same with this study. Comparing short-term siffness, moment at service condition, yield moment and ultimate moment with predictions using current code equation, the predictions agreed well with the test results. Especially, the prediction of equation overestimated the cracking moment of Du et al. model. Thus, the existing method for the comparison parameters except for the cracking moment can be applied to the AAC beams.

Chapter 5. Shear Test for Geopolymer Concrete Beams

5.1 Scope and Objectives

This test was planned to evaluate whether the shear performance calcaulated by KDS 14 20 22: 2022 is satisfied for shear failure, which is one of the main failure modes of the structure. The shear specimens using SD500 rebars as stirrups were tested with the spacing of stirrups, concrete strength, and shear span as variables. All specimens were induced to occur shear failure before flexural yield.

5.2 Variables and Specimen Details

In the shear tests, test variables are concrete types (normal concrete, geopolymer concrete), stirrup spacing, shear span-to-depth ratio (a/d), compressive strength of concrete and Table 5-1 shows test parameters. In specimen name, 'S' means shear test specimen, 'G' and 'N' denote geopolymer concrete and normal concrete, respectively. S-N1 is a control specimen using normal concrete and does not have stirrup. S-G1 is a specimen using geopolymer concrete and does not have stirrup, S-G2 to S-G4 are specimens using geopolymer concrete and have stirrups which spacing is 220 mm, 150 mm, 110 mm, respectively. All specimens used SD500 D10 rebar for stirrup.

In specimens S-G5 to S-G8, the rebar details of beams are same with S-G1 to S-G4, and concrete was poured on the same day. But higher strength of concrete, 60 MPa was considered due to longer concrete curing, 28 days. S-G9 to S-G12 are specimens that *a*/*d*, shear span ratio is 3.9 and the rebar details of beams are same with S-G1 to S-G4, only span length increased to 4,200 mm.

Figure 5-1 shows the detail of beam shear specimens. The spacing of stirrups are determined for the main variables to check shear behavior of geopolymer concrete. The span length between 2 loading points, the width of beams (b), the height of beams (h) is 800 mm, 350 mm, 500 mm, respectively for all specimens. The total length of specimens is 3,600 mm (a/d = 2.5) and 4,800 mm (a/d = 3.9), respectively. As an example, S-G1 and S-G4 in Figure 5-1 are specimens without stirrups and specimens with a stirrup spacing of 220 mm, respectively. They also have same cross-section detail.

Table 5-1 Variables of beam shear tests

<table>
<tr><th>Variables</th><th>Specimens</th><th>Length
L (mm)</th><th>Shear span
a (mm)</th><th>a/d</th><th>Height
h (mm)</th><th>f_c'*
(MPa)</th><th>Stirrup spacing
s
(mm)</th></tr>
<tr><td>Control Specimen
(normal concrete)</td><td>S-N1</td><td rowspan="9">3000</td><td rowspan="9">1100</td><td rowspan="9">2.5</td><td rowspan="13">500</td><td rowspan="5">45</td><td>-</td></tr>
<tr><td>a/d = 2.48</td><td>S-G1</td><td>-</td></tr>
<tr><td>D10 $d/2$ spacing</td><td>S-G2</td><td>220</td></tr>
<tr><td>D10 $d/3$ spacing</td><td>S-G3</td><td>150</td></tr>
<tr><td>D10 $d/4$ spacing</td><td>S-G4</td><td>110</td></tr>
<tr><td rowspan="4">Strength of concrete
(28 days curing)
based on
S-G1~G4</td><td>S-G5</td><td rowspan="4">60</td><td>-</td></tr>
<tr><td>S-G6</td><td>220</td></tr>
<tr><td>S-G7</td><td>150</td></tr>
<tr><td>S-G8</td><td>110</td></tr>
<tr><td rowspan="4">a/d = 3.9
based on
S-G1~G4</td><td>S-G9</td><td rowspan="4">4200</td><td rowspan="4">1700</td><td rowspan="4">3.9</td><td rowspan="4">45</td><td>-</td></tr>
<tr><td>S-G10</td><td>220</td></tr>
<tr><td>S-G11</td><td>150</td></tr>
<tr><td>S-G12</td><td>110</td></tr>
</table>

*f_c' = 45 MPa (design compressive strength of geopolymer concrete, 5~14 days)
f_c' = 60 MPa (design compressive strength of geopolymer concrete, 28 days, strength difference according to age of same concrete)

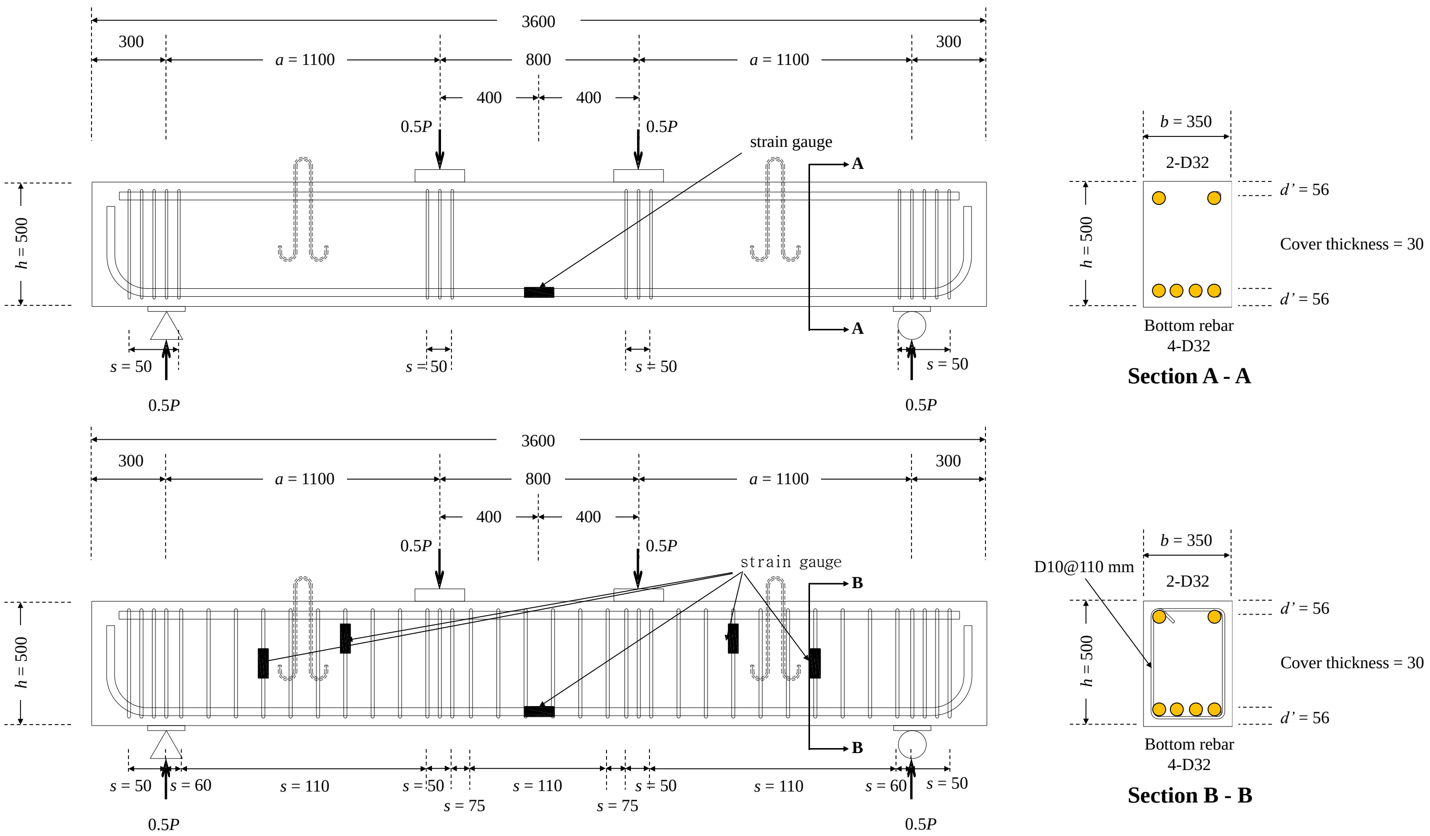

Figure 5-1 Shear specimen detail (S-G1, S-G4)

S-N1, S-G1 to S-G8 which are the specimens with a shear span-to-depth ratio a/d = 2.5, used 4-D32 (SD600) for longitudinal bars, and S-G9 to S-G12 specimens with a/d = 3.9 increased flexural strength by using 5-D32 (SD600) for longitudinal bars to induce shear failure. All stirrups are D10 (SD500).

Design results are shown as Table 5-2. All specimens induced shear failure. Therefore, (nominal shear strength/shear force causing flexural strength) was designed to be less than 1, and the design results were 0.25 to 0.95, all of which were less than 1, leading to shear failure.

To prevent local damage to the loading point and the reaction point during the test, transverse reinforcement was placed at spacings of 50 mm at the loding and reaction point.

To measure the strain of rebar during the tests, 1 to 5 gauges were attached for each specimen (see Figure 5-1). A total of five (six for 2-layers) were attached by attaching one to the center of the bottom longitudinal bars (two for 2-layers), two to the transverse bar located in the center of the left and right shear span, respectively.

Table 5-2 Design results of beam shear tests

Specimens	f_c' (MPa)	a/d	Longitudinal rebar ratio	Stirrup	Stirrup spacing s (mm)	V_c (kN)	V_s (kN)	V_n (kN)	V_m (kN)	V_n/V_m
S-N1	46.1	2.5	4-D32 (2.04%)	-	-	175.9	0.0	175.9	694.3	0.25
S-G1	47.0			-	-	177.6	0.0	177.6	696.7	0.25
S-G2				SD500 D10	220	177.6	160.0	337.6	696.7	0.48
S-G3					150	177.6	234.7	412.3	696.7	0.59
S-G4					110	177.6	320.0	497.6	696.7	0.71
S-G5	60.2			-	-	201.0	0.0	201.0	724.8	0.28
S-G6				SD500 D10	220	201.0	160.0	361.0	724.8	0.50
S-G7					150	201.0	234.7	435.7	724.8	0.60
S-G8					110	201.0	320.0	521.0	724.8	0.72
S-G9	42.7	3.9	5-D32 (2.56%)	-	-	160.1	0.0	160.1	485.0	0.33
S-G10				SD500 D10	220	160.1	160.0	311.5	485.0	0.64
S-G11					150	160.1	234.7	382.1	485.0	0.79
S-G12					110	160.1	320.0	462.8	485.0	0.95

*f_c' = compressive strength of geopolymer concrete on test day
V_n = nominal shear strength
V_m = shear force causing nominal moment M_n

5.3 Test Setup

Figure 5-2 shows the setup for loading. 1500 kN actuator was used for the 4 points loading. During the test, the strain of the rebars, load and displacement were measured in real time using a data logger. Loading was applied at a speed of 1 to 2 mm/min.

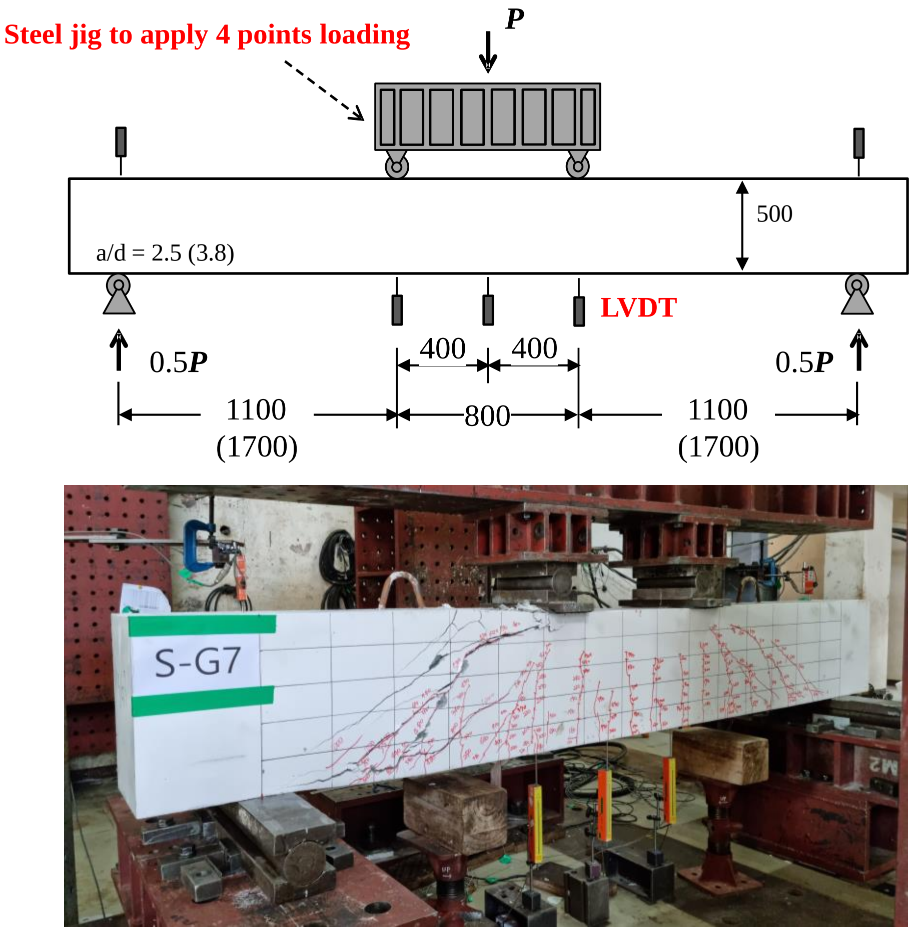

Figure 5-2 Beam shear test setup (unit: mm)

5.4 Material Tests

The concrete pouring, curing, and material test methods are the same as described in '**4.4 Material Tests**'. The shear test specimens correspond to group 2, 3, 6, and 7 in Table 4-3. The compressive strength of each specimen is shown in Table 5-3.

Table 5-3 Compressive strength of specimens

Group	Specimens	f_c' on test day (MPa)
2	S-G1, S-G2, S-G3, S-G4	47.0
3	S-G9, S-G10, S-G11, S-G12	42.7
6 (normal)	S-N1	46.1
7 (28 days)	S-G5, S-G6, S-G7, S-G8	60.2

Stirrups used for shear test were D10 rebars, longitudinal rebars were D32 rebars. 4 rebar specimens of 600 mm length were manufactured for D10, and 4 rebar specimens of 700 mm length were manufactured for D32, and tensile tests were performed. The test methods were the same as described in '**4.4 Material Tests**'. D10 rebars were SD500, and D32 rebars were SD600. The test results of steel tensile tests are shown in Table 5-4 and Figure 5-3.

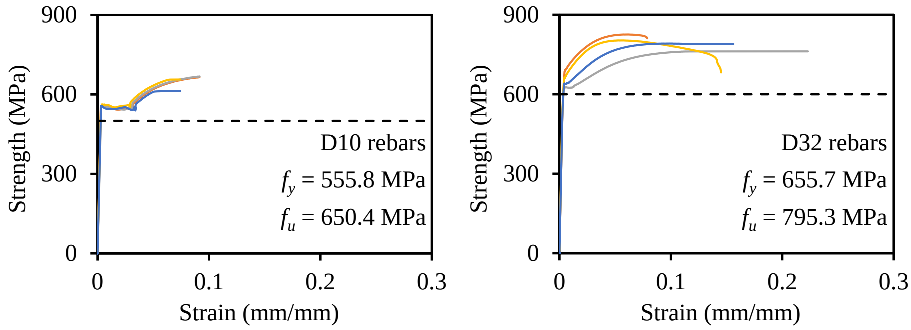

* Dotted line : Nominal yield strength

Figure 5-3 Results of the steel tensile test (shear test)

Table 5-4 Results of the steel tensile test (shear test)

Diameter	Yield strength, f_y (MPa)	Tensile strength, f_u (MPa)
D10	555.8	650.4
D32	655.7	795.3

5.5 Test Results

A total of 13 shear tests were performed. Figure 5-4 shows the shear force-deflection curve of S-N1, S-G1 to S-G4 which shear span-to-depth ratio is 2.5. Figure 5-5 shows the shear force-deflection curve of S-G5 to S-G8 which shear span-to-depth ratio is 2.5 and they are long-term curing specimens. Figure 5-6 shows the shear force-deflection curve of S-G9 to S-G12 which shear span-to-depth ratio is 3.9.

A horizontal dotted line represents nominal shear strength (V_n) which was calculated using current design code KDS and a circular mark represents peak shear strength (V_u). Some specimens (S-G8, S-G11, and S-G12) showed when the shear force was reached at the flexural strength by a dash-dotted line (V_m). These specimens are designed with V_n/V_m = 0.72 to 0.95, but their actual shear strength exceeds the nominal shear strength calculated by KDS, resulting in flexural failure.

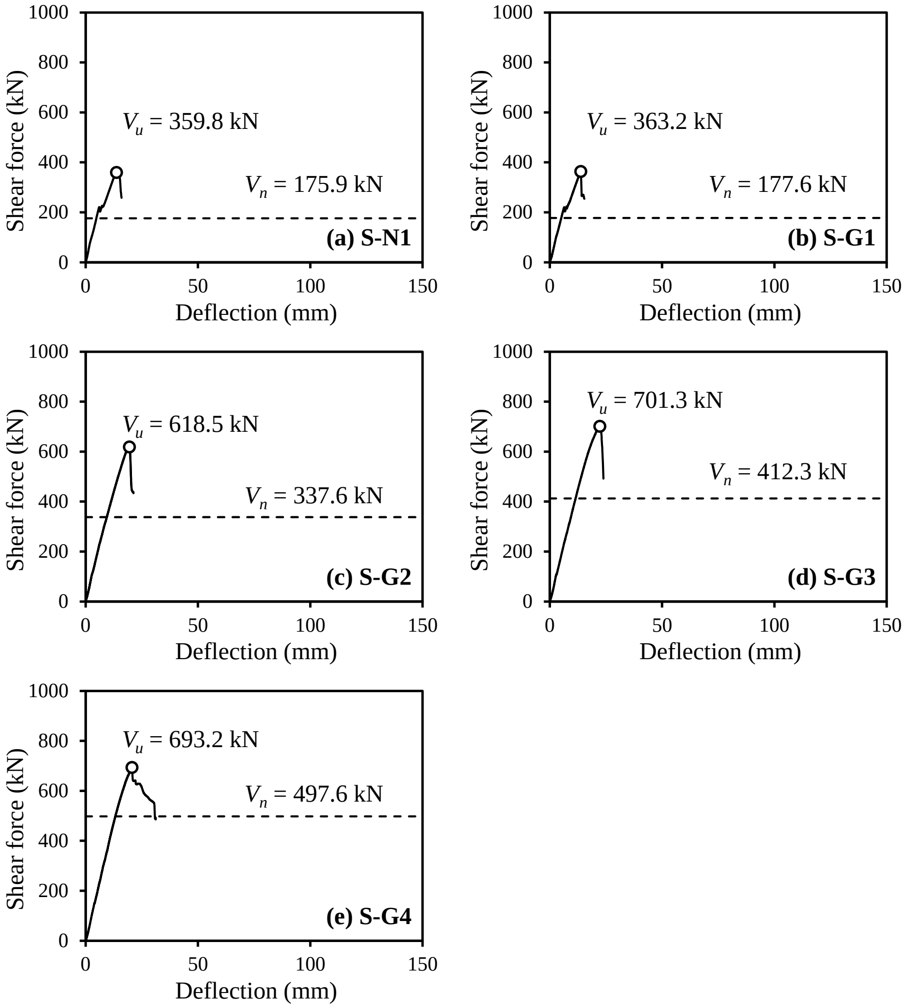

Figure 5-4 Shear force-deflection relationships of specimens

(a/d = 2.5, f_c' = 47.0 MPa (geopolymer concrete),

f_c' = 46.1 MPa (normal concrete))

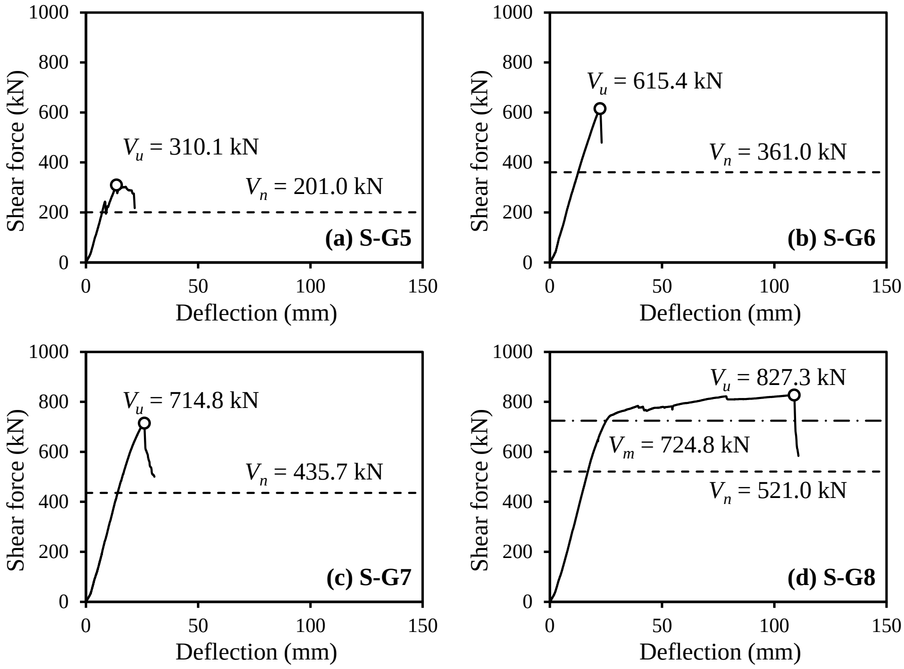

Figure 5-5 Shear force-deflection relationships of specimens

(aging 28 days, $a/d = 2.5$, $f_c' = 60.2$ MPa)

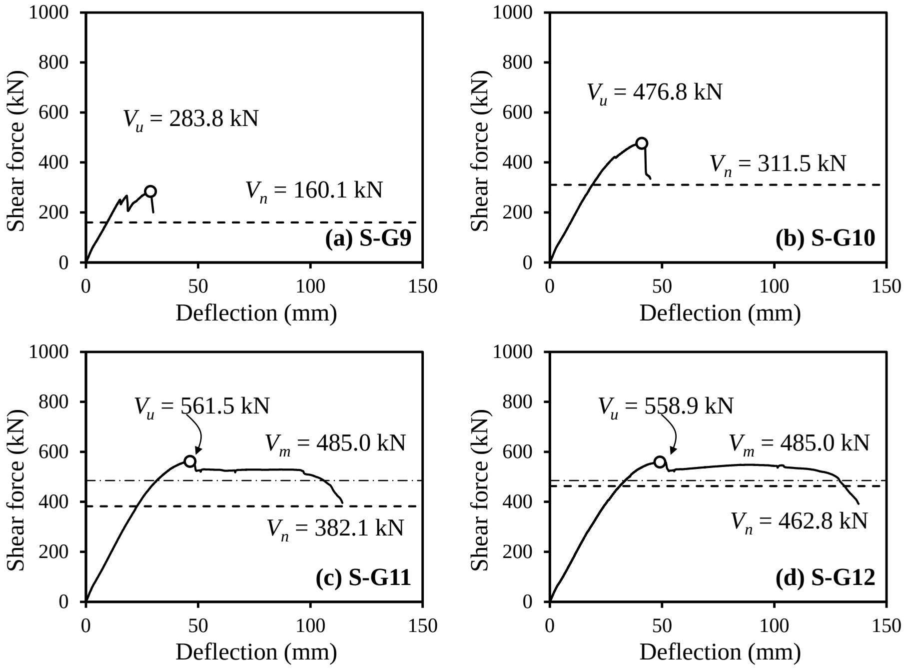

Figure 5-6 Shear force-deflection relationships of specimens

(a/d = 3.9, f_c' = 42.7 MPa)

The peak shear force of S-N1 is 359.8 kN (Figure 5-4 (a)). The nominal strength calculated by KDS is V_n = 175.9 kN. The peak shear force/nominal shear strength is 2.05. The peak shear force of S-G1 is 363.2 kN (Figure 5-4 (b)). The nominal shear strength is V_n = 177.6 kN, and the ratio between peak shear force and nominal shear strength is 2.05, which met the current code. The peak shear force of S-G2, the specimen which spacing of stirrup is 220 mm, was 618.5 kN (Figure 5-4 (c)) and the nominal strength is V_n = 337.6 kN. The peak force/nominal strength is 1.83 and it met the current code. The peak force of S-G3, the specimen which spacing of stirrup is 150 mm, was 701.3 kN

(Figure 5-4 (d)) and the nominal strength is V_n = 412.3 kN. The peak force/nominal strength is 1.70 and it met the current code. The peak force of S-G4, the specimen which spacing of stirrup is 110 mm, was 693.2 kN (Figure 5-4 (e)) and the nominal strength is V_n = 497.6 kN. The peak force/nominal strength is 1.39 and it met the current code.

The same results were found in S-G5 to S-G8, specimens that increased the aging date to 28 days, with the same rebar details as in S-G1 to S-G4. The peak shear force of S-G5 was 310.1 kN (Figure 5-5 (a)). The nominal shear strength is V_n = 201.0 kN and the ratio of peak shear force and nominal shear strength is 1.54, which met the current code. The peak shear force of S-G6, the specimen which spacing of stirrup is 220 mm, was 615.4 kN (Figure 5-5 (b)) and the nominal strength is V_n = 361.0 kN. The peak force/nominal strength is 1.70 and it met the current code. The peak force of S-G7, the specimen which spacing of stirrup is 150 mm, was 714.8 kN (Figure 5-5 (c)) and the nominal strength is V_n = 435.7 kN. The peak force/nominal strength is 1.64 and it met the current code. The peak force of S-G8, the specimen which spacing of stirrup is 110 mm, was 827.3 kN (Figure 5-5 (d)) and the nominal strength is V_n = 521.0 kN. The peak force/nominal strength is 1.59 and it met the current code.

Even in S-G9 to S-G12, all specimens that increased the shear span-to-depth ratio to 3.8, showed the strength greater than nominal strength. The peak shear force of S-G9 was 283.8 kN (Figure 5-6 (a)). The nominal shear strength is V_n = 160.1 kN and the ratio of peak shear force and nominal shear strength is 1.77, which met the current code. The peak shear force of S-G10, the specimen which spacing of stirrup is 220 mm, was 476.8 kN (Figure 5-6 (b)) and the nominal strength is V_n = 311.5 kN. The peak force/nominal strength is 1.53 and it met the current code. The peak force of S-G11, the specimen which spacing of stirrup is 150 mm, was 561.5 kN (Figure 5-6 (c)) and the nominal strength is V_n = 382.1 kN. The peak force/nominal strength is 1.47 and it met the current code. The peak force of S-G12, the specimen which spacing of stirrup is 110 mm, was 558.9 kN (Figure 5-6 (d)) and the nominal strength is V_n = 462.8 kN. The peak force/nominal strength is 1.21 and it met the current code.

Figure 5-7 compares the measured peak shear strength and nominal strength of all shear specimens. y=x graph is baseline and the result above the baseline indicates the measured peak strength is greater than nominal strength. All 13 normal and geopolymer concrete specimens are located above the baseline. The current design code safely predicted the test results, showing the average value of V_u/V_n = 1.65 and COV. = 0.145.

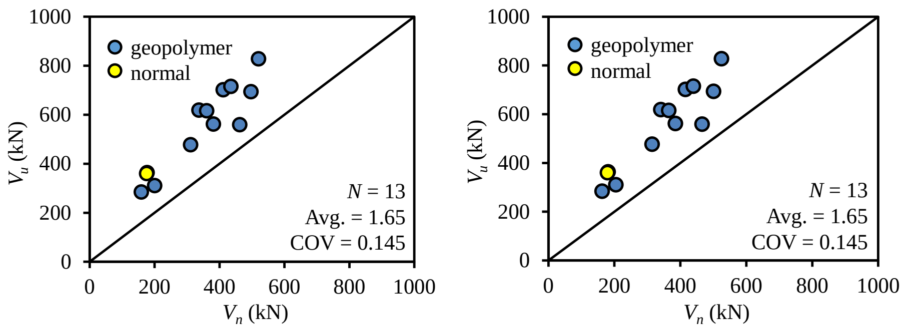

(a) KDS (b) ACI

Figure 5-7 Comparison between the test results and predictions (Shear)

Table 5-5 summarizes the shear test results for all specimens. In all specimens, V_u/V_n values are 1.21 to 2.05. Also, there was no big difference compared to normal concrete specimens.

Table 5-5 Summary of shear test results

Speci mens	f_c' (MPa)	a/d	Stirrups	Spacing s (mm)	V_u (kN)	V_n (kN)	V_u/V_n	Failure mode
S-N1	46.1	2.5	-	-	359.8	175.9	2.05	Shear
S-G1	47.0	2.5	-	-	363.2	177.6	2.05	Shear
S-G2	47.0	2.5	SD500 D10	220	618.5	337.6	1.83	Shear
S-G3	47.0	2.5	SD500 D10	150	701.3	412.3	1.70	Shear
S-G4	47.0	2.5	SD500 D10	110	693.2	497.6	1.39	Shear
S-G5	60.2	2.5	-	-	310.1	201.0	1.54	Shear
S-G6	60.2	2.5	SD500 D10	220	615.4	361.0	1.70	Shear
S-G7	60.2	2.5	SD500 D10	150	714.8	435.7	1.64	Shear
S-G8	60.2	2.5	SD500 D10	110	827.3	521.0	1.59	Flexural + Shear
S-G9	42.7	3.9	-	-	283.8	160.1	1.77	Shear
S-G10	42.7	3.9	SD500 D10	220	476.8	311.5	1.53	Shear
S-G11	42.7	3.9	SD500 D10	150	561.5	382.1	1.47	Flexural + Shear
S-G12	42.7	3.9	SD500 D10	110	558.9	462.8	1.21	Flexural + Shear

where f_c' is compressive strength of concrete specimens
V_n = nominal shear strength
V_u = peak shear force

In other words, the shear span-to-depth ratio (a/d = 2.5, 3.9), spancing of stirrups (no stirrup, s = 110 mm, 150 mm, 220 mm) and concrete strength, which are the design variables considered in these tests, can be safely designed with the current strength equation in all specimens.

5.6 Failure Mode

Figure 5-8 to Figure 5-20 shows failure mode of the shear specimens, respectively. Most specimens showed typical shear failure. The initial flexural crack spread to the shear span, followed by the angle of the crack being inclined and developed into a flexural-shear crack. After that, shear failure occurred due to diagonal cracks. The tests were finished because shear failure occurred, and the load decreased rapidly. There was no big difference between normal concrete specimen and geopolymer concrete specimen.

In some specimens (S-G8, S-G11, S-G12, Figure 5-16, Figure 5-19, Figure 5-20), the test results exceeded the shear strength (V_m) calculated by KDS as shown in the load-defelction curve. After that, at the peak load, concrete collapsed at the load point or at the center and behaved flexibly.

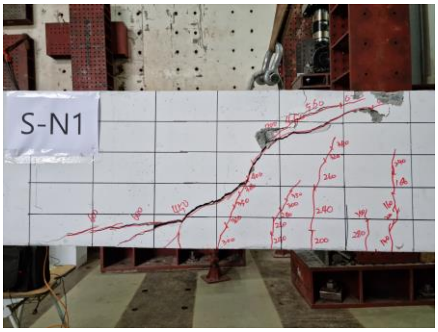

(a) Left shear span

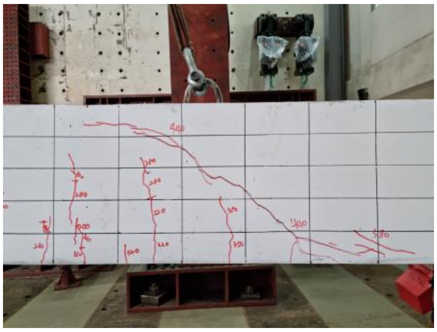

(b) Right shear span

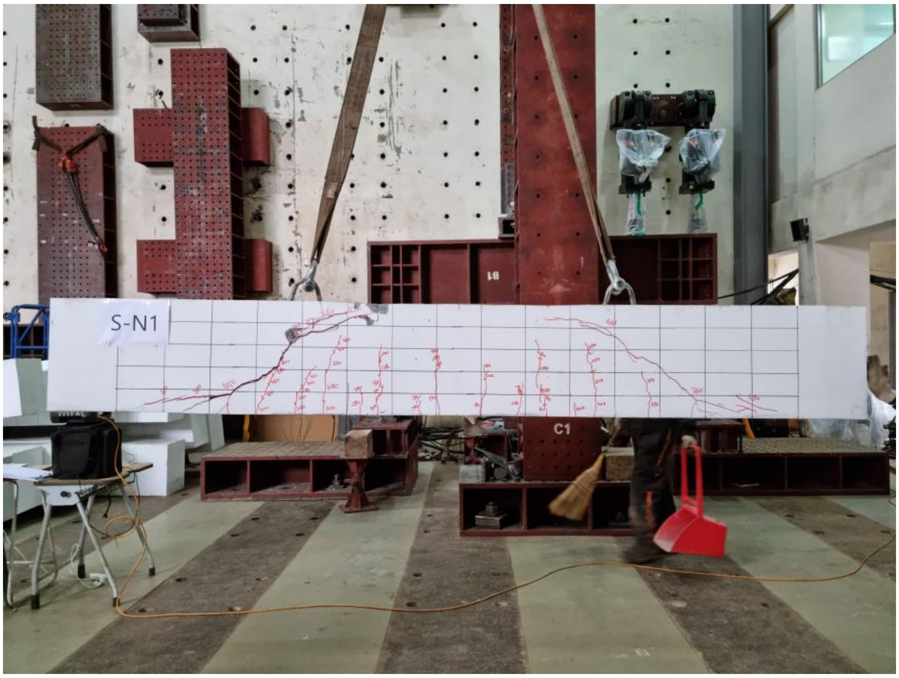

(c) Failure – Concrete collapse at right load point

Figure 5-8 Failure mode of S-N1

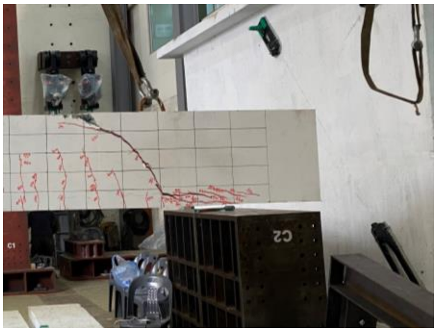

(a) Left shear span

(b) Right shear span

(c) Failure – Concrete collapse at right load point

Figure 5-9 Failure mode of S-G1

(a) Left shear span

(b) Right shear span

(c) Failure – Concrete collapse at right load point

Figure 5-10 Failure mode of S-G2

(a) Left shear span

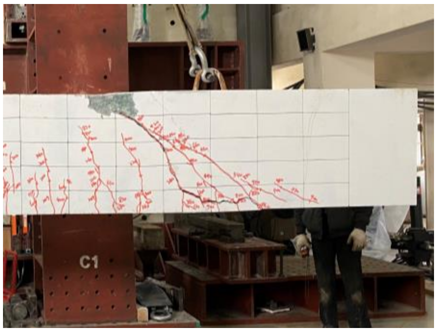

(b) Right shear span

(c) Failure – Concrete collapse at right load point

Figure 5-11 Failure mode of S-G3

(a) Left shear span

(b) Right shear span

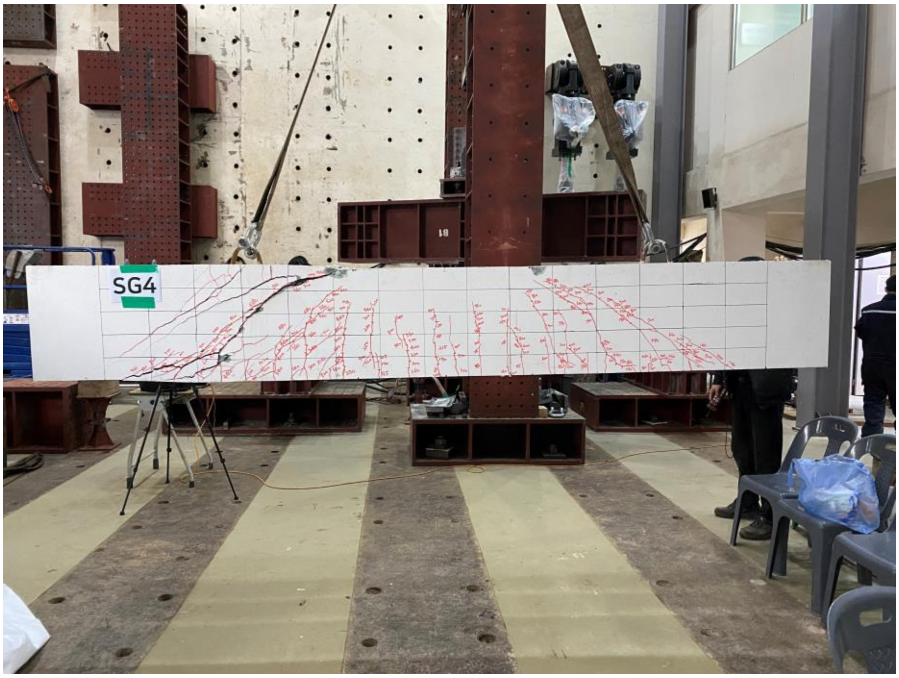

(c) Failure – Concrete collapse at right load point

Figure 5-12 Failure mode of S-G4

(a) Left shear span

(b) Right shear span

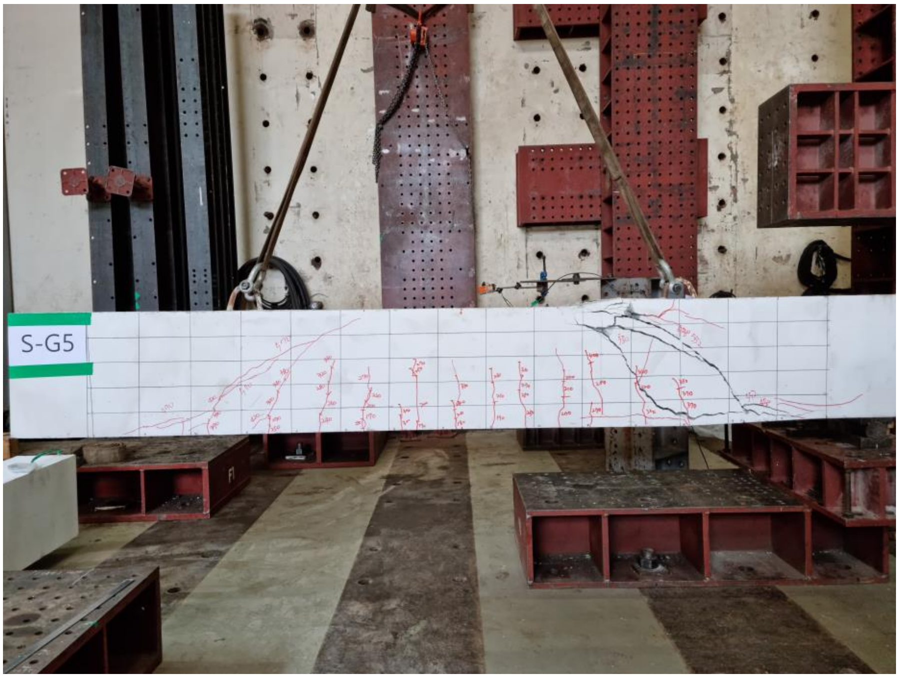

(c) Failure – Concrete collapse at right load point

Figure 5-13 Failure mode of S-G5

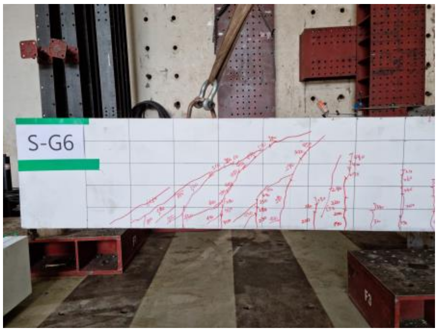

(a) Left shear span

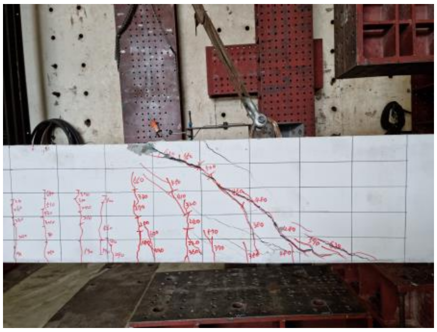

(b) Right shear span

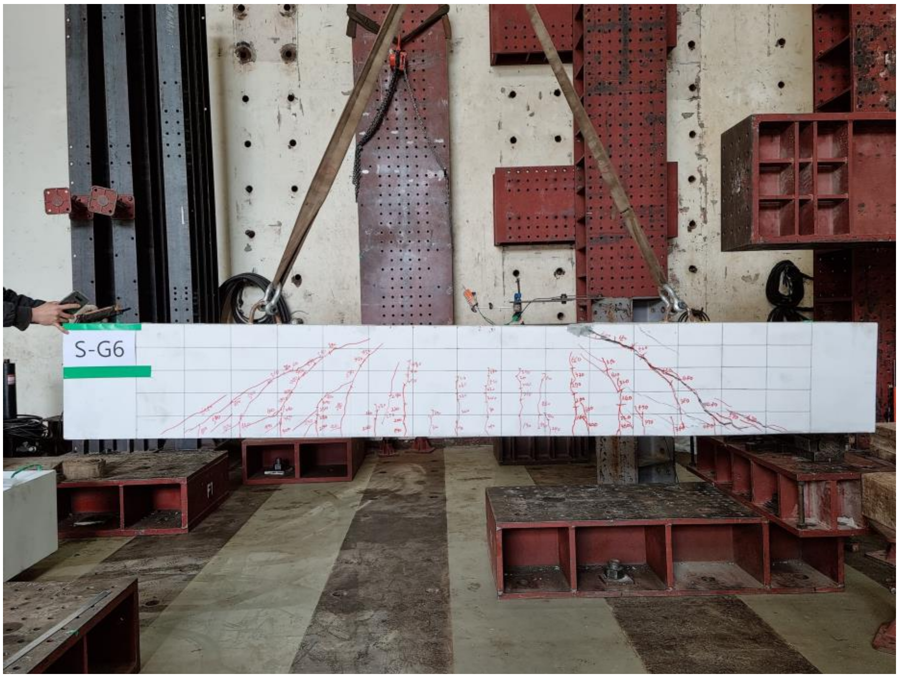

(c) Failure – Concrete collapse at right load point

Figure 5-14 Failure mode of S-G6

(a) Left shear span

(b) Right shear span

(c) Failure – Concrete collapse at right load point

Figure 5-15 Failure mode of S-G7

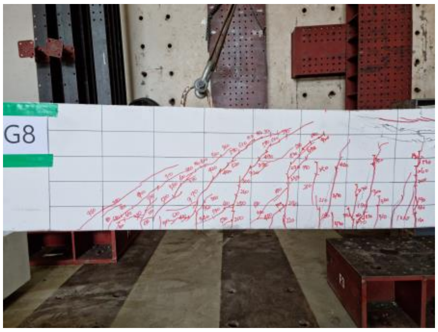

(a) Left shear span

(b) Right shear span

(c) Failure – Concrete collapse at right load point

Figure 5-16 Failure mode of S-G8

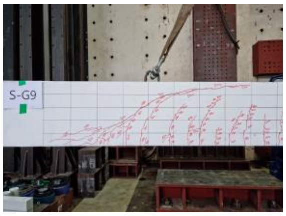

(a) Left shear span

(b) Uniform *M* section

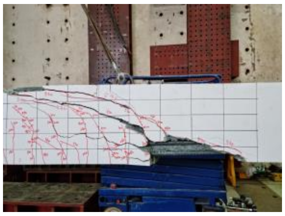

(c) Right shear span

(d) Failure – Concrete collapse at right load point

Figure 5-17 Failure mode of S-G9

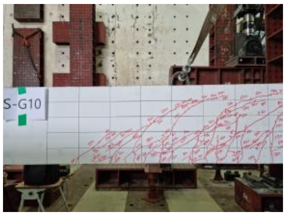

(a) Left shear span

(b) Uniform *M* section

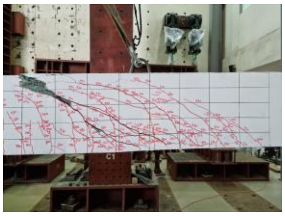

(c) Right shear span

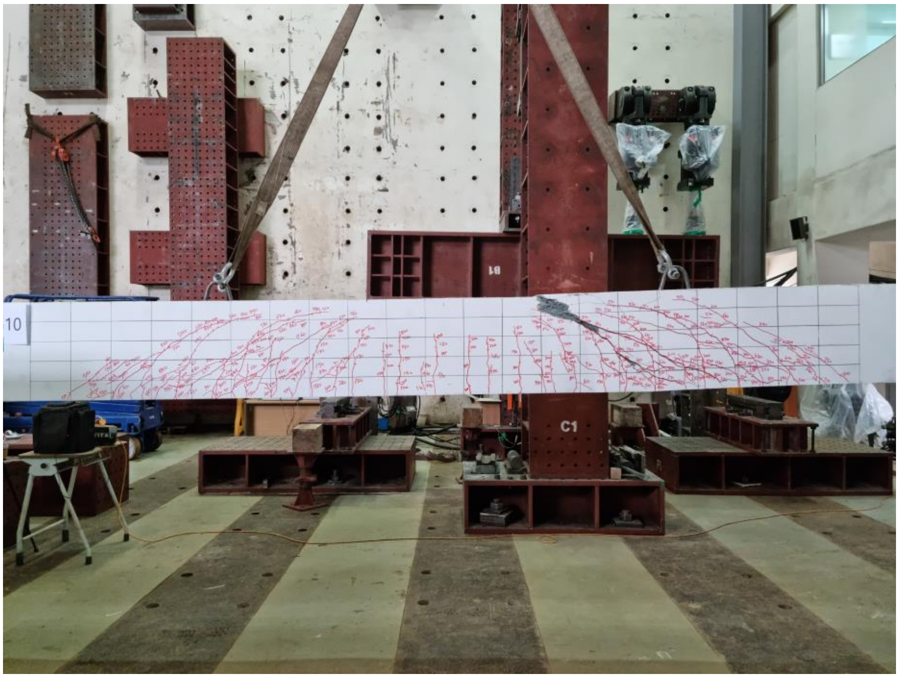

(d) Failure – Concrete collapse at right load point

Figure 5-18 Failure mode of S-G10

(a) Left shear span

(b) Uniform *M* section

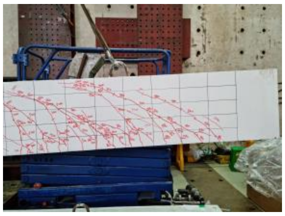

(c) Right shear span

(d) Failure – Concrete collapse at right load point

Figure 5-19 Failure mode of S-G11

(a) Left shear span

(b) Uniform *M* section

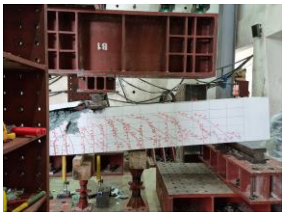

(c) Right shear span

(d) Failure – Concrete collapse at right load point

Figure 5-20 Failure mode of S-G12

Table 5-6 Approximate numbers and spacing of cracks (unit: ea, mm)

Specimens	Cracks	Left shear span	Mid span	Right shear span
S-N1	numbers	7	6	7
	spacing (avg.)	137.5	114.2	137.5
S-G1	numbers	8	9	6
	spacing (avg.)	122.2	80	157.1
S-G2	numbers	6	7	8
	spacing (avg.)	150	110	122.2
S-G3	numbers	7	8	7
	spacing (avg.)	112.5	88.8	112.5
S-G4	numbers	9	7	9
	spacing (avg.)	110	100	110
S-G5	numbers	5	5	4
	spacing (avg.)	150	133.3	140
S-G6	numbers	7	6	6
	spacing (avg.)	137.5	114.2	157
S-G7	numbers	9	7	6
	spacing (avg.)	110	100	128.5
S-G8	numbers	9	14	8
	spacing (avg.)	110	53.3	122.2
S-G9	numbers	10	7	12
	spacing (avg.)	136.3	100	115.3
S-G10	numbers	16	6	14
	spacing (avg.)	100	114.2	113.3
S-G11	numbers	16	11	14
	spacing (avg.)	100	66.6	113.3
S-G12	numbers	14	9	12
	spacing (avg.)	100	80	130.7

5.7 Strain of Stirrups and Longitudinal Bars

Figure 5-21 shows the stirrup strain for the mid span deflection. Regardless of the failure mode and the number of stirrups of the specimens, the stirrups yielded as planned in all specimens. Figure 5-22 shows the longitudinal rebar strain, which measured at the mid span, for the mid span deflection. In the specimens in which shear failure occurred, the strain of the longitudinal rebars did not reach the yield strain or partially reached. On the other hand, in S-G8, S-G11, and S-G12, which are specimens in which flexural failure occurred due to higher shear strength than expected, the longitudinal rebars yielded and their failure modes were same.

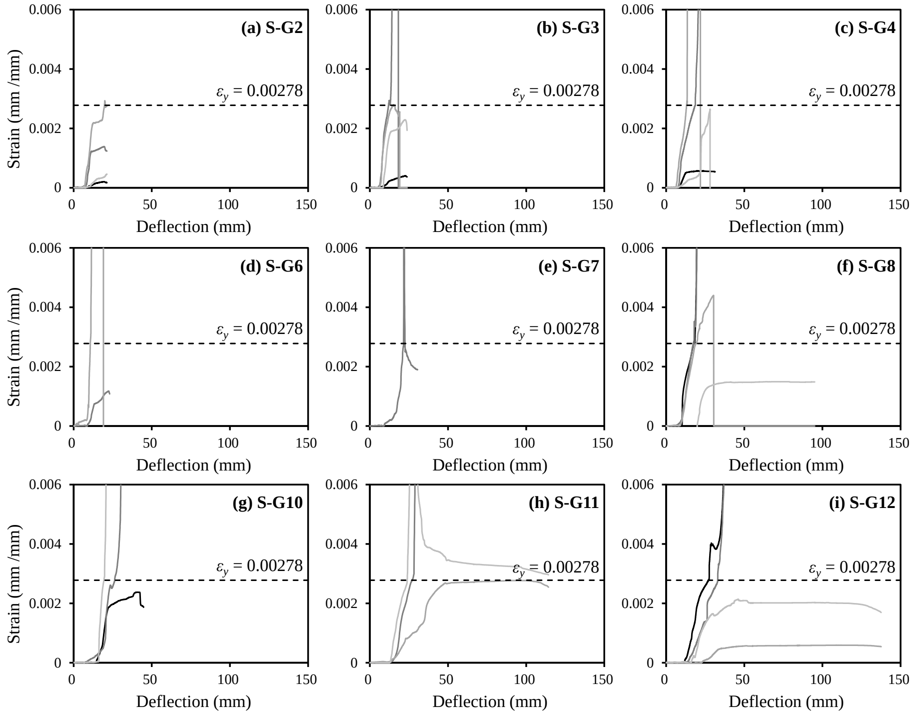

Figure 5-21 Strain of stirrups

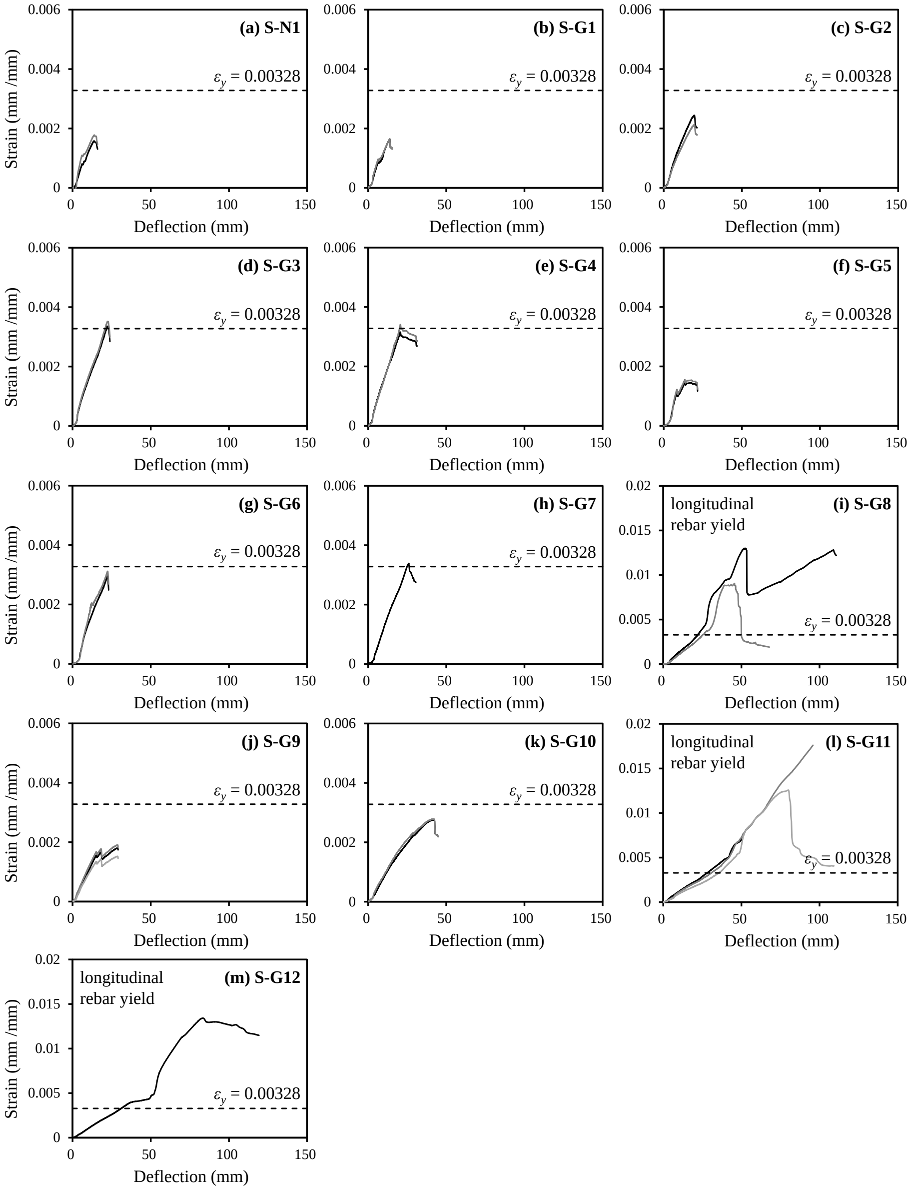

Figure 5-22 Strain of longitudinal bars

5.8 Discussion

In the shear test, a four-point loading test was performed with a total of 13 members as variables such as shear span-to-depth ratio (a/d = 2.5, 3.9), spacing of stirrups (s = none, 110 mm, 150 mm, 220 mm), and compressive strength of concrete (45 MPa, 60 MPa). The stirrup of the specimens was SD500 rebars. The results showed greater than shear strength calculated by KDS 14 20 22: 2022 at the design strength level of 45 MPa and the long-term strength of 60 MPa for specimens with no stirrups or with spacing of stirrups d/4 to d/2. The ratio of the nominal strength to the experimental strength was 1.21 to 2.05, with an average of 1.65 and the coefficient of variation of 0.134, which can be reasonably predicted. Most specimens were showed diagonal shear failure, and, in some specimens, shear strength was greater than expected, showing flexural failure due to upper concrete collapse. Also, there was no big difference compared to normal concrete specimens.

When comparing S-N1, a normal concrete specimen which is a control specimen, with S-G1, a specimen with the same cross-section and different materials, the ratio between the experimental strength and the nominal strength is same as 2.05. In the case of the failure modes of the two specimens, they were also equally failed by the diagonal crack. The average spacing of cracks at the bottom of the mid-span of the two specimens was similar to 114.2 to 80 mm, and the maximum length of diagonal cracks was also similar to about 900 mm.

The Shibayama et al. model showed shear tests that conducted on 10 FA-based geopolymer concrete beams. The experimental parameters were the shear span ratio, concrete strength and the transverse shear reinforcement ratio. The settings of Du et al. model was different with this study. While the settings of this study have symmetrical loading and reaction point, the setting of Du et al. model is not. Nevertheless, the thing that the ultimate shear capacity of beams is greater for lower shear span ratios and higher concrete strengths is same with this study. Existing design code equations can be applied to evaluate the ultimate shear capacity of beams made of FA-based geopolymer concrete subjected to double-curvature bending. The AIJ mean and AIG min equations could evaluate the test results with high accuracy. The JSCE standard can be used to evaluate the ultimate shear capacity. The ACI 318-14 simplified and detailed equation underestimated the test results, regardless of the shear span ratio and loading type.

Chapter 6. Lap Splice Test for Geopolymer Concrete Beams

6.1 Scope and Objectives

The basic premise of “Strength Design Method” is that bond failure with concrete should not occur until rebars meet yield strength. Accordingly, the lap spice test was planned to evaluate the bond performace of rebars. There are 4 ways for testing bond strength of rebars, as shown in Figure 6-1. Pull-out test (Figure 6-1 (a)) is simple and possible for short bond length, but the bond length and reaction force conditions are different from the actual member conditions, so the bond strength can be overestimated. Beam-end test (Figure 6-1 (b)) and beam anchorage test (Figure 6-1 (c)) mainly evaluates the bond strength when anchoring a single rebar, but they are difficult to accurately reflect the effect of concrete cracks and confinement effect caused by transverse rebars. On the other hand, lap splice test (Figure 6-1 (d)) is most widely used test method for evaluating the bond strength of rebars because they can simulate actual lap splice conditions.

The advantages of the lap splice test are as follows. It is possible to simulate the actual load conditions, so it is possible to evaluate the actual bond strength (ACI 408R-03). The current design code KDS 14 20 52: 2022, ACI 318, Eurocode 2 were developed from the same lap splice test results. In particular, since the lap splice length section is a moment-constant section, the same tensile force is applied to the lap splice rebar.

Therefore, in this study, it was evaluated whether the lap splice test satisfies the bond performance (splice length) calculated by KDS 14 20 52: 2022.

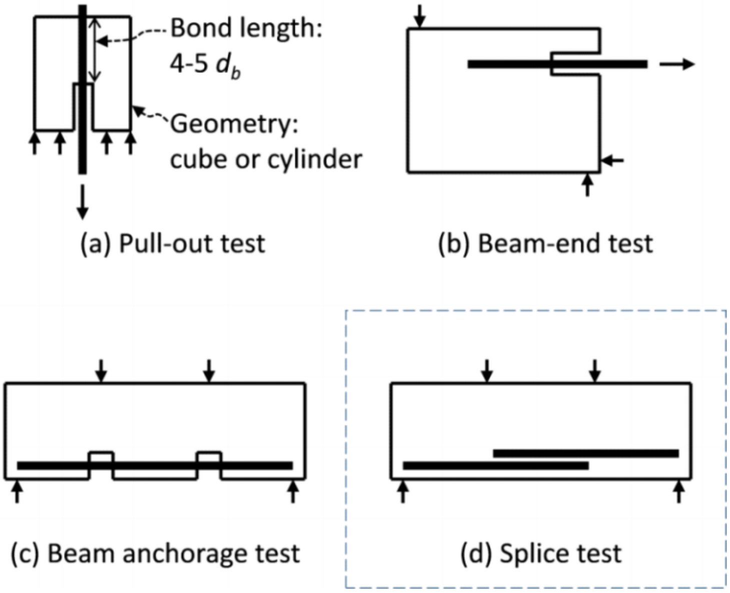

Figure 6-1 Bond strength test method of rebar

6.2 Variables and Specimen Details

The lap splice specimens were designed as variables for the type of concrete (normal concrete, geopolymer concrete), cover thickness, stirrups, diameter of longitudinal bars, and concrete strength, and the test parameters were summarized in Table 6-2.

In specimen name, ‘L’ means lap splice test specimen, ‘G’ and ‘N’ denote geopolymer concrete and normal concrete, respectively. L-N1~N2, L-G1~G2 are specimens that the lap splice length is 50% of the required lap splice length based on KDS in order to induce bond failure. L-G3 and L-G4 are specimens that induced the yield of the longitudinal bars with the lap splice length as 100% of the required lap splice length based on KDS (i.e., $c_b = c_{so} = 43$ mm).

L-G5 and L-G6 are specimens that cover thickness increased to $c_b = c_{so} = 53$ mm, and manufactured as 50% and 100% of the required lap splice length based on KDS, respectively, leading to bond failure and yield of longitudinal rebars. L-G7 and L-G8 are specimens that satisfy 100% of the required lap splice length based on KDS without stirrups in the lap splice section. $c_b = c_{so} = 53$ mm and 63 mm, respectively.

L-G9 and L-G10 are specimens in which the lap splice length is 100% of the ACI 318 code and is 16% longer than the current KDS code, L-G11 and L-G12 are specimens that apply the same detail as L-G3 and L-G4, but the concrete strength increased to 60 MPa (same geopolymer concrete, 28 days) ($c_b = c_{so} =$ 43 mm).

Table 6-1 Variables of lap splice tests (plan)

<table>
<tr><th>Specimens</th><th>Longitudinal bars , d_b (㎜)</th><th>ACI 318 (㎜)</th><th>KDS (㎜)</th><th>l_s (㎜)</th><th>l_s/ ACI 318</th><th>l_s/ KDS</th><th>f_c' (MPa)</th><th>f_y (MPa)</th><th>c_b (㎜)</th><th>c_{so} (㎜)</th><th>c_{si} (㎜)</th><th>K_{tr}</th></tr>
<tr><td>L-N1</td><td>25.4</td><td>1235</td><td>1063</td><td>530</td><td>0.43</td><td>0.5</td><td rowspan="12">45</td><td rowspan="14">600</td><td>43</td><td>43</td><td>106.2</td><td rowspan="8">25.3</td></tr>
<tr><td>L-N2</td><td>31.7</td><td>1541</td><td>1327</td><td>660</td><td>0.43</td><td>0.5</td><td>43</td><td>43</td><td>93.6</td></tr>
<tr><td>L-G1</td><td>25.4</td><td>1235</td><td>1063</td><td>530</td><td>0.43</td><td>0.5</td><td>43</td><td>43</td><td>106.2</td></tr>
<tr><td>L-G2</td><td>31.7</td><td>1541</td><td>1327</td><td>660</td><td>0.43</td><td>0.5</td><td>43</td><td>43</td><td>93.6</td></tr>
<tr><td>L-G3</td><td>25.4</td><td>1235</td><td>1063</td><td>1060</td><td>0.86</td><td>1.0</td><td>43</td><td>43</td><td>106.2</td></tr>
<tr><td>L-G4</td><td>31.7</td><td>1541</td><td>1327</td><td>1330</td><td>0.86</td><td>1.0</td><td>43</td><td>43</td><td>93.6</td></tr>
<tr><td>L-G5</td><td rowspan="2">25.4</td><td>1235</td><td>1063</td><td>530</td><td>0.43</td><td>0.5</td><td>53</td><td>53</td><td>96.2</td></tr>
<tr><td>L-G6</td><td>1235</td><td>1063</td><td>1060</td><td>0.86</td><td>1.0</td><td>53</td><td>53</td><td>96.2</td></tr>
<tr><td>L-G7</td><td>25.4</td><td>1235</td><td>1063</td><td>1060</td><td>0.86</td><td>1.0</td><td>53</td><td>53</td><td>96.2</td><td rowspan="2">-</td></tr>
<tr><td>L-G8</td><td>31.7</td><td>1549</td><td>1334</td><td>1330</td><td>0.86</td><td>1.0</td><td>63</td><td>63</td><td>73.6</td></tr>
<tr><td>L-G9</td><td>25.4</td><td>1235</td><td>1063</td><td>1230</td><td>1.0</td><td>1.16</td><td>43</td><td>43</td><td>106.2</td><td rowspan="2">25.3</td></tr>
<tr><td>L-G10</td><td>31.7</td><td>1541</td><td>1327</td><td>1540</td><td>1.0</td><td>1.16</td><td>43</td><td>43</td><td>93.6</td></tr>
<tr><td>L-G11</td><td>25.4</td><td>1070</td><td>921</td><td>920</td><td>0.86</td><td>1.0</td><td rowspan="2">60</td><td>43</td><td>43</td><td>106.2</td><td rowspan="2">25.3</td></tr>
<tr><td>L-G12</td><td>31.7</td><td>1335</td><td>1149</td><td>1150</td><td>0.86</td><td>1.0</td><td>43</td><td>43</td><td>93.6</td></tr>
</table>

where, planned compressive strength of concrete are 45 MPa (design compressive strength of geopolymer concrete) and 60 MPa (28 days compressive strength) (Table 6-1).

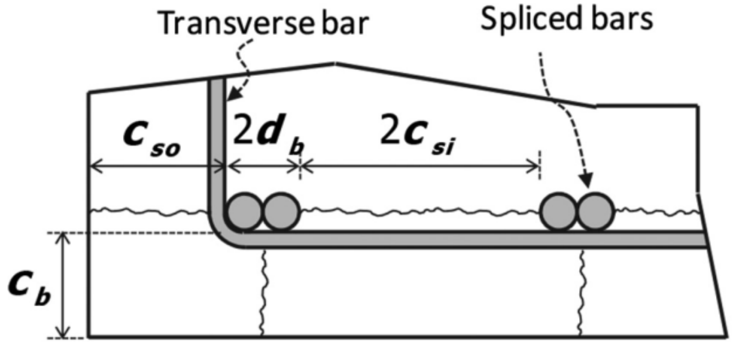

Figure 6-2 Cover thickness of lap splice specimens

where, c_b is length from beam bottom surface to spliced bars surface, c_{so} is length from beam side surface to spliced bars surface, and c_{si} is half of length between spliced bars (Figure 6-2).

The cross-section size of the lap splice specimens is 400 mm width and 500 mm depth. The total length of the specimens is 5,000 mm (L-N1 ~ L-G2, L-G5), 5,600 mm (L-G3 ~ L-G4, L-G6 ~ L-G9, L-G11 ~ L-G12), 5,800 mm (L-G10), respectively. The cover thickness was planned for $c_b = c_{so} = 43$, 53, 63 mm. These are the value of the spacer (30, 40, 50 mm) for rebar arrangement plus the diameter of the D13 stirrups, 13 mm.

D13 stirrups were arranged at spacing of 200 mm in all sections including lap splice section, and at spacings of 100 mm to prevent local failure near the load point and reaction point. Stirrups of L-G7 and L-G8 specimens were not arranged at the lap splice section ($K_{tr} = 0$).

In order to prevent local stress concentration near the load point, the distance between lap splice section and load point of specimens was manufactured as wide as the effective depth of the specimens. This is to prevent local stress concentration so to prevent over-evaluation of bond strength.

The actual cover thickness and lap splice length were measured when manufacturing the specimens (Table 6-2). Because of construction error, there was a little difference between actual value and test plan for cover thickness and lap splice. The lap splice length was recalculated in consideration of the actual material strength and the actual cover thickness.

Table 6-2 Planned and actual value of cover thickness and lap splice length

Specimens	c_{so} (mm)					l_s (mm)				
	Plan	Actual		vs. plan		Plan	Actual	Recalculated	Actual / recalculated l_s	Remark
		Left	Right	Left	Right					
L-N1	43	43	43	0	0	530	530	577	0.92	0.5 l_s
L-N2	43	44	43	1	0	660	660	692	0.95	0.5 l_s
L-G1	43	46	43	3	0	530	530	571	0.93	0.5 l_s
L-G2	43	43	43	0	0	660	660	685	0.96	0.5 l_s
L-G3	43	43	40	0	-3	1060	1060	1187	0.89	1.0 l_s
L-G4	43	48	48	5	5	1330	1330	1425	0.93	1.0 l_s
L-G5	53	55	53	2	0	530	533	571	0.93	0.5 l_s
L-G6	53	48	53	-5	0	1060	1065	1142	0.93	1.0 l_s
L-G7	53	43	48	-10	-5	1060	1060	1242	0.85	1.0 l_s
L-G8	63	70	80	7	17	1330	1330	1559	0.85	1.0 l_s
L-G9	43	43	40	0	-3	1230	1230	1187	0.89	ACI 318
L-G10	43	45	43	2	0	1540	1540	1371	0.97	
L-G11	43	42	40	-1	-3	920	922	1004	0.92	1.0 l_s
L-G12	43	43	45	0	2	1150	1145	1205	0.95	1.0 l_s

Table 6-3 Variables of lap splice tests (acutal)

<table>
<tr><th>Specimens</th><th>Longitudinal bars, d_b (㎜)</th><th>ACI 318 (㎜)</th><th>KDS (㎜)</th><th>Actual l_s (㎜)</th><th>l_s/ KDS (or ACI 318)</th><th>f_c' (MPa)</th><th>f_y (MPa)</th><th>c_b (㎜)</th><th>c_{so} (㎜)</th><th>c_{si} (㎜)</th><th>K_{tr}</th></tr>
<tr><td>L-N1</td><td>25.4</td><td>1339</td><td>1153</td><td>530</td><td>0.46</td><td rowspan="2">46.1</td><td rowspan="14">658.6
(D25)

633.5
(D32)</td><td>43</td><td>43</td><td>106.2</td><td rowspan="8">25.3</td></tr>
<tr><td>L-N2</td><td>31.7</td><td>1608</td><td>1384</td><td>660</td><td>0.48</td><td>43</td><td>44</td><td>92.6</td></tr>
<tr><td>L-G1</td><td>25.4</td><td>1327</td><td>1142</td><td>530</td><td>0.46</td><td rowspan="2">47</td><td>43</td><td>46</td><td>103.2</td></tr>
<tr><td>L-G2</td><td>31.7</td><td>1592</td><td>1371</td><td>660</td><td>0.48</td><td>43</td><td>43</td><td>93.6</td></tr>
<tr><td>L-G3</td><td>25.4</td><td>1379</td><td>1187</td><td>1060</td><td>0.89</td><td rowspan="2">43.5</td><td>43</td><td>43</td><td>106.2</td></tr>
<tr><td>L-G4</td><td>31.7</td><td>1655</td><td>1425</td><td>1330</td><td>0.93</td><td>43</td><td>48</td><td>88.6</td></tr>
<tr><td>L-G5</td><td rowspan="2">25.4</td><td>1327</td><td>1142</td><td>533</td><td>0.47</td><td>47</td><td>53</td><td>55</td><td>94.2</td></tr>
<tr><td>L-G6</td><td>1326</td><td>1142</td><td>1065</td><td>0.93</td><td rowspan="4">43.5</td><td>53</td><td>53</td><td>96.2</td></tr>
<tr><td>L-G7</td><td>25.4</td><td>1442</td><td>1242</td><td>1060</td><td>0.85</td><td>53</td><td>48</td><td>101.2</td><td rowspan="2">-</td></tr>
<tr><td>L-G8</td><td>31.7</td><td>1811</td><td>1559</td><td>1330</td><td>0.85</td><td>63</td><td>80</td><td>56.6</td></tr>
<tr><td>L-G9</td><td>25.4</td><td>1379</td><td>1187</td><td>1230</td><td>0.89</td><td>43</td><td>43</td><td>106.2</td><td rowspan="2">25.3</td></tr>
<tr><td>L-G10</td><td>31.7</td><td>1592</td><td>1371</td><td>1540</td><td>0.97</td><td>47</td><td>43</td><td>45</td><td>91.6</td></tr>
<tr><td>L-G11</td><td>25.4</td><td>1166</td><td>1004</td><td>922</td><td>0.92</td><td rowspan="2">60.8
(28 days)</td><td>43</td><td>43</td><td>106.2</td><td rowspan="2">25.3</td></tr>
<tr><td>L-G12</td><td>31.7</td><td>1400</td><td>1205</td><td>1145</td><td>0.95</td><td>43</td><td>44</td><td>92.6</td></tr>
</table>

where, planned compressive strength of concrete are 45 MPa (design compressive strength of geopolymer concrete) and 60 MPa (28 days compressive strength) (Table 6-2).

In addition, as a result of considering actual compressive strength of specimens and the rebar strength, the originally planned lap splice length and test variables were modified as shown in Table 6-3 above. The lap splice length of bond failure specimens was planned to be $0.5l_s$, but they were slightly shortened to $0.46 \sim 0.48l_s$. Also, the lap splice length of flexural failure specimens was planned to be $1.0l_s$, but they were slightly shortened to $0.85 \sim 0.95l_s$.

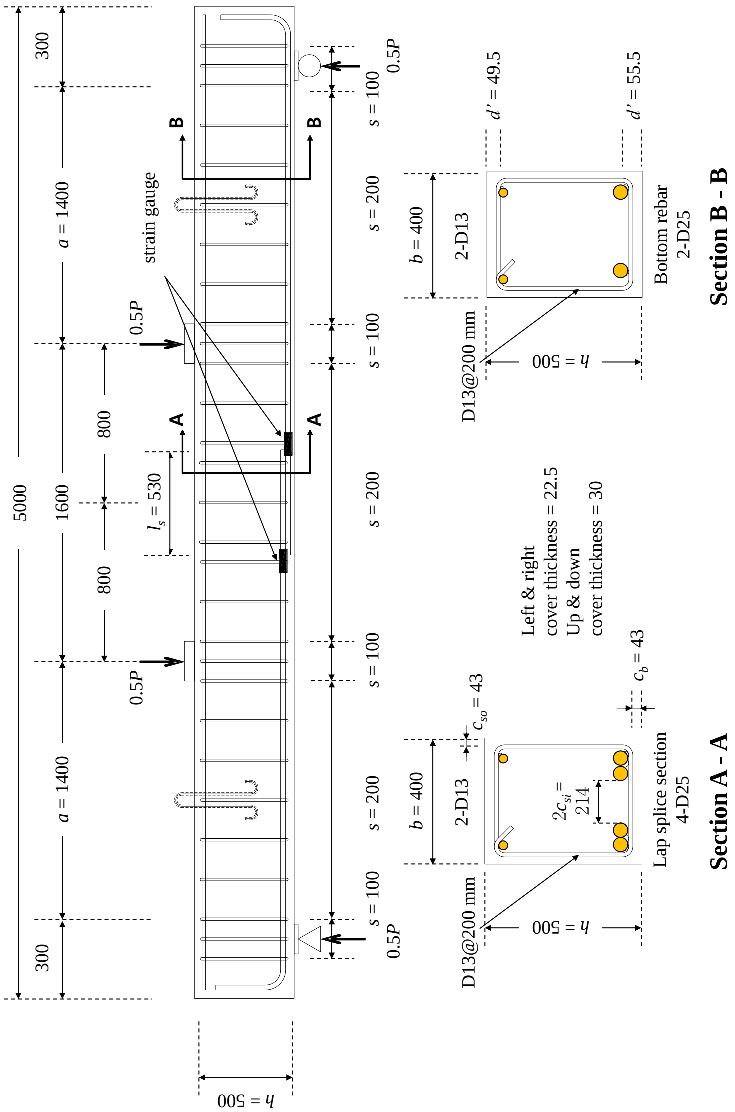

(a) L-G1 specimen detail

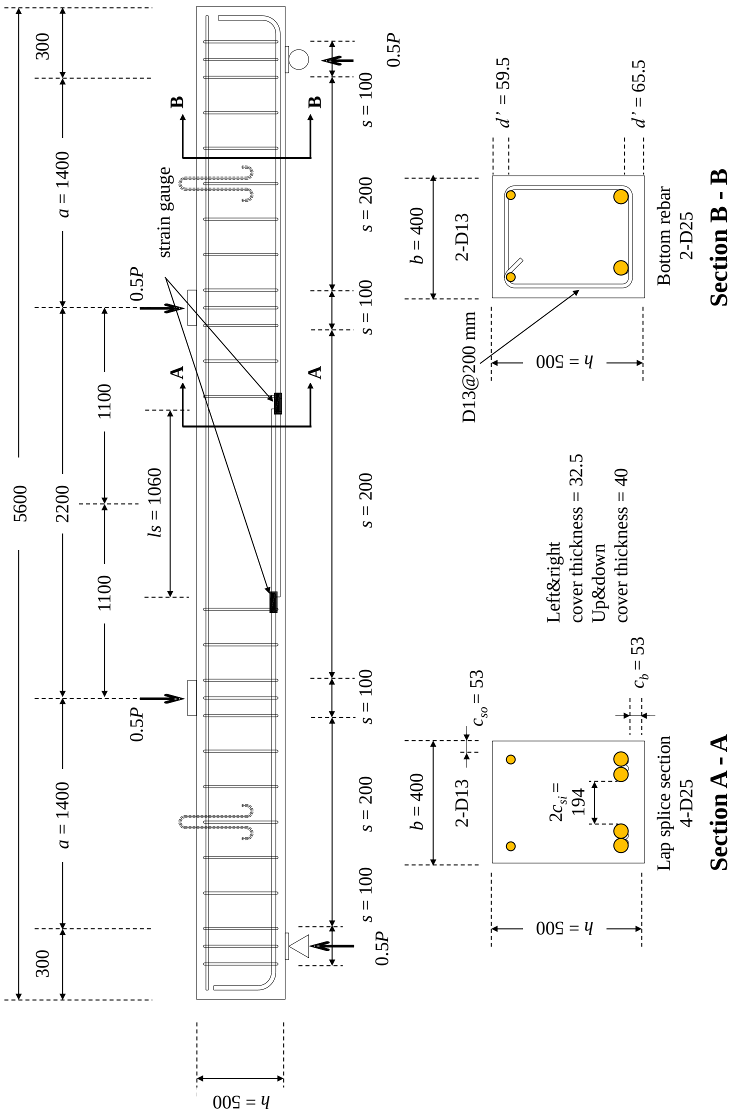

(b) L-G7 specimen detail

Figure 6-3 Lap splice specimen detail (L-G1, L-G7)

6.3 Test Setup

Figure 6-4 shows the setup for loading. 1500 kN actuator was used for the 4 points loading. During the test, the strain of the bottom rebars, load and displacement were measured in real time using a data logger. Loading was applied at a speed of 1 to 2 mm/min.

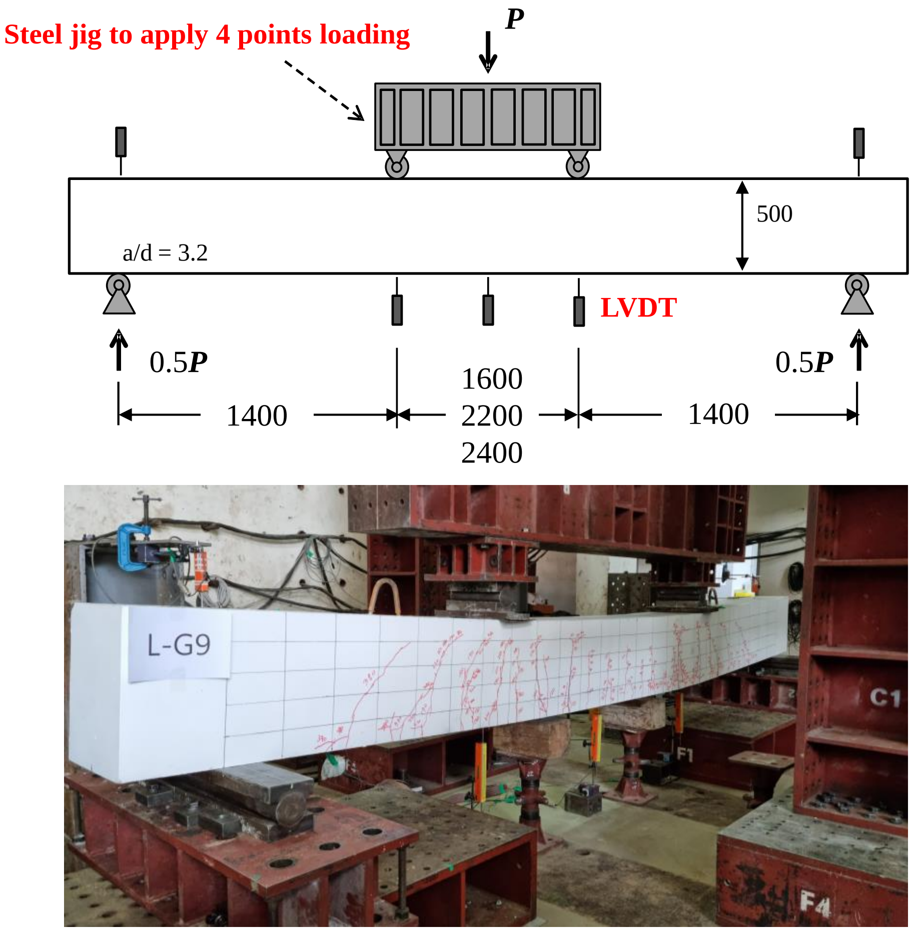

Figure 6-4 Beam flexural test setup (unit: mm)

6.4 Material Tests

The concrete pouring, curing, and material test methods are the same as described in '**4.4 Material Tests**'. The lap splice test specimens correspond to group 4, 5, 6, and 8 in Table 4-3. The compressive strength of each specimen is shown in Table 6-4.

Table 6-4 Compressive strength of specimens

Group	Specimens	f_c' on test day (MPa)
4	L-G3, L-G4, L-G6, L-G7, L-G8, L-G9	43.5
5	L-G1, L-G2, L-G5, L-G10	47.0
6 (normal)	L-N1, L-N2	46.1
8 (28 days)	L-G11, L-G12	60.8

Stirrups used for lap splice test were D13 rebars, longitudinal rebars were D25, D32 rebars. 4 rebar specimens of 600 mm length were manufactured for D13 and D25, and 4 rebar specimens of 700 mm length were manufactured for D32, and tensile tesst were performed. The test methods were the same as described in '**4.4 Material Tests**'. D13 rebars were SD500, and D25, D32 rebars were SD600. The results of rebar tensile tests are shown in Table 6-5 and Figure 6-5.

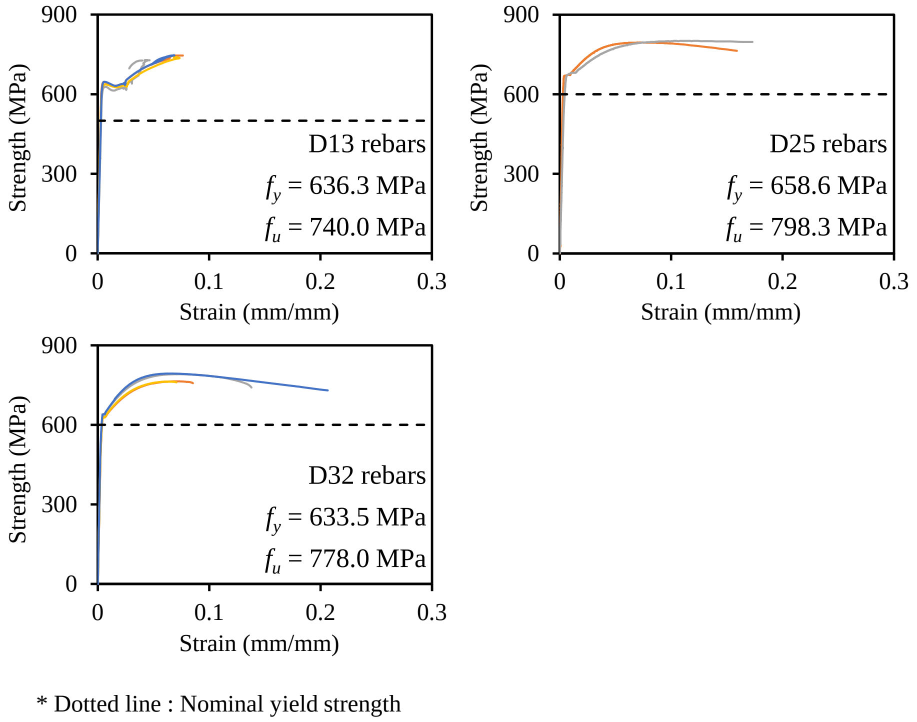

Figure 6-5 Rebar tensile test results (shear test)

Table 6-5 Rebar tensile test results (lap splice test)

Diameter	Yield strength, f_y (MPa)	Tensile strength, f_u (MPa)
D13	636.3	740.0
D25	658.6	798.3
D32	655.7	795.3

6.5 Test Results

A total of 14 lap splice tests were performed. Figure 6-6 shows the load (P)-deflection curve of L-N1, L-G1, L-G3, and L-G7 using D25 rebars for longitudinal bars. Figure 6-7 shows the curve of L-N2, L-G2, L-G4, and L-G8 using D32 rebars for longitudinal bars. Figure 6-8 shows the curve of the specimens that changed cover thickenss and the specimens that satisfied the required lap splice length based on ACI 318. Figure 6-9 shows the curve of the specimens that curing for 28 days. Circular mark means peak experimental load (P_u), a horizontal dash-dotted line refers to the yield strength (P_y) at the time of yield of the longitudinal bars calculated by cross-sectional analysis. A horizontal dotted line refers to the nominal strength (P_n) calculated by the ratio of the actual lap splice length to the required lap splice length stipulated by KDS.

In Figure 6-6, in the 50% length of required lap splice length specimens (a) L-N1, and (b) L-G1, the bond failure occurred due to the lack of lap splice length regardless of the type of concrete (normal vs. geopolymer concrete). In all specimens, the experimental strength exceeding the nominal strength was shown.

The 100% length of required lap splice length specimens (c) L-G3, and (d) L-G7 satisfied the required lap splice length of KDS code, test results exceeded the nominal strength, and the longitudinal rebars yielded and met the yield strength. However, L-G7, which did not use stirrups in lap splice section, showed bond failure due to the fall of covered concrete after yield.

In Figure 6-7, the same results are shown when D32 rebars were used as longitudinal bars. In the 50% length of required lap splice length specimens (a) L-N2, and (b) L-G2, the bond failure occurred due to the lack of lap splice length regardless of the type of concrete (normal vs. geopolymer concrete). Also, 100% length of required lap splice length specimens (c) L-G4, and (d) L-G8 satisfied the required lap splice length of KDS code, test results exceeded the nominal strength, and the longitudinal rebars yield and met the yield strength. However, L-G8, which did not use stirrups in lap splice section, showed bond failure due to the fall of covered concrete after yield.

The cover thickness change specimens (a) L-G5, and (b) L-G6 in Figure 6-8, L-G5 made of half required lap splice length of KDS, but bond failure occurred before the yield strength, and L-G6 satisfying the required length showed ductile behavior after yield. In (c) L-G9, and (d) L-G10 satisfying required lap splice length of ACI 318, flexural failure occurred after longitudinal bars yield. This is because the required lap splice length of ACI 318 is longer than the length based on KDS.

In Figure 6-9, (a) L-G11, and (b) L-G12 which were 100% of the required lap splice length and cured for 28 days, the longitudinal bars equally yielded and met the yield strength. Later, the crach width of L-G11 expanded at the end of the lap splice section, and the lower concrete of L-G12 was collapsed.

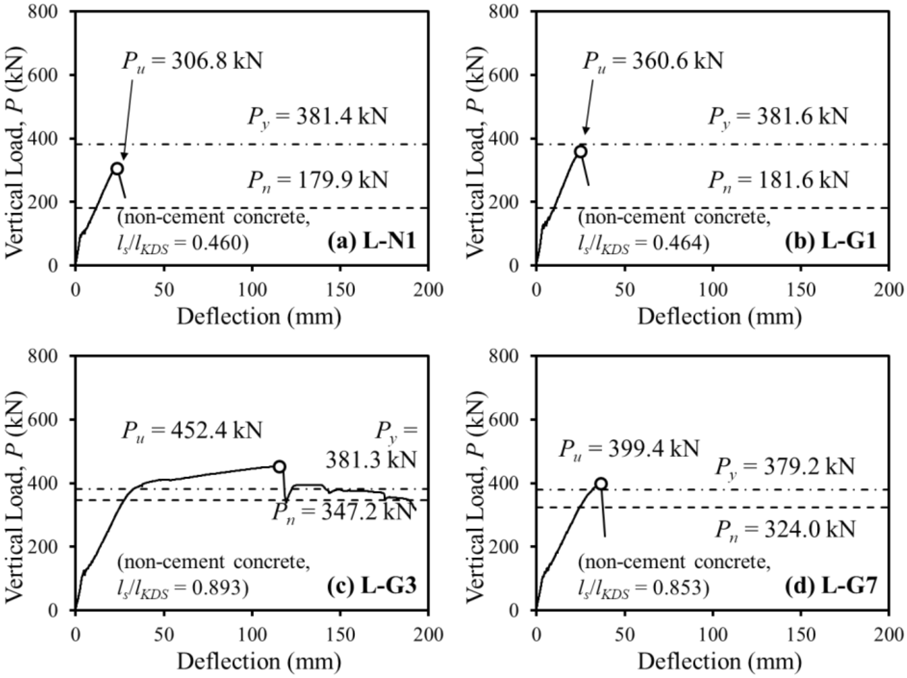

Figure 6-6 Load-deflection curve (D25 rebars)

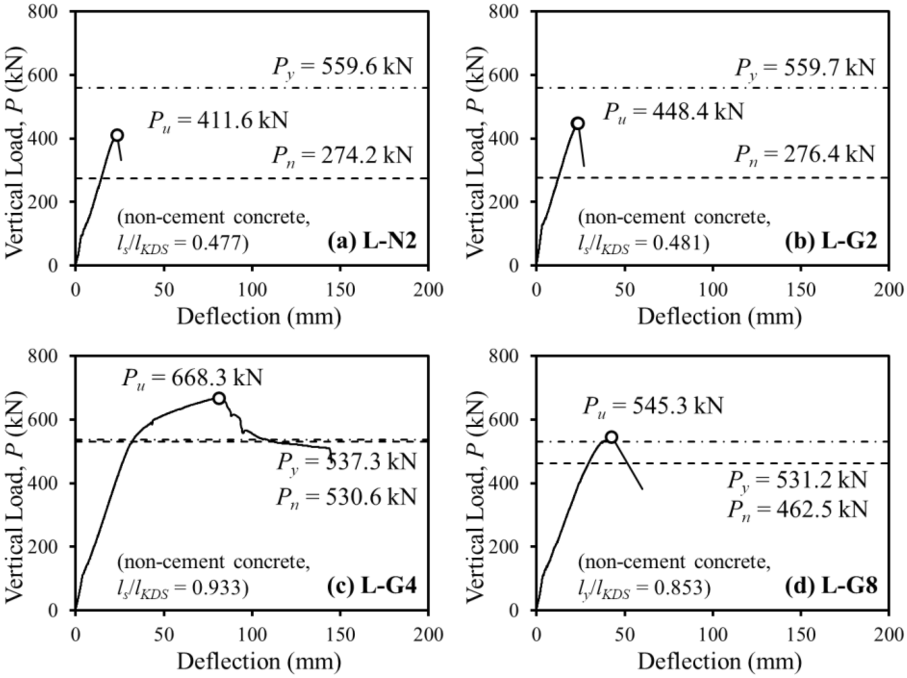

Figure 6-7 Load-deflection curve (D32 rebars)

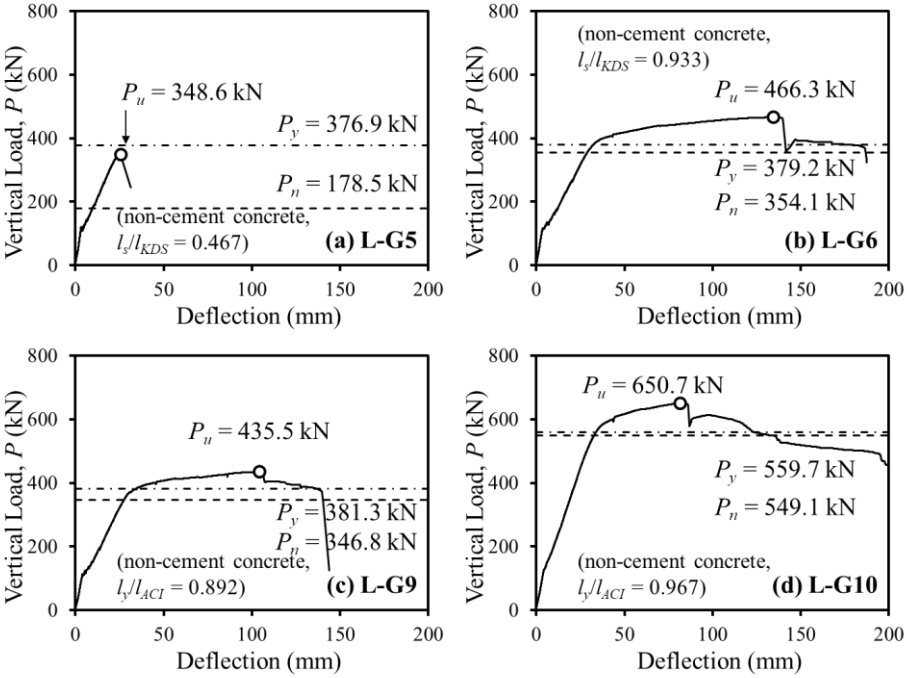

Figure 6-8 Load-deflection curve (cover thickness, ACI 318)

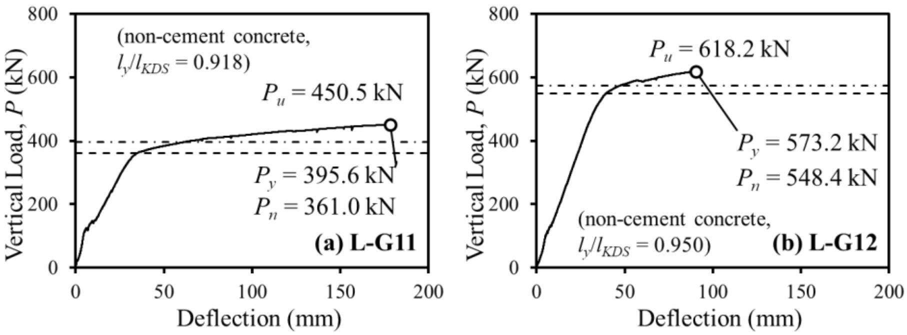

Figure 6-9 Load-deflection curve (28 days)

To calculate the nominal strength (P_n) and yield strength (P_y) of the specimens, nonlinear cross-sectional analysis was performed under the following conditions.

※ Nonlinear cross-sectional analysis

Nonlinear cross-sectional analysis was performed by using strain compatibility of section of specimens. The stress-strain relationship of rebars and concrete used in the analysis considering the tension (+) and compression (-) values is as follows.

The material model of concrete was Hognestad's model (Equation (6-1)). The entire cross section of the beam is non-restrained condition because the restraints by the stirrups are not considered, and the tensile strength of the concrete is ignored.

$$\sigma_n = f_{ck}\left[\frac{2\varepsilon}{\varepsilon_{co}} + \left(\frac{\varepsilon}{\varepsilon_{co}}\right)^2\right] \text{ for } -\varepsilon_{cu} \le \varepsilon \le 0 \qquad (6\text{-}1)$$

Where, σc = stress of non-restrained concrete, f_{ck} = compressive strength of concrete (results of material tests), ε_{co} = strain corresponding to the compressive strength of concrete (= 0.002), ε_{cu} = extreme strain of concrete (= 0.003), and if the strain is greater than the extreme strain, the stress is assumed to be 0 due to the occurrence of concrete collapse.

For the material model of rebars, a bilinear model (Bi-linear) with strain hardening, and the hardening coefficient (E_{sh}) is 0.01.

$$-f_y \leq \sigma_r = E\varepsilon \leq f_y \ \text{ for } -\varepsilon_y \leq \varepsilon \leq \varepsilon_y \tag{6-2}$$

$$\sigma_r = f_y + E_{sh}(\varepsilon - \varepsilon_y) \ \text{ for } \ \varepsilon > \varepsilon_y \tag{6-3}$$

$$\sigma_r = -f_y + E_{sh}(\varepsilon + \varepsilon_y) \ \text{ for } \ \varepsilon < -\varepsilon_y \tag{6-4}$$

where, σ_r = stress of rebars, f_y = yield strength of rebars, E = elastic coefficient of rebars, E_{sh} = hardening coefficient of rebars (= 0.01), and ε_y = yield strain of rebars and it is the starting point of strain hardening.

Figure 6-10 shows the ratio of experimental strength and nominal strength of lap splice specimens. The nominal strength was calculated as the strength when the strain (f_s) of the longitudinal bars had the ratio of KDS required lap splice length to the actual lap splice length (l_s) through cross-sectional analysis (Equation (6-5)). Based on the strain of longitudinal bars causing the nominal strength, results of cross-sectional analysis are compared with the test results and summarized in Table 6-6. All specimens showed test results exceeding the nomnial strength calculated by cross-sectional analysis, with an average of 1.42 and a coefficient of variation of 0.205.

$$f_s = \frac{l_s}{l_{KDS}} \varepsilon_y \tag{6-5}$$

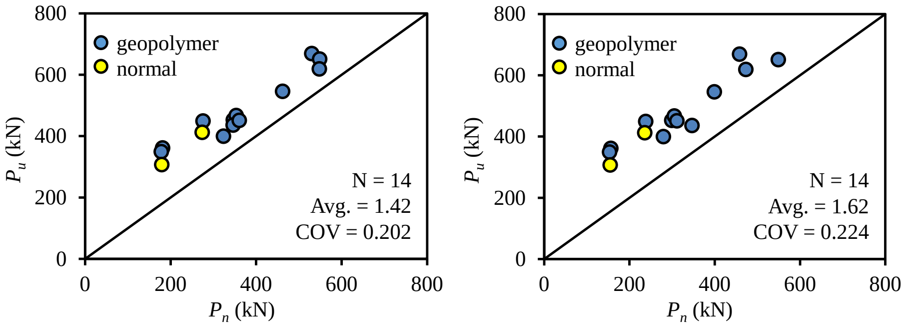

(a) KDS (b) ACI

Figure 6-10 Comparison between peak and nominal strength (lap splice)

Table 6-6 Comparison between results of cross-sectional analysis and test results

	Lap splice length and strain					Cross-sectional analysis		Test results	Comparison	
Specimens	l_s	l_{KDS}	l_s/l_{KDS}	ε_y	f_s	P_n	P_y	P_u	P_u/P_n	P_u/P_y
L-N1	530	1153	0.460	0.003293	0.001514	179.8	381.4	306.8	1.71	0.80
L-N2	660	1384	0.477	0.003168	0.001510	274.1	559.6	411.6	1.50	0.74
L-G1	530	1142	0.464	0.003293	0.001528	181.7	381.6	360.6	1.99	0.94
L-G2	660	1371	0.481	0.003168	0.001525	276.7	559.7	448.4	1.62	0.80
L-G3	1060	1187	0.893	0.003293	0.002941	347.2	381.3	452.4	1.30	1.19
L-G4	1330	1425	0.933	0.003168	0.002956	532.4	537.3	668.3	1.26	1.24
L-G5	533	1142	0.467	0.003293	0.001537	178.4	376.9	348.6	1.95	0.92
L-G6	1065	1142	0.933	0.003293	0.003072	354.0	379.2	466.3	1.32	1.23
L-G7	1060	1353	0.783	0.003293	0.002579	297.8	379.2	399.4	1.34	1.05
L-G8	1330	1432	0.929	0.003168	0.002941	502.8	531.2	545.3	1.08	1.03
L-G9	1230	1187	0.892	0.003293	0.002937	346.9	381.3	435.5	1.26	1.14
L-G10	1540	1371	0.967	0.003168	0.003063	551.7	559.7	650.7	1.18	1.16
L-G11	922	1004	0.918	0.003293	0.003024	361.1	395.6	450.5	1.25	1.14
L-G12	1145	1205	0.950	0.003168	0.003009	548.4	573.2	618.2	1.13	1.08

Figure 6-11(a) shows the ratio of experimental strength and yield strength of bond failure specimens (lap splice length = 0.46 ~ 0.48 l_s). The average of ratio is 0.84 and coefficient of variation is 0.106. The bond failure specimens did not meet the yield strength because it was intentionally designed to lack the lap splice length. However, as a result of cross-sectional analysis, the strain of longitudinal bars at the peak experimental strength was $\varepsilon_{s,\,peak}$ = 0.72 ~ 0.93 ε_y, indicating bond strength greater than 50% of the laps splice length/required lap splice length ratio (Table 6-7).

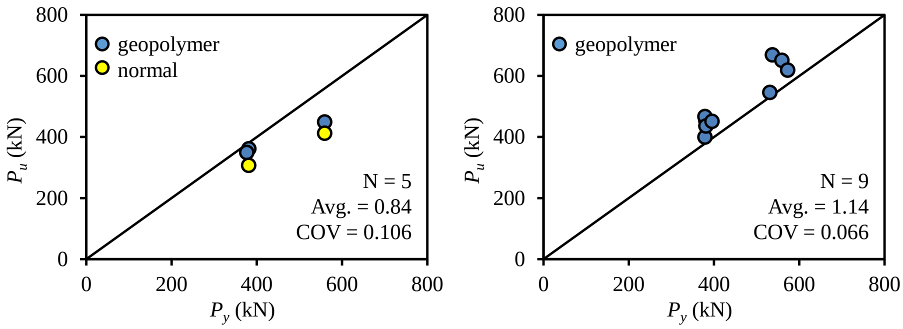

(a) 50% requied length

(b) 100% required length

Figure 6-11 Comparison between peak and yield strength

Table 6-7 Cross-sectional analysis results of 50% required length specimens

Specimens	Actual length / required length	Yield strain ε_y	Strain at peak strength $\varepsilon_{s,\ peak}$	$\varepsilon_{s,\ peak}/\varepsilon_y$
L-N1	0.460	0.003293	0.00259	0.79
L-N2	0.477	0.003168	0.002276	0.72
L-G1	0.464	0.003293	0.003046	0.93
L-G2	0.481	0.003168	0.002482	0.78
L-G5	0.467	0.003293	0.003015	0.92

Figure 6-11(b) shows the ratio of experimental strength and yield strength of flexural failure specimens (lap splice length = 0.85 ~ 0.96 l_s). The average of ratio is 1.14 and coefficient of variation is 0.076. All specimens met the yield strength. Table 6-8 summarizes the ratio of the actual lap slplice length and the KDS required lap splice lenngth, and the comparison between experimental strength and yield strength for each specimen.

Table 6-8 Cross-sectional analysis results of 100% required length specimens

Specimens	Actual length / required length	P_u	P_y	P_u/P_y
L-G3	0.893	452.4	381.3	1.19
L-G4	0.933	668.3	537.3	1.24
L-G6	0.933	466.3	379.2	1.23
L-G7	0.783	399.4	379.2	1.05
L-G8	0.929	545.3	531.2	1.03
L-G9	0.892	435.5	381.3	1.14
L-G10	0.967	650.7	559.7	1.16
L-G11	0.918	450.5	395.6	1.14
L-G12	0.950	618.2	573.2	1.08

Table 6-9 summarizes the results of lap splice test for all specimens. As described before, the specimens manufactured with 50% of the required lap splice length did not reach the yield strength, resulting in bond failure, and in all specimens satisfying the required lap splice length, P_u/P_y exceeded 1.0 and showed flexural failure.

Table 6-9 Summary of lap splice test results

Specimens	Longitudinal rebars d_b (㎜)	f_c' (MPa)	c_b (㎜)	c_{so} (㎜)	c_{si} (㎜)	K_{tr}	f_y (MPa)	KDS req. (㎜)	ACI 318 req. (㎜)	Actual length l_s (㎜)	l_s/ KDS (or ACI 318)	P_u (kN)	P_n (kN)	P_y (kN)	P_u/P_n	Failure mode
L-N1	25.4	46.1	43	43	106.2	25.3	658.6	1153	1339	530	0.46	306.8	179.8	381.4	1.71	Bond
L-N2	31.7		43	43	93.6		633.5	1384	1608	660	0.48	411.6	274.1	559.6	1.50	Bond
L-G1	25.4	47.0	43	43	106.2		658.6	1142	1327	530	0.46	360.6	181.7	381.6	1.99	Bond
L-G2	31.7	47.0	43	43	93.6		633.5	1371	1592	660	0.48	448.4	276.7	559.7	1.62	Bond
L-G3	25.4	43.5	43	40	106.2		658.6	1187	1379	1060	0.89	452.4	347.2	381.3	1.30	Flexural
L-G4	31.7	43.5	43	48	93.6		633.5	1425	1655	1330	0.93	668.3	532.4	537.3	1.26	Flexural
L-G5	25.4	47.0	53	53	96.2		633.5	1142	1327	533	0.47	348.6	178.4	376.9	1.95	Bond
L-G6		43.5	53	48	96.2		633.5	1142	1326	1065	0.93	466.3	354.0	379.2	1.32	Flexural
L-G7	25.4	43.5	53	43	96.2	-	633.5	1242	1442	1060	0.85	399.4	297.8	379.2	1.34	Bond after yield
L-G8	31.7	43.5	63	70	73.6		658.6	1559	1811	1330	0.85	545.3	502.8	531.2	1.08	Bond after yield
L-G9	25.4	43.5	43	40	106.2	25.3	633.5	1187	1379	1230	0.89	435.5	346.9	381.3	1.26	Flexural
L-G10	31.7	47.0	43	43	93.6		658.6	1371	1592	1540	0.97	650.7	551.7	559.7	1.18	Flexural
L-G11	25.4	60.8	43	40	106.2		633.5	1004	1166	922	0.92	450.5	361.1	395.6	1.25	Flexural
L-G12	31.7	60.8	43	43	93.6		658.6	1205	1400	1145	0.95	618.2	548.4	573.2	1.13	Bond after yield

To summarize the test results, the current lap splice design code can be applied to the deisgn variables considered in these tests, such as concrete type (normal concrete, geopolymer concrete), cover thickness, stirrups, diameter of longitudinal bars, and concrete strength.

6.6 Failure Mode

Figure 6-12 ~ 6-25 show the failure modes of the lap splice specimens, respectively. Failure modes can be largely divided into 3 types as seen in the load-deflection curves. They are bond failure (L-N1, N2, G1, G2, and G5), flexural failure (L-G3, G4, G6, G7, G8, and G9), and bond failure after yield (L-G7, G8, and G12). In the case of bond failure, flexural and diagonal cracks occurred in the beginning, and ultimately, they were failed when longitudinal bars cracks occurred in the lower concrete. There was no difference between normal concrete and geopolymer concrete. In the case of flexural failure, flexural and diagonal cracks occurred, and the crack width at the end of the lap splice section occurred intensively. After that, collapse began in the upper concrete and reached the peak strength, and then showed ductile behavior. In the case of bond failure after yield, the longitudinal bars yielded, but specimens showed brittle failure when the lower concrete was failed due to the absence of stirrups after the peak strength.

(a) Left shear span

(b) Right shear span

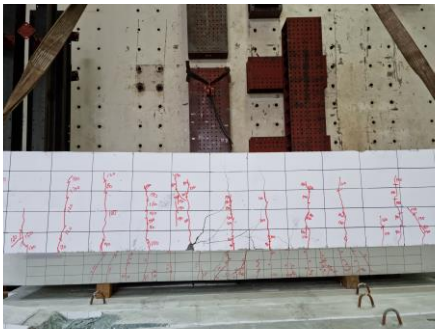

(c) Lap splice section

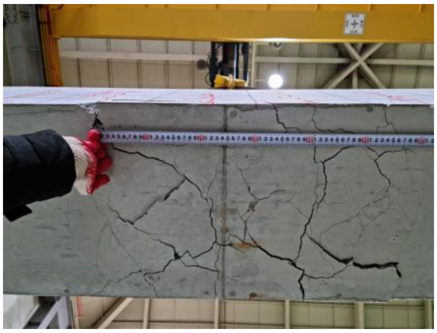

(d) Bottom part

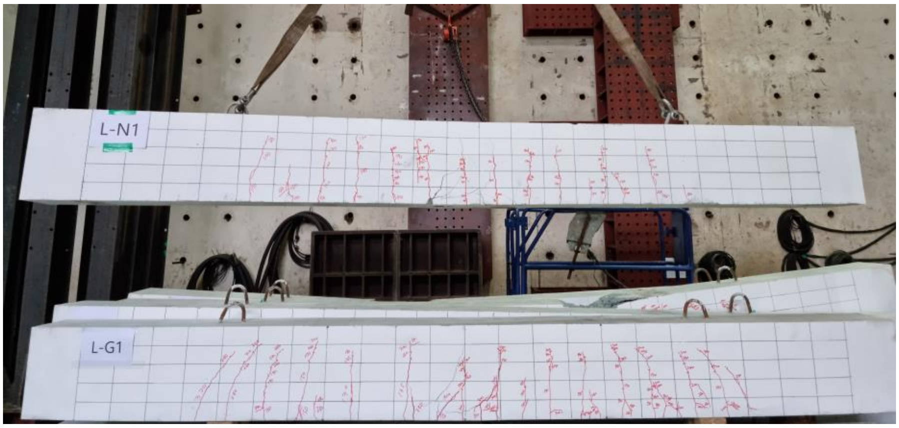

(e) Failure – Bond failure

Figure 6-12 Failure mode of L-N1

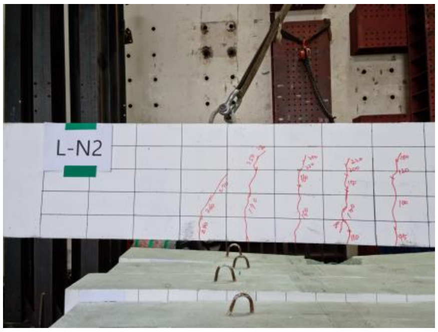

(a) Left shear span

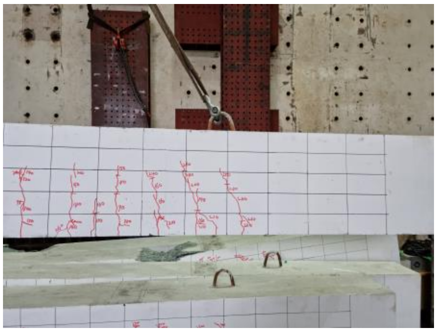

(b) Right shear span

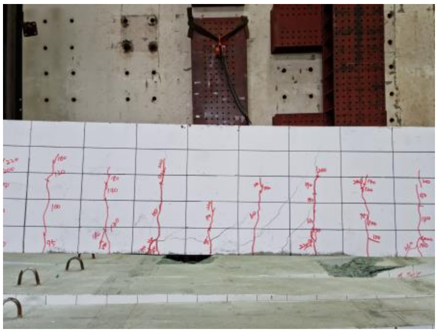

(c) Lap splice section

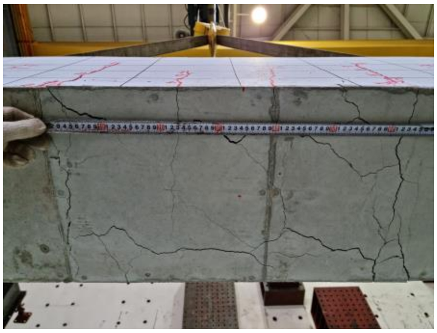

(d) Bottom part

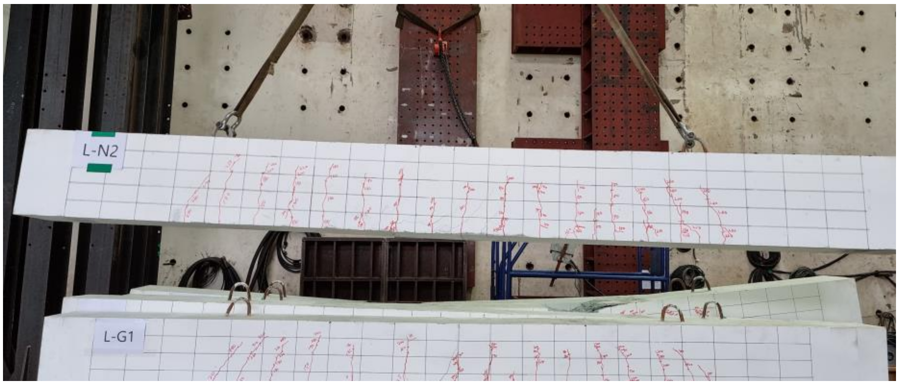

(e) Failure – Bond failure

Figure 6-13 Failure mode of L-N2

(a) Left shear span

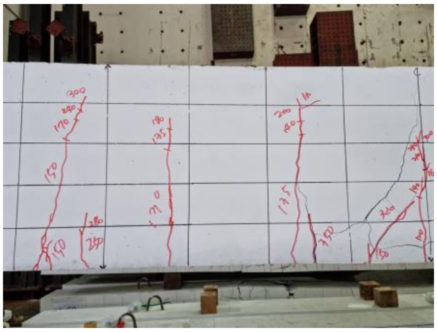

(b) Left lap splice section

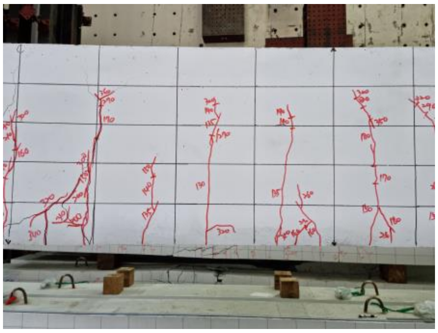

(c) Right lap splice section

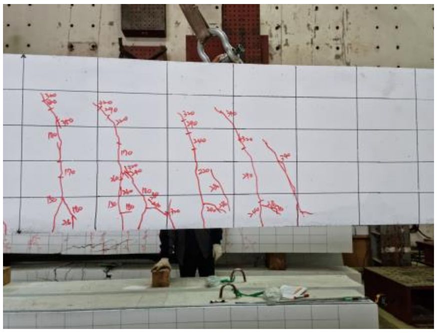

(d) Right shear span

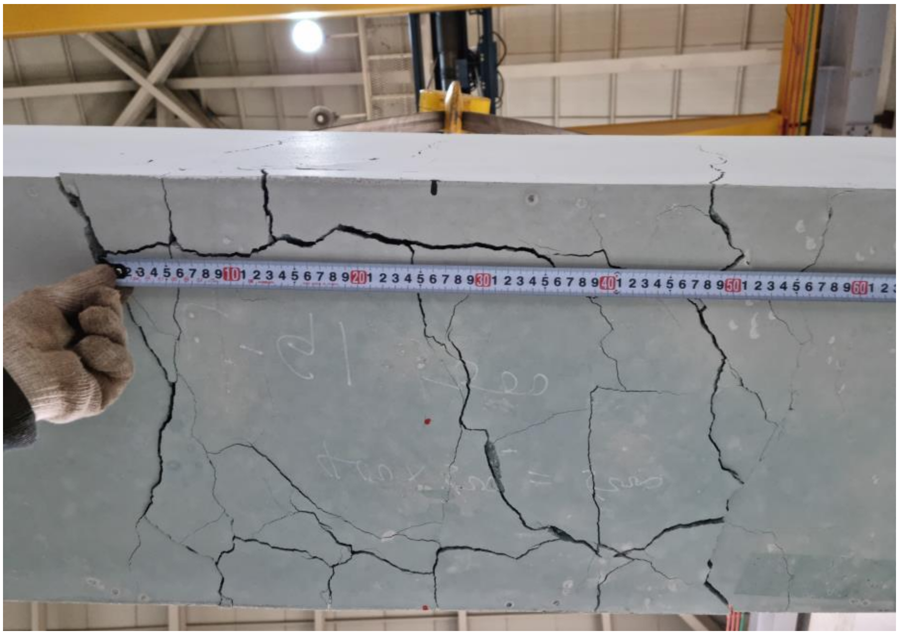

(e) Bottom part

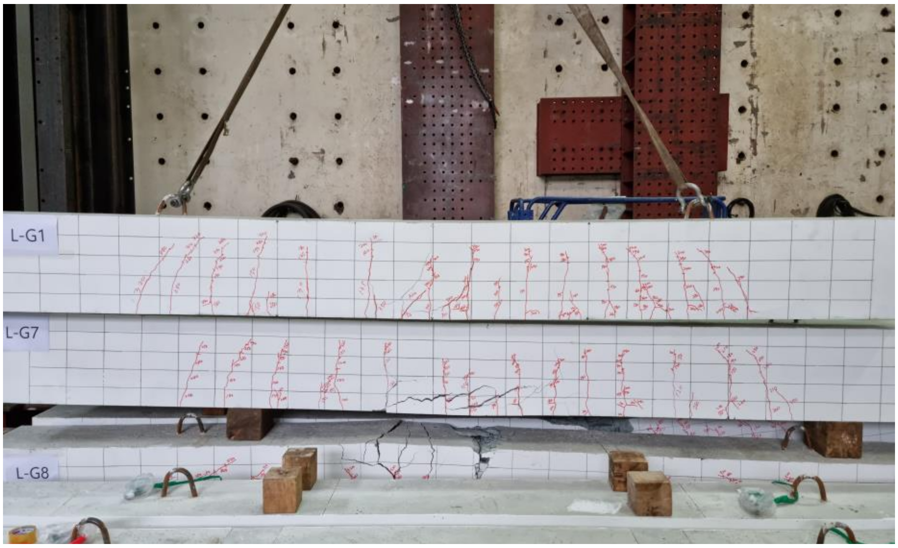

(f) Failure – Bond failure

Figure 6-14 Failure mode of L-G1

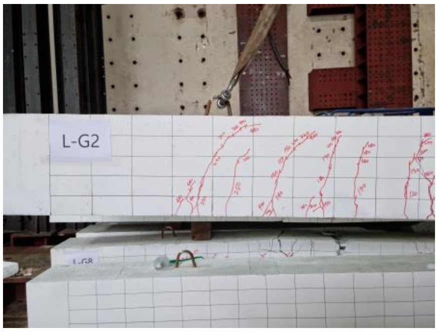

(a) Left shear span

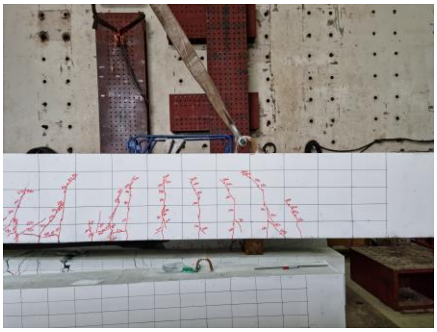

(b) Right shear span

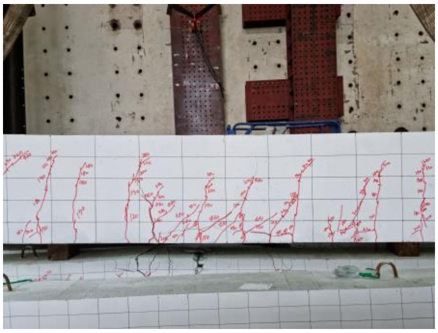

(c) Lap splice section

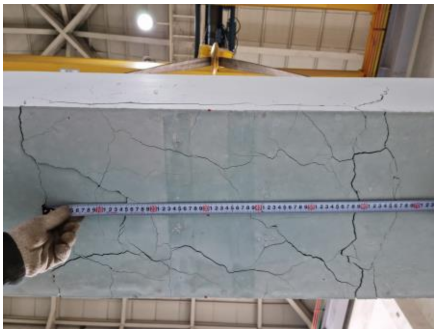

(d) Bottom part

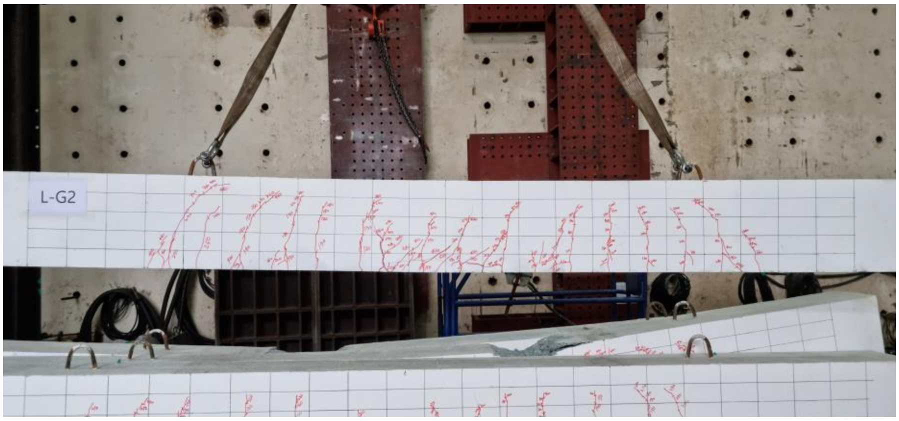

(e) Failure – Bond failure

Figure 6-15 Failure mode of L-G2

(a) Left shear span

(b) Left lap splice section

(c) Right lap splic section

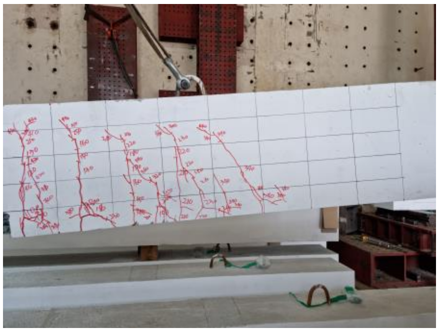

(d) Right shear span

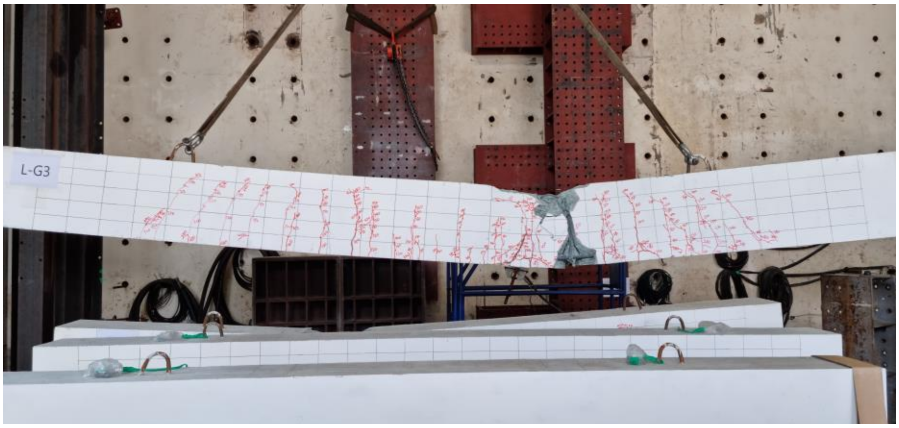

(e) Failure – Concrete collapse at right load point

Figure 6-16 Failure mode of L-G3

(a) Left shear span

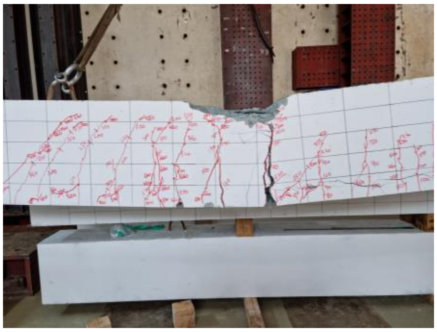

(b) Left lap splice section

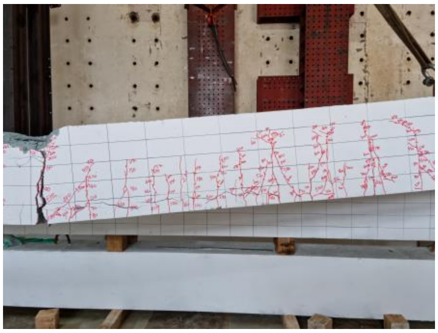

(c) Right lap splice section

(d) Right shear span

(e) Failure – Bond failure

Figure 6-17 Failure mode of L-G4

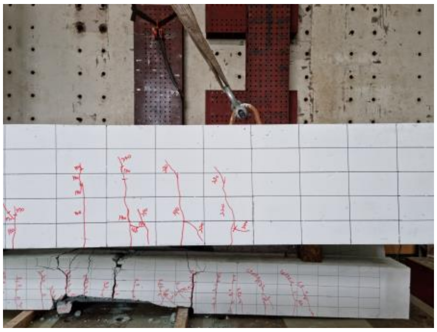

(a) Left shear span (b) Right shear span

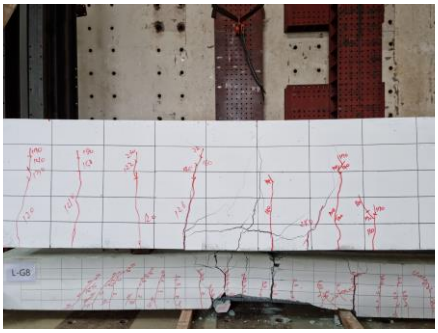

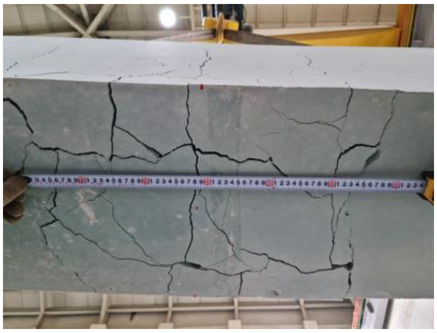

(c) Lap splice section (d) Bottom part

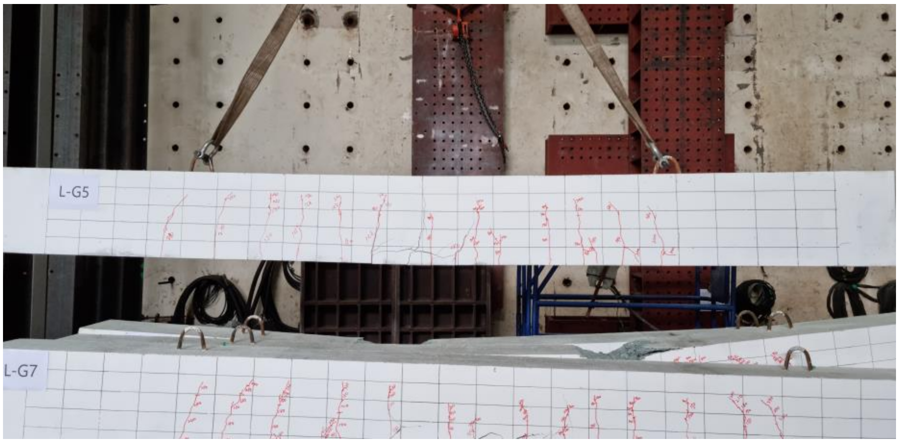

(e) Failure – Bond failure

Figure 6-18 Failure mode of L-G5

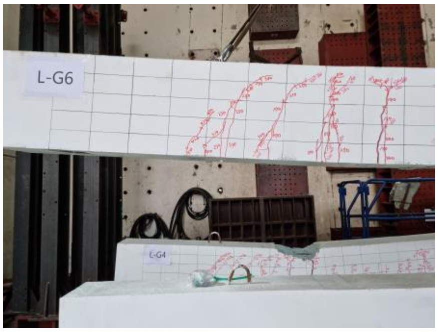

(a) Left shear span

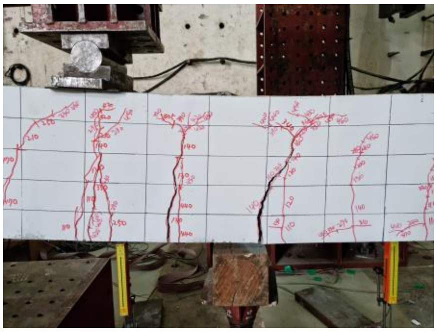

(b) Left lap splice section

(c) Right lap splice section

(d) Right shear span

(e) Failure – Concrete collapse at right load point

Figure 6-19 Failure mode of L-G6

(a) Left shear span

(b) Right shear span

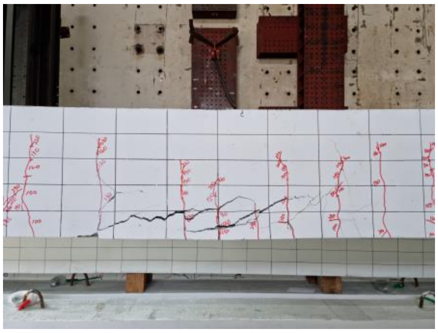

(c) Lap splice section

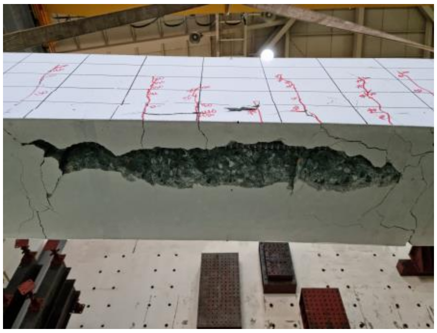

(d) Bottom part

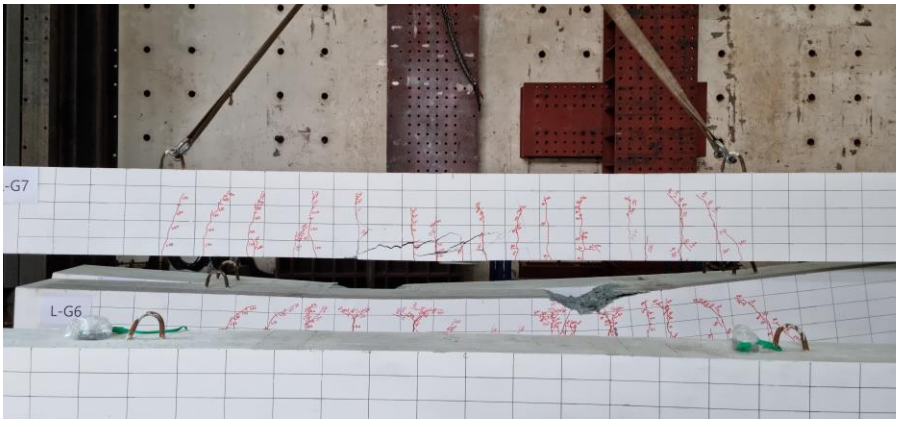

(e) Failure – Concrete collapse at bottom

Figure 6-20 Failure mode of L-G7

(a) Left shear span

(b) Right shear span

(c) Lap splice section

(d) Bottom part

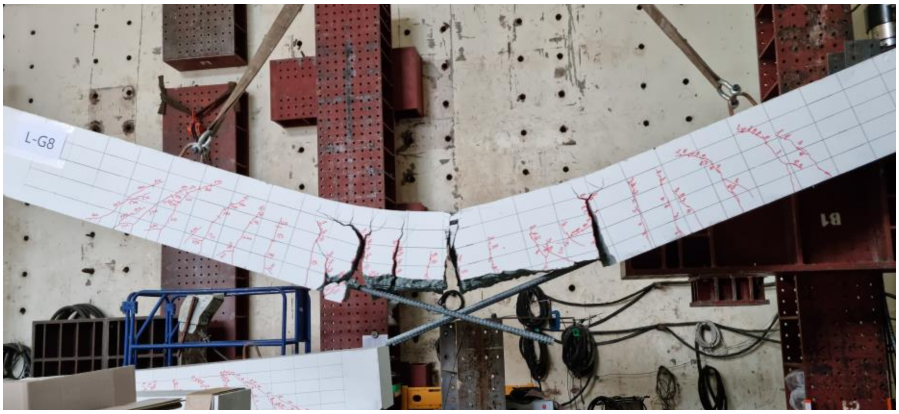

(e) Failure – Bond failure

Figure 6-21 Failure mode of L-G8

(a) Left shear span

(b) Right shear span

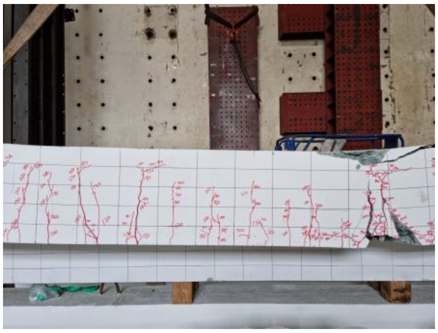

(c) Lap splice section

(d) Fracture of longitudinal bars

(e) Failure – Concrete collapse at right load point

Figure 6-22 Failure mode of L-G9

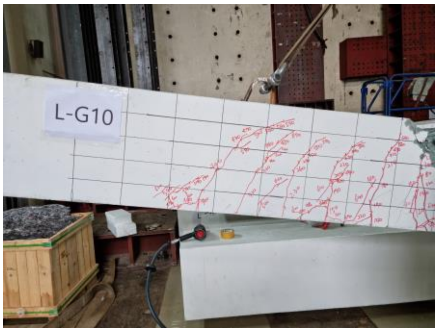

(a) Left shear span

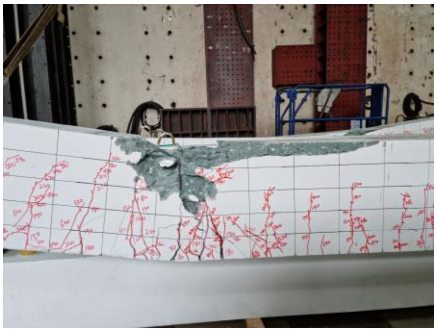

(b) Right shear span

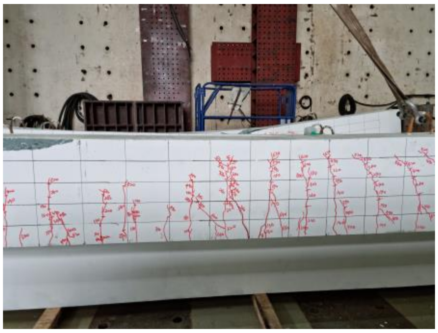

(c) Lap splice section

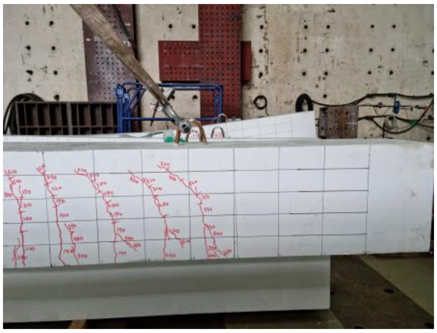

(d) Bottom part

(e) Failure – Concrete collapse at left load point

Figure 6-23 Failure mode of L-G10

(a) Left shear span

(b) Right shear span

(c) Lap splice section

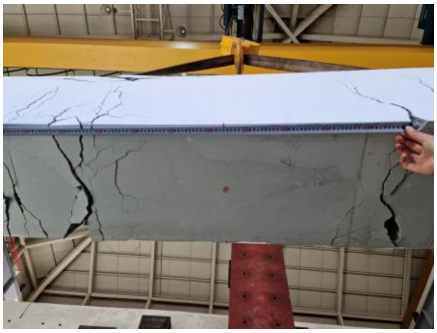

(d) Bottom part

(e) Failure – Concrete collapse at rigth load point

Figure 6-24 Failure mode of L-G11

(a) Left shear span

(b) Right shear span

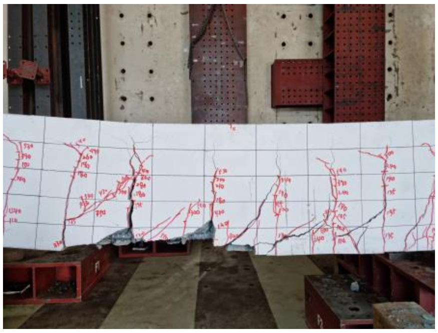

(c) Lap splice section

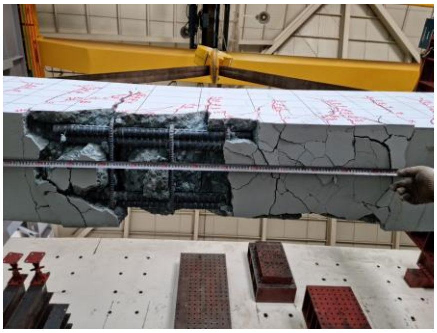

(d) Bottom part

(e) Failure – Concrete collapse at bottom

Figure 6-25 Failure mode of L-G12

Table 6-10 Approximate numbers and spacing of cracks (unit: ea, mm)

Specimens	Cracks	Left shear span	Mid span	Right shear span
L-N1	numbers	3	11	3
	spacing (avg.)	150	133.3	150
L-N2	numbers	4	10	5
	spacing (avg.)	160	145.4	133.3
L-G1	numbers	7	12	7
	spacing (avg.)	100	123	100
L-G2	numbers	8	13	6
	spacing (avg.)	88.8	114.2	142.8
L-G3	numbers	5	24 (collapse)	9
	spacing (avg.)	133.3	88	100
L-G4	numbers	7	23	9
	spacing (avg.)	125	91.6	60
L-G5	numbers	3	9	3
	spacing (avg.)	200	160	150
L-G6	numbers	6	18	7
	spacing (avg.)	114.2	115.7	100
L-G7	numbers	4	12	4
	spacing (avg.)	120	169	120
L-G8	numbers	7	13 (collapse)	4
	spacing (avg.)	125	157	160
L-G9	numbers	9	21 (collapse)	9
	spacing (avg.)	120	100	100
L-G10	numbers	9	25	6
	spacing (avg.)	100	92.3	114.2
L-G11	numbers	7	23	7
	spacing (avg.)	100	91.6	100
L-G12	numbers	6	16 (collapse)	9
	spacing (avg.)	142.8	129.4	100

6.7 Strain of Longitudinal Bars

The strain gauges of lap splice specimens are located 30 mm outside the end of lap splice section.

Figure 6-26 shows the results of longitudinal rebar gauge of bond failure specimens (L-N1, N2, G1, G2, G5, and lap splice length = 0.46 ~ 0.48 l_s). Because of the lack of lap splice length, not all longitudinal rebars yielded, but some longitudinal rebars yielded. This shows similar results to $\varepsilon_{s,\,peak}$ = 0.72 ~ 0.93 ε_y, which is the strain of the longitudinal rebars at the peak test strength, and there was no difference between the normal concrete specimens and geopolymer concrete specimens.

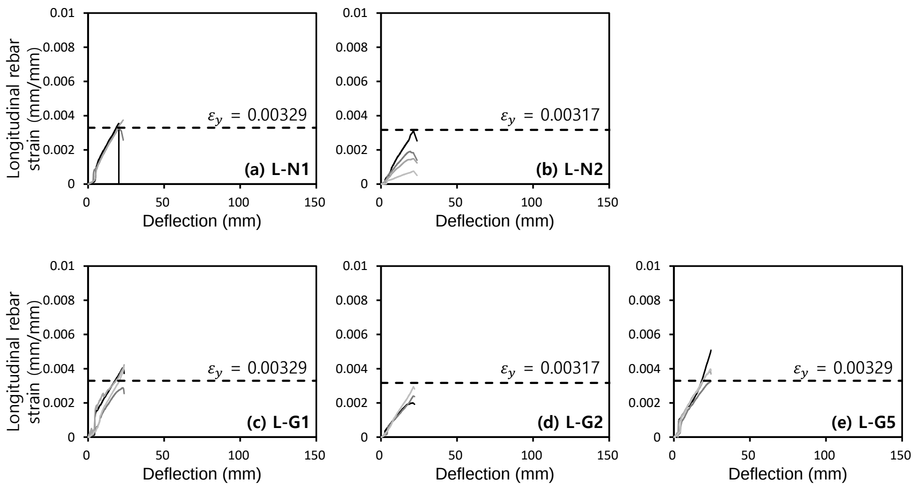

Figure 6-26 Strain results of longitudinal rebars (bond failure specimens)

Figure 6-27 shows the results of longitudinal rebar gauge of flexural failure specimens (L-G7, and G8) that did not use stirrups. The peak experimental strength exceeded yield strength, but after that, the load was rapidly reduced due to bond failure due to the failure of the lower cover concrete. In the actual strain measurement results, all longitudinal rebars except for one rebar yielded.

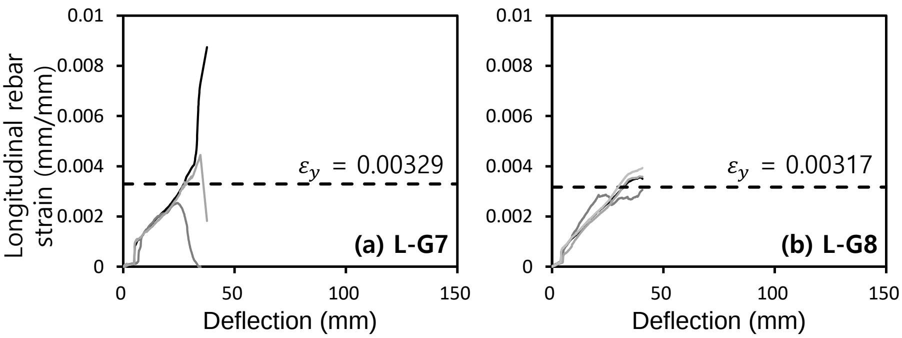

Figure 6-27 Strain results of longitudinal rebars (L-G7, and G8)

Figure 6-28 shows the results of longitudinal rebar gauge of flexural failure specimens (L-G3, G4, G6, G9, G10, G11, and G12) that used stirrups. As the ductile behavior was exhibited after reaching the peak strength, all the longitudinal rebars showed plastic strain after yield. After the yield load, the rebar gauge was damaged due to excessive plastic deflection of the rebars, resulting in a decrease in the strain measurement.

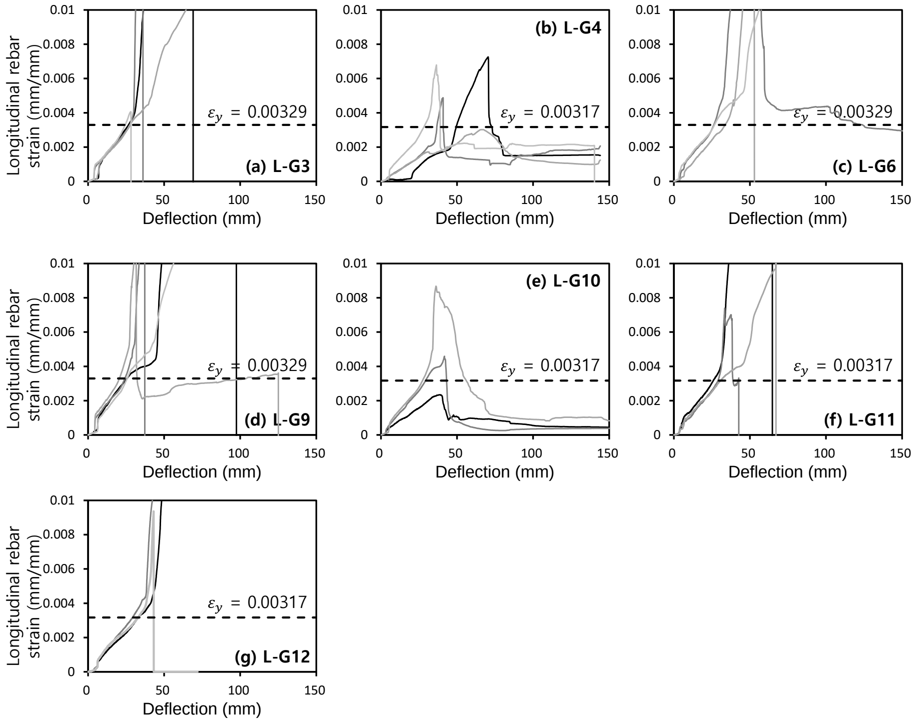

Figure 6-28 Strain results of longitudinal rebars

(L-G3, G4, G6, G9, G10, G11, and G12)

6.8 Discussion

In the lap splice test, a four-point loading test was performed with a total of 14 members as variables such as diameter of longitudinal bars (D25, D32), cover thickness, and compressive strength of concrete (45 MPa, 60 MPa). The bond strength of the splice bar was evaluated by simulating the actual lap splice conditions. The longitudinal bar of the specimens was D25 or D32 of SD600 rebars, and cover thickness was 30 mm to 50 mm (thickness to longitudinar bars was 43 mm to 63 mm). Regardless of the concrete type, all specimens showed greater than nominal strength calculated by nonlinear cross-sectional analysis. The ratio of the nominal strength to the experimental strength was 1.42 on average and the coefficient of variation was 0.205, confirming the bond performance between concrete and rebars.

In 9 specimens that satisfied lap splice length of KDS 14 20 52: 2022, the longitudinal bars yielded. The ratio of yield strength to the experimental strength was 1.03 to 1.24, with an average of 1.14 and the coefficient of variation was 0.076. In some specimens in which stirrups were not used in lap splice section, bond failure occurred after the yield of longitudinal bars, but most of them showed flexural failure. On the other hand, 5 specimens that intentionally reduced the required lap splice length in half did not reach the yield moment due to the lack of the lap splice length specified in KDS 14 20 52: 2022, but the strain of the longitudinal bars at the peak strength of the test was 0.72 ~ 0.93ε_y.

When comparing L-N1, a normal concrete specimen which is a control specimen, with L-G1, a specimen with the same cross-section and different materials, the nominal strength is very similar, but there was a slight difference in experimental strength, so the ratio was 1.71 and 1.99. In the case of the failure modes of the two specimens, they were equally failed by a longitudinal bond crack that occurred on the bottom of the beam in the lap splice section. The average interval of cracks at the bottom of the mid-span of the two specimens was similar to 133.3 to 123 mm, and the maximum length of the cracks was also similar to about 400 mm.

Similar results were found in the case of L-N2 and L-G2, which were specimens with different longitudinal rebar diameters using D32 rebars. The ratio between the nominal strength and the experimental strength was 1.50 and 1.62.

The Hwang et al. model showed two types of settings, 3-point loading and 4-point loading. Comparing experimental results of tensile strength of bar splices with current code equation, ACI 318-19 underestimated the tensile strength, and the prediction was conservative. ACI 408R-03 overestimated the tensile strength. Eurocode 2 and fib Model Code 2010 showed similar results. GB 50010-2010 showed the most conservative prediction.

Comparing experimental results of rebar tensile strength of the Hwang et al. model, ACI 408R-03 provided the best prediction of noncontact lap splices. ACI 318-19 underestimated the rebar tensile strength of noncontact lap splices. Eurocode2, fib Model Code 2010, and GB 50010-2010 underestimated the rebar tensile strength of noncontact lap splices.

Concluding Remarks

For normal concrete applicable to the current design code, KDS, the replacement ratio of cement replacement materials is limited to 70% or less (KCS 14 20 01 :2022). Geopolymer concrete used in this study is a concrete that replaces cement with 100% ground granulated blast-furnace slag (GGBS), and there is no standard for use as a structural material in the current design code, KDS. Therefore, in this study, the suitalbility of KDS 14 20 00 was evaluated for the use of structural materials for geopolymer concrete, which is a newly developed material. Accordingly, the material developed through material tests and structural tests was evaluated whether it could be designed with the current KDS 14 20 00.

For the material tests, specimens were manufactured according to KS F 2403, and then a compressive strength, flexural strength, and tensile splitting strength tests were performed by requesting an external institution (KS F 2405, KS F 2408, KS F 2423). The results are as follows.

(1) A total of 70 specimens (55 for Ø100×200 mm and 15 for Ø150×300 mm) were conducted for each age date for the compressive strength. As a result of the tests, the compressive strength was 21.6 MPa on the 1st day of age, and on the 28th was 45 MPa or more, which is the design standard compressive strength.

(2) A total of 15 specimens (100×100×400 mm) were conducted for each age date for the flexural strength (modulus of rupture). As a result of the tests, the modulus of rupture was 1.20 to 1.30 times the current strength of KDS 14 20 30 :2021 until the age of 28th, so the flexural strength of geopolymer concrete can be conservatively evaluated by the current KDS equation.

(3) A total of 30 specimens (15 for Ø100×200 mm and 15 for Ø150×300 mm) were conducted for each age date for the tensile splitting strength. The tests were performed by comparing the current specimen diameter Ø150 and the existing specimen diameter Ø100 (KS F 2403). Regardless of the size of the specimens, the tensile splitting strength of geopolymer concrete can be conservatively evaluated by the design code evaluation formula as it shows 1.13 to 1.27 times the foreign design code evaluation formula (ACI 363, ACI 318, fib) until the age of 28.

For the structural tests, the materials developed through structural tests (flexural, shear, lap splice) were evaluated with the current KDS 14 20 00. The results are as follows.

(1) The flexural strength was evaluated through beam flexural tests. In the flexural tests, a four-point force test was conducted with a total of 7 specimens as variables such as rebar ratio, cross-sectional depth, and concrete compressive strength, etc. SD600 rebars were used as the

longitudinal rebars of the specimens. The results showed greater than the flexural strength calculated by KDS 14 20 20 for the minimum rebar ratio (0.25%) to the maximum rebar ratio (2.0%), and for the design standard strength level of 45 MPa and the long-term strength of 60 MPa. The ratio of experimental strength / nominal strength was 1.00 to 1.36, with an average of 1.13 and the coefficient of variation of 0.13, so the flexural strength of geopolymer concrete could be reasonably predicted by the current KDS. All specimens showed typical flexural failure.

When comparing F-N1, a normal concrete specimen which is a control specimen, with F-G3, a specimen with the same cross-section and different materials, the ratio between the experimental strength and the nominal strength is very similar to 1.05 and 1.07. In the case of the failure modes of the two specimens, they were also equally failed by the fraction of the lower longitunidal rebars. The average interval of cracks at the bottom of the mid-span of the two specimens was similar to 50 to 60 mm, and the maximum length of cracks was also similar to about 400 mm.

(2) The shear strength was evaluated through beam shear tests. In the shear tests, a four-point force test was conducted with a total of 13 specimens as variables such as shear span ratio, spacing of stirrups, and concrete compressive strength, etc. SD500 rebars were used as the stirrups of the specimens. The results showed greater than the shear strength calculated by KDS 14 20 22 for the spacing of the stirrups (s = none, $d/4$, $d/3$, $d/2$), and for the design standard strength level of 45 MPa and the long-term strength of 60 MPa. The ratio of experimental strength / nominal strength

was 1.21 to 2.05, with an average of 1.61 and the coefficient of variation of 0.145, so the shear strength of geopolymer concrete could be reasonably predicted by the current KDS. Most of the specimens showd shear failure due to diagonal crack, but in some specimens, the shear strength showed higher than the shear force that reached flexural strength, showing flexural failure. Therefore, the actual shear strength was evaluated to be greater than the experimental strength.

When comparing S-N1, a normal concrete specimen which is a control specimen, with S-G1, a specimen with the same cross-section and different materials, the ratio between the experimental strength and the nominal strength is same as 2.05. In the case of the failure modes of the two specimens, they were also equally failed by the diagonal crack. The average interval of cracks at the bottom of the mid-span of the two specimens was similar to 100 to 130 mm, and the maximum length of diagonal cracks was also similar to about 900 mm.

(3) The bond strength of the rebars were evaluated by conducting lap splice tests on the beam. In the lap splice test, a four-point loading test was performed with a total of 14 members as variables such as diameter of longitudinal bars, cover thickness, and compressive strength of concrete. The objective is to evaluate whether the bond failure between the concrete and rebars occurred until the yield strength development of the rebars, which is the basic premise of the ‘strength design method' by simulating the actual lap splice conditions. The longitudinal bar of the

specimens was D25 or D32 of SD600 rebars, and cover thickness was 30 mm to 50 mm (thickness to longitudinar bars was 43 mm to 63 mm). Regardless of the concrete type, all specimens showed greater than nominal strength (when the lap splice length did not satisfy KDS required length) calculated by nonlinear cross-sectional analysis or flexural yield strength (when the lap splice length satisfied KDS required length) of beam. The ratio of the nominal strength to the experimental strength was 1.42 on average and the coefficient of variation was 0.205, confirming the bond performance between concrete and rebars.

When comparing L-N1, a normal concrete specimen which is a control specimen, with L-G1, a specimen with the same cross-section and different materials, the nominal strength is very similar, but there was a slight difference in experimental strength, so the ratio was 1.71 and 1.99. In the case of the failure modes of the two specimens, they were equally failed by a longitudinal bond crack that occurred on the bottom of the beam in the lap splice section. The average interval of cracks at the bottom of the mid-span of the two specimens was similar to 120 to 130 mm, and the maximum length of the cracks was also similar to about 400 mm.

Similar results were found in the case of L-N2 and L-G2, which were specimens with different longitudinal rebar diameters using D32 rebars. The ratio between the nominal strength and the experimental strength was 1.50 and 1.62.

Concluding Remarks

Based on the experimental results, it was found that the precast beam for ordinary moment resisting frames made of geopolymer concrete (design standard compressive strength of 45 MPa or less) can be structured by applying the current design code, KDS 14 20 00, “concrete structural design (strength design method).”

References

[1] KCS 14 20 01. *General Information on Concrete Construction*. Korea Constrution Standards Center. 2022

[2] KCS 14 20 10. *General Concrete*. Korea Construction Standards Center. 2022

[3] KDS 14 20 00. *Concrete Structural Design* (*Strength Design Method*). Korea Construction Standards Center. 2022

[4] KDS 14 20 01. *General Information on Concrete Structural Design* (*Strength Design Method*). Korea Construction Standards Center. 2022

[5] KDS 14 20 10. *Structural Analysis and Design Principle on Concrete*. Korea Construction Standards Center. 2021

[6] KDS 14 20 20. *Flexural and Compressive Design Code on Concrete Structure*. Korea Construction Standards Center. 2022

[7] KDS 14 20 22. *Shear and Torsional Deisgn Code on Concrete Structure*. Korea Construction Standards Center. 2022.

[8] KDS 14 20 30. *Usability Design Code on Concrete Structure*. Korea Construction Standards Center. 2021.

[9] KDS 14 20 50. *Rebar Detail Design Code on Concrete Structure*. Korea Construction Standards Center. 2022.

[10] KDS 14 20 52. *Development and Splice Design Code on*

Concrete Structure. Korea Construction Standards Center. 2022

[11] KDS 14 20 60. *Prestressed Concrete Structure Design Code*. Korea Construction Standards Center. 2022.

[12] KS F 2403. *Standard Test Method for Making and Curing Concrete Specimens*. Korean Standards & Certifications. 2019.

[13] KS F 2405. *Standard Test Method for Compressive Strength of Concrete*. Korean Standards & Certifications. 2017.

[14] KS F 2408. *Standard Test Method for Flexural Strength of Concrete*. Korean Standards & Certifications. 2021.

[15] KS F 2423. *Standard Test Method for Tensile Splitting Strength of Concrete*. Korean Standards & Certifications. 2021.

[16] ACI *Committee 318. Building Code Requirements for Structural Concrete* (*ACI 318-19*) *and Commentary* (*ACI 318R-19*). American Concrete Institute. Farmington Hills. MI. 2019.

[17] ACI Committee 318. *Building Code Requirements for Structural Concrete* (*ACI 318-99*) *and Commentary* (*ACI 318R-99*). American Concrete Institute. Farmington Hills. MI. 1999.

[18] ACI Committee 363. *State-of-the-Art on High-Strength Concrete* (*ACI 363R-92*). American Concrete Institute. Farmington Hills. MI. reapproved 1997.

[19] ACI Committee 408. *Bond and Development of Straight Reinforcing Bars in Tensions*. American Concrete Institute. Farmingon Hills. MI. 2003.

[20] fib Model Code for Concrete Structures 2010.

[21] Eurocode 2: Design of concrete structures. The European Standard EN 1992-1-1: 2004.

[22] Alex, A.G., Tewele, T.G., Kemal, Z. and Subramanian, R.B. (2022). *Flexural Behavior of Low Calcium Fly Ash Based Geopolymer Reinforced Concrete Beam*, International Journal of Concrete Structures and Materials, Vol. 16, No. 5, pp.689-699.

[23] Chang, E.H. (2009). *Shear and Bond Behaviour of Reinforced Fly Ash-Based Geopolymer Concrete Beams*, Curtin University of Technology.

[24] Tekle, B.H., Khennane, A., Kayali, O. (2017). *Bond of Spliced GFRP Reinforcement Bars in Alkali Activated Cement Concrete*, Engineering Structures 147 (2017), pp.740-751.

[25] Atsushi SHIBAYAMA, Minehiro NISHIYAMA. *Shear Strength of Reinforced Fly-Ash-based Geopolymer Concrete Beams with and without Shear Reinforcement*, Structures-D-22-04575

[26] Du, Y., Wang, J., Shi, C., Hwang, H.J., Li, N. (2021). *Flexural Behavior of Alkali-Activated Slag-Based Concrete Beams*, Engineering Structures, Vol. 229, 111644.

[27] Hwang, H.J., Yang, F., Ma, G. (2022). *Effect of Noncontact Lap Splices in Reinforced Concrete Beams*, ACI Structural Journal, Vol. 119, Issue 2, p3-18. 16p.

국문 초록

최근, 전세계적으로 탄소배출량 증가에 따른 기후변화에 대응하기 위해 세계각국에서 탄소배출량 감축목표를 설정하는 조치가 이루어졌다. 교토의정서 (1997)과 파리협정 (2015)에서는 국가의 탄소배출 감소의무를 규정하였고, 정부는 2050 탄소중립 정책을 시행하였다.

건설분야에서는 건축원자재의 생산, 운송과 건축시공, 그리고 폐기과정에서 발생하는 탄소인 Embodied Carbon을 저감하는 탄소저감형 콘크리트를 연구 중에 있다. 일반적으로, 시멘트 1톤 생산 시 약 1톤의 이산화탄소가 배출된다. 그리고 이 양은 전세계 이산화탄소 배출량의 약 7%를 차지한다.

현행 콘크리트 설계기준인 KDS 14 20 01에 따르면, 한국산업표준에 규정되지 않은 시멘트를 사용할 경우 성능실험이 필수적이다. 따라서, 탄소저감형 콘크리트가 현행 설계기준으로 설계 가능 여부를 평가하기 위해 보의 휨, 전단 및 겹침이음 실험을 진행하였다. 보 휨 실험에서 콘크리트 종류, 휨철근비, 실험체 단면 깊이, 콘크리트 압축강도 등을 변수로 실험을 진행하였다. 보 전단 실험에서는 콘크리트 종류, 전단경간비, 횡철근 간격, 콘크리트 압축강도 등을 변수로 실험을 진행하였다. 보 겹침이음 실험에서는 콘크리트 종류, 겹침이음길이, 겹침이음구간에서 횡철근의 유무,

순피복두께, 콘크리트 압축강도 등을 변수로 실험을 진행하였다. 모든 휨 실험체의 실험강도가 KDS와 ACI 기준식에 의한 공칭강도를 넘어섰고 휨 파괴로 파괴되었다. 모든 전단 실험체의 실험강도 또한 KDS와 ACI 기준식에 의한 공칭강도를 넘어섰다. 대부분의 전단 실험체는 사인장 균열에 의한 전단파괴로 파괴되었으나 일부 실험체에서 KDS식으로 계산한 휨 강도 도달시의 전단력을 넘어서 휨 파괴를 보였다. 겹침이음 실험체 또한 모든 실험체의 실험강도가 KDS와 ACI 기준식에 의한 공칭강도를 넘었다. 겹침이음 실험체의 경우 겹침이음길이에 따른 차이가 있었는데, KDS 요구겹침길이를 만족한 실험체는 항복강도에 도달하여 주철근이 항복하였으나, 의도적으로 요구겹침길이를 절반으로 감소시킨 실험체는 항복강도에 도달하지 못하고 파괴되었다.

실험결과를 종합했을 때 무시멘트 탄소저감형 콘크리트로 제작된 프리캐스트 보는 현행 설계기준인 KDS를 적용하여 구조설계를 수행할 수 있는 것으로 나타났다.

주요어: 탄소저감 콘크리트, 압축 강도, 휨 강도, 전단 강도, 부착 강도, 겹침이음, 프리캐스트 보.

학번: 2021- 28039

감사의 글

길다면 길고 짧다면 짧은 기간의 대학원 생활 동안 가르침을 주신 교수님을 비롯하여 도움을 주신 많은 분들께 감사의 말을 전합니다.

먼저, 미흡한 저를 제자로 받아주시고 이끌어주신 스승님, 박홍근 교수님께 진심으로 감사드립니다. 교수님의 제자로 대학원 생활을 시작하고 끝마친 것이 저에게는 굉장한 행운이었습니다. 연구를 본격적으로 시작하기 전 마이애미 빌딩 붕괴에 대해 공부한 것은 구조에 대해 견문을 넓히는 데에 큰 도움이 되었습니다. 연구를 본격적으로 시작한 후에도 지오폴리머 콘크리트와 성능 실험에 대해 제대로 배울 수 있었습니다. 이 논문을 작성하면서도 훌륭한 가르침을 주시고 좋은 아이디어를 계속 제시해 주셔서 완성할 수 있었습니다. 부족한 저를 이끌어주신 덕분에 대학원 생활 잘 마무리하고 좋은 회사에 취직도 할 수 있었습니다. 일 열심히 배우고 좋은 엔지니어가 되어 교수님께 보답하겠습니다.

또한, 자세한 피드백을 주셔서 한 번 더 논문을 점검할 수 있게 해주시고 연구자로서의 자세를 보여주신 홍성걸 교수님, 열정적인 강의를 해주시고 공학에 대해 수학적으로 자세히 가르쳐주신 이철호 교수님, 재미있는 강의로 프리스트레스 콘크리트에 대해 배울 수 있게 해주신 강현구 교수님, 논문을 쓸 수 있게 연구에

많은 도움을 주신 김창수 교수님, 황현종 교수님. 매 학기 훌륭한 강의를 해주시고 논문을 완성할 수 있게 도움을 주셔서 감사합니다.

석사 기간 동안 대학원 생활에 도움을 준 BSSL 식구 여러분께도 감사드립니다. 초반에 정신을 차리게 해주시고 대학원 생활을 잘 마무리할 수 있게 해주신 현진이 형, 연구 기간 동안 여러모로 큰 도움을 주신 광원이 형, 꿀팁도 많이 주시고 많이 도와주신 현근이 형, 재밌는 장난과 농담을 던져주신 종훈이 형, 항상 친절했던 목인이 형, 일적으로도 공부로도 많이 가르쳐주신 유상이 형, 학회 때 친해져서 재밌었던 동갑내기 진영, 말 늦게 놓은 게 아쉬울 정도로 잘 대해준 재한이 형, 입학 때부터 졸업까지 많이 챙겨준 자형이 형, 같은 연구하면서 고생하고 많이 도와준 한세, 실험체 만들고 실험할 때 도와준 은상까지 소중한 시간, 같이 나눠서 즐거웠습니다. 여러분들의 미래에 꿈같은 일들만 가득하기를 진심으로 기원합니다.

같이 건축구조에 대해 공부했던 대학교 형들, 내가 힘들고 지쳤을 때 웃게 해주고 나와 재밌게 놀아줬던 친구들 린우, 준모, 진오, 병훈이, 재용이, 그리고 다른 소중한 친구들 모두 고맙습니다.

마지막으로, 대학원을 갈 수 있다고 격려해 주고 믿어주시고 밀어주신 아버지, 힘들어할 때 응원해 주시고 웃게 해주신 엄마, 같이 살며 짜증 내는 거 받아주고 하나하나 도와준 누나 고마워요. 여러분이 있어서 해낼 수 있었습니다. 항상 고맙고 사랑합니다.

석사과정을 마치면서 많이 도와주셨지만, 언급 못 한 분들이 많습니다. 그분들께도 모두 감사의 말씀을 전합니다. 고맙습니다.

2023년 2월

김 도 훈